Max-Planck-Institut für Molekulare Pflanzenphysiolgie Potsdam-Golm

„Pflanzen-Mikroben-Interaktionen“

Analysis of *Medicago truncatula* transcription factors involved in the arbuscular mycorrhizal symbiosis

Dissertation

Zur Erlangung des akademischen Grades

„doctor rerum naturalium“

Dr. rer. nat.

in der Wissenschaftsdisziplin „Molekulare Pflanzenphysiologie“

eingereicht an der

Mathematisch-Naturwissenschaftlichen Fakultät

der Universität Potsdam

von

Silvia Bortfeld

geboren am 18. Januar 1983

Potsdam, den 26. Juni 2013

Published online at the
Institutional Repository of the University of Potsdam:
URL http://opus.kobv.de/ubp/volltexte/2014/7066/
URN urn:nbn:de:kobv:517-opus-70664
http://nbn-resolving.de/urn:nbn:de:kobv:517-opus-70664

Contents

Tables

Figures

Abbreviations

Ac	acetate
AM	arbuscular mycorrhizal
AMF	arbuscular mycorrhizal fungus
arb cells	arbuscule-containing cells
A. rhizogenes	*Agrobacterium rhizogenes*
A. tumefaciens	*Agrobacterium tumefaciens*
bp	base pairs
CDS	coding sequence
cDNA	complementary deoxyribonucleic acid
cm	centimeter
cor cells	cortical cells of non-mycorrhizal roots
Ct	threshold cycle
DEPC	diethylpyrocarbonate
ddH_2O	double destilled water
DMF	NN-dimethyl formamide
DNA	deoxyribonucleic acid
DNAse	deoxyribonuclease
dNTPs	deoxyribosenucleotides
dpi	days post inoculation
dsRNA	double stranded RNA
DTT	dithiothreitol
E. coli	*Escherichia coli*
EDTA	1-ethyl-3-(3-dimethylaminopropyl) carbodiimide
EMS	ethyl methanesulfonate
EST	expressed sequence tags
et al.	and others
EtBr	ethidium bromide
EtOH	ethanol
gDNA	genomic DNA
g	gram
x g	gravitation acceleration
GdmCl	guanidinium chloride
h	hour
kb	kilo base pairs
l	litre

LAM	Laser Assisted Microdissection
LCM	Laser Capture Microdissection
LFC	log2-fold change
M	molar
M. truncatula	*Medicago truncatula*
MES	2-(N-mopholino)ethanesulfonic acid
mg	milligram
min	minutes
miRNA	microRNA
miR	mature microRNA
miR*	microRNA star strand
mg	milligram
ml	milliliter
MOPS	3-(N-morpholino)propanesulfonic acid
mM	millimolar
mRNA	messenger ribonucleic acid
myc	mycorrhizal
nac cells	non-arbsucule-containing cells of mycorrhizal roots
ng	nanogram
N. benthamina	*Nicotiana benthamiana*
nonmyc	non-mycorrhizal
nt	nucleotides
PBS	phosphate buffered saline
PCR	Polymerase-Chain-Reaction
P_i	inorganic phosphate
piwiRNA	piwi interacting RNA
pg	pictogram
pre-miRNA	precursor microRNA
qRT-PCR	quantitative real-time PCR
RISC	RNA induced silencing complex
RNA	ribonucleic acid
rpm	round per minute
SDS	sodium dodecyl sulfate
siRNA	small interfering ribonucleic acid
TAE	Tris-acetate-EDTA
TC	tentative sequence

TF	transcription factor
Tnt1 mutant	tobacco retrotransposon insertion mutant
Tris	Tris(hydroxymethyl)aminomethane
UTR	untranslated region
wpi	weeks post inoculation
v/v	volume/volume
v/w	volume/weight
µg	microgram
µM	micromol
µl	microliter

Publications:

Parts of this thesis were published

Nicole Gaude, **Silvia Bortfeld**, Nina Duensing, Marc Lohse and Franziska Krajinski* (2012) Arbuscule-containing and non-colonized cortical cells of mycorrhizal roots undergo extensive and specific reprogramming during arbuscular mycorrhizal development, The Plant Journal 69, 510–528, DOI: 10.1111/j.1365-313X.2011.0481

1 Introduction

1.1 The arbuscular mycorrhizal symbiosis

Arbuscular mycorrhizal (AM) symbiosis (the name derived from "mycos"= fungi and "rhiza"= root) is a mutualistic interaction between 80 % of vascular land plants and obligat biotrophic fungi (Newman and Reddell, 1987; Smith and Read, 1997). Arbuscular mycorrhizal fungi (AMF) were already found in the first land plants, more than 400 million year ago and might play a key role in colonization of the land by plants (Pirozynski and Malloch, 1975; Simon et al., 1993; Remy et al., 1994; Redecker et al., 2000). Today around 150 AMF species are known, which belong to the phylum *Glomeromycota*, a sister clade of the *Asco*- and *Basidiomycota* (Schüssler et al., 2001). The AMF provide water and mineral nutrients, such as phosphate, nitrate, sulfur, zinc and copper, to the plant (Marschner and Dell, 1994; Clark et al., 2001; Karandashov and Bucher, 2005; Allen and Shachar-Hill, 2009; Tian et al., 2010; Soltis et al., 2011). Furthermore, plant fitness is improved *via* induction of plant growth and activation of defense mechanisms against biotic and abiotic stresses (Smith and Read, 1997; Auge, 2001; Morandi et al., 2002; Barker et al., 2005; Liu et al., 2007). On the other hand, the AMF are enabled to fulfill their lifecycle by consumption of up to 20 % of the plant derived photosynthesis products (Bago et al., 2000; Zhu et al., 2003). Although the AMF are obligat biotrophs, spore germination is induced by exogenous stimuli, e.g. CO_2 and volatiles, in the absence of a host plant (Becard and Piche, 1989; Gianinazzi-Pearson and Gianinazzi, 1989; Nair et al., 1991). Morphologically two fungal growth patterns in the host root can be distinguished, the "*Arum*- " and the "*Paris*-"type (Smith and Read, 1997; Cavagnaro et al., 2003). In the following text the development of a symbiotic interaction between host plants and an AMF of the "*Arum*"-type will be described.

During the presymbiotic phase a molecular dialogue is established between plant and fungus. Plant-derived hormones, also referred as strigolactones, are secreted with the root exudates and induce fungal spore germination, respiration and hyphae branching (figure 1) (Parniske, 2005; Akiyama and Hayashi, 2006; Besserer et al., 2008; Gomez-Roldan et al., 2008). On the other hand, the fungus secretes a so called Myc-factor, consisting of a mixture of sulphated tetrameric and non-sulfated pentameric lipochito-oligosaccharides (Myc-LCOs) (Olsson and Johansen, 2000; Maillet et al., 2011). Myc-LCOs are recognized by Lys-M receptor-like kinases, which are localized in the plasma membrane of epidermal cells (Op den Camp et al., 2011). These fungal signaling molecules activate the host root branching and symbiosis-related gene expression (Olah et al., 2005). Upon recognition of the Myc-LCOs by Lys-M receptor-like kinases, calcium oscillation and expression of symbiosis-relevant genes, such as *ENOD11*, is induced *via* the components of a common *sym* pathway (Kosuta et al., 2003; Kosuta et al., 2008), which is described in detail in chapter 1.3.

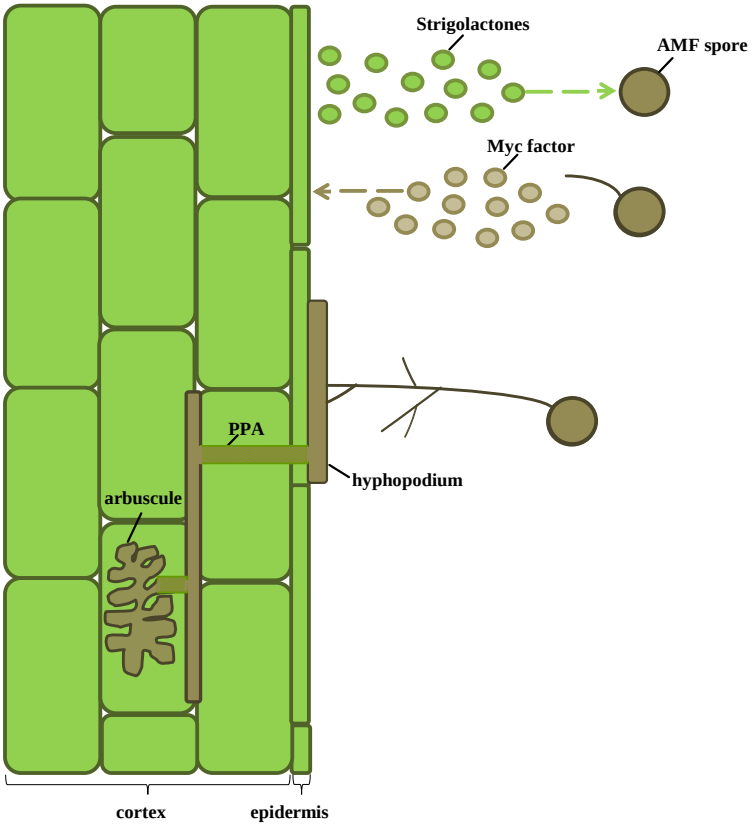

Figure 1: Colonization process of a plant root by arbuscular mycorrhizal fungi (based on Parniske, 2008).

The symbiosis starts with a molecular dialogue. Plant-derived strigolactones are secreted from the host roots and lipochito-oligosaccharides (Myc-LCOs) are secreted by the AMF. Afterwards the beneficial symbiont generates an infection structure (hyphopodium) on the epidermal cell surface. The entering of plant cells and growths of hyphae through the epidermal cells is facilitated by a pre-penetration apparatus (PPA). In the root cortex a runner hyphae is growing along the root axis, before the cortex cells are entered by PPA structures. In the inner cortical cells dichotomous hyphae branching leads to the formation of tree like structures (arbuscules). These structures are surrounded by an extension of the plant plasma membrane, known as periarbuscular membrane, which harbors numerous nutrient transporters to manage the nutrient exchange.

The formation of a fungal infection structure (hyphopodium) on the surface of the epidermal cells facilitates the infection of root cells (Voets et al., 2006). Four to five weeks after hyphopodia formation, a massive reorganization of the epidermal cells occurs (Genre et al., 2005; Siciliano et al., 2007). Calcium oscillation followed by the movement of the epidermal nucleus to the fungal contact site of the epidermal cell leads to the formation of a new infection structure, also referred as pre-penetration apparatus (PPA) (Genre et al., 2005; Genre et al., 2008; Sieberer et al., 2012; Takeda et al., 2012). This plasma bridge consists of cytoskeletal fibres, extensions of the endoplasmatic reticulum, golgi stacks and golgi vesicles (Genre et al., 2005; Genre et al., 2008). The PPA permits fungal hyphae to cross the epidermal cells and colonize the cortex (Genre et al., 2005; Genre et al., 2008). In the cortex, the hyphae grow along the root axis, before the inner cortical cells are entered (Genre et al., 2005; Genre et al., 2008). Upon dichotomous hyphae branching the nutrient exchange structures, referred as arbuscules (latin = little tree), are built up in the cortical cells (figure 1) (Alexander et al., 1988; Alexander et al., 1989). This leads to massive cytoskeletal rearrangements (Genre and Bonfante, 1997, 1998; Fester et al., 2001; Genre and Bonfante, 2002). Golgi bodies arrange around the arbuscule branch nodes and indicate exocytosis processes, which are required for the establishment of a plant-derived periarbuscular membrane (Pumplin and Harrison, 2009; Genre et al., 2012). The membrane separates the

arbuscules from the plant cytosol and enables nutrient exchange by harbouring numerous nutrient transporter proteins like the mycorrhizal-specific phosphate transporter *MtPt4* (Cox and Tinker, 1976; Ferrol et al., 2002; Harrison et al., 2002; Javot et al., 2007b). Due to the short life-span of arbuscules (5-8 days), one cortical cell can be colonized several times by fungal hyphae (Alexander et al., 1988; Alexander et al., 1989; Javot et al., 2007b). Interestingly, the life-time of an arbuscule is dependent on the phosphate transport efficiency and the functionality of the mycorrhizal-specific phosphate transporter *MtPt4* (Harrison et al., 2002; Javot et al., 2007b). Accordingly, the colonization of the root cortex is an asynchronous process including permanent formation and degradation of fungal structures (Gianinazzi-Pearson and Brechenmacher, 2004). Consequently, fungal structures of different developmental stages are simultaneously present in mycorrhizal roots during AM symbiosis (Alexander et al., 1988; Alexander et al., 1989; Javot et al., 2007b).

1.2 Studying the symbiosis-related reprogramming *via* transcriptome analyses

As mentioned above, root cortical cells undergo a massive reorganization process during the colonization by AMF. In the last decades genes involved in this reorganization process were identified *via* different transcriptomic approaches, such as the generation of Expressed Sequence Tags (EST), Suppression Subtractive Hybridization (SSH-) libraries, qRT-PCR analyses and microarray hybridizations.

By establishment and sequencing of ESTs and Tentative Consensus Sequences (TCs) based on cDNA libraries, mycorrhizal-specific genes, e.g. *MtGst1*, *MtPt4*, *MtBcp1*, as well as NBS-LRR resistance–like proteins, and lectins were identified (Harrison et al., 2002; Journet et al., 2002; Wulf et al., 2003; Frenzel et al., 2005). These EST and TC libraries enabled the spotting of macro- and microarrays (Liu et al., 2003). First cDNA microarrays were established by Liu and co-workers in 2003. In a time course experiment the down-regulation of defence genes like PR3 proteins and chitinases could be monitored in *Glomus versiforme* inoculated *Medicago truncatula* roots (Liu et al., 2003). In the following years legume microarrays were improved and deep sequencing data sets were generated (Küster et al., 2004; Devers et al., 2011) . A Mt16k-Rit macro- and microarray hybridization was performed to identify co-induced genes in *Rhizophagus irregularis*- and *Sinorhizobium meliloti*- inoculated *M. truncatula* roots (Manthey et al., 2004). Additionally, 201 significantly co-regulated (2-fold induced) genes in *Funneliformis mosseae*- and *R. irregularis*- inoculated *M. truncatula* roots were detected upon Mt16K-Rit microarray hybridization (Hohnjec et al., 2005). Affymetrix GeneChip® Medicago genome array experiments (including ~52000 *M. truncatula*, 1900 *Medicago sativa* probes as well as 8000 *Sinorhizobium meliloti* probes) facilitated a genome wide transcript profiling of leaf, root and symbiotic tissues originating from *M. truncatula* and *M. sativa* (Benedito et al., 2008).

Especially, mycorrhizal-induced genes were identified in AMF-inoculated *M. truncatula* and *Lotus japonicus* roots (Gomez et al., 2009; Guether et al., 2009; Hogekamp et al., 2011).

Due to the short life-time of arbuscules, permanent reinfection processes of cortical cells take place, which lead to the presence of colonized and non-colonized cells in mycorrhizal roots (Javot et al., 2007b). This leads to dilution effects in whole root transcriptome analyses. These dilution effects can be overcome by cell type-specific transcriptome analyses. Several methods enable the isolation of single cells or specific cell-types from the surrounding tissue (Nakazono et al., 2003; Nelson et al., 2006). The sampling of cell sap or whole cell content *via* glass microcapillaries, generation of protoplasts or peeling of cell layers of interest belong to the most common techniques (Kehr, 2001; Birnbaum et al., 2003; Jones and Grierson, 2003). But, these methods massively influence metabolic and transcriptomic processes like the induction of defense genes by wounding and bear a high contamination risk. Furthermore, these techniques provide not sufficient analyte (RNA) amounts for downstream analyses, such as northern blot and microarray hybridization (Brandt et al., 1999; Brandt et al., 2002).

Laser Assisted Microdissection systems (LAM) facilitate specific and efficient isolation of distinct cell types without influencing the transcription or metabolism of the target cells. The method is based on a microscope coupled with a laser (typically infrared (IR) laser, UV- or nitrogen-laser) that facilitates the microdissection of the target tissue or target cells from tissue sections mounted on microscope slides (Emmert-Buck et al., 1996; Day et al., 2005). The first system was used for dissection of animal tissues and was provided by Arcturus (Pixcell® II system, *Arcturus*, USA) (Emmert-Buck et al., 1996). In case of Laser Capture Microdissection (LCM) a focused UV-laser beam dissects the surrounding tissue by photo decompensation (figure 2A, B) (Day et al., 2005; Nelson et al., 2006). Afterwards the cells were catapulted *via* the photon pressure of a laser beam into a special collection tube containing a sticky membrane to fix the target cells (Nelson 2006). With this ablative dissection, heat-damage of the analytes (nucleic acids, proteins and metabolites) is prevented, because the wavelength of the UV-laser is higher than the absorption wavelength of proteins and nucleic acids (Day et al., 2005). An important factor for a successful isolation of target cells is the tissue preparation. The identification and sampling of target cells requires a microscopically thin section with highly preserved morphology (Goldsworthy et al., 1999). But the extractability of analytes and tissue preservation have to be balanced during tissue fixation (Kerk et al., 2003). RNA with sufficient quality and quantity was obtained from cryosections and ethanol or acetone fixated tissues (Goldsworthy et al., 1999; Nakazono et al., 2003; Casson et al., 2005). Although the plant tissue microdissection is more challenging as compared to animal tissues, several LAM protocols for plant tissues are available. In 2002, Asano and co-workers used LCM to isolate phloem cells from cryodissected rice leaves and established cDNA libraries upon RNA isolation and amplification (Asano et al., 2002).

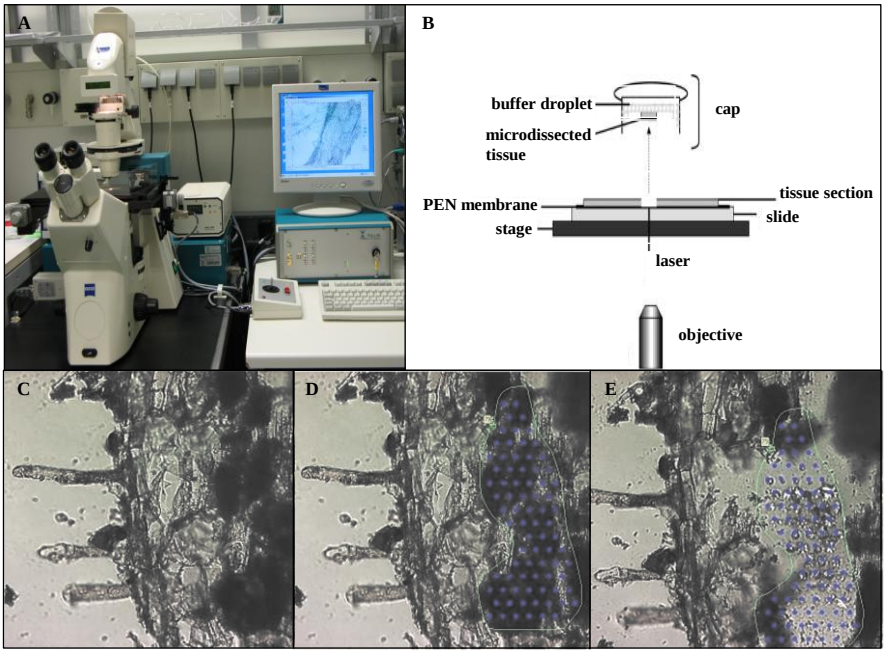

Figure 2: Laser Capture Microdissection assisted sampling of root cortex cells (Rodriguez-Gonzalez, 2012, modified). In this work the P.A.L.M.® Microbeam 020207 system was used to enable the LCM of *M. truncatula* cortical root cells. The system consists of an epifluorescence microscope coupled to an UV-laser (A). Computer controlled laser settings and a high definition microscope stage facilitate the selection of target cells. B) Paraffin sections mounted on membrane-sealed slides (PEN slides) can be dissected by a laser pulse, which is directed through the objective. The target cells are catapulted *via* a laser beam into the lid of an adhesive cap, containing a buffer droplet. (C-E) In this work, longitudinal *M. truncatula* root cryosections were mounted on glass slides (C) and numerous laser spots were applied on one cell *via* the laser function "Auto-LPC" to dissect the tissue (D). (E) Root section after microdissection.

Another advantage of LCM is the compatibility with nearly all kinds of downstream analyses. The combination of LCM and microarray hybridization enabled the transcriptome analyses of epidermal cells and vascular tissues sampled from cryodissected maize coleoptiles (Nakazono et al., 2003). A combination of LAM and microarray hybridization was used to study the transcriptional reprogramming of leaf tissues upon pathogen infections (Chandran et al., 2010; Hacquard et al., 2010). Further, the transcriptome analysis of different compartments of the ectomycorrhiza fungus *Tuber melanosporum* upon root tip colonization of *Corylus avellana* L. was facilitated by LAM and microarray hyrbidizations (Hacquard et al., 2013). Coupling LAM and qRT-PCR facilitated to unravel the cell-specific expression of phosphate transporters during the AM symbiosis (Balestrini et al., 2007; Gomez-Ariza et al., 2009). In recent studies, LCM and qRT-PCR were combined to investigate the transcriptional reprogramming of different *M. truncatula* and *L. japonicus* cortical cell types during AM symbiosis (Gomez et al., 2009; Guether et al., 2009; Hogekamp et al., 2011). Further, LCM of paraffin embedded roots was combined with Affymetrix® GeneChip hybridization (Hogekamp et al., 2013). In this work, cDNA samples from cortex cells selected from cryosections of mycorrhizal and nonmycorrhizal *Medicago truncatula* roots were used for Affymetrix® GeneChip hybridization (figure 2C-E).

1.3 Root endosymbioses share a common signal transduction pathway

The AM symbiosis (400 million years old) is more ancient than the 60 million years old root nodule (RN) symbiosis, formed between nitrogen fixing *Rhizobia* and legumes (Sprent and James, 2007). As mentioned earlier, both symbioses start with a molecular dialogue between host and symbiont mediated by the exchange of signaling molecules (Nod- and Myc-factors) (Denarie et al., 1996; Olah et al., 2005; Gough and Cullimore, 2011). Nod-and Myc-factors are lipochito-oligosaccharides (LCOs) components (Maillet et al., 2011). It is supposed, that Myc-factors might represent ancestors of Nod-factors (Maillet et al., 2011). Both signaling molecules are recognized by plant receptor-like kinases, localized in the plasma membrane of epidermal cells (Limpens et al., 2003; Madsen et al., 2003; Radutoiu et al., 2003; Op den Camp et al., 2011). Nod-factors bind to NOD FACTOR PERCEPTION NFP (LjNFR5) and LYS-M RECEPTOR-LIKE KINASE MtLYK3 (LjNFR1) (Limpens et al., 2003; Madsen et al., 2003; Radutoiu et al., 2003). Analysis of *Parasponia andersonii* and *M. truncatula* revealed that NFP may also be involved in the perception of sulfated Myc-LCOs and induction of root branching (Maillet et al., 2011; Op den Camp et al., 2011). Furthermore, MtLYR1 might be involved in the recognition of Myc-LCOs (Gomez et al., 2009). In both symbioses signal perception and formation of infection structures (PPA during AM symbiosis and infection thread during RN symbiosis) is activated by components of the common *sym* pathway, as shown in figure 3 (Kistner and Parniske, 2002; Stracke et al., 2002; Genre et al., 2005; Oldroyd and Downie, 2008; Sieberer et al., 2012; Takeda et al., 2012). These components are involved in the activation and perception of a periodic calcium oscillation in and around the nucleus, named calcium spiking (Oldroyd and Downie, 2006; Kosuta et al., 2008; Oldroyd and Downie, 2008). Upstream of the calcium spiking, extracellular signals from symbionts (Myc- and Nod-factors) activate a leucine-rich repeat receptor-like kinase, known as DOES NOT MAKE INFECTION 2 in *M. truncatula* (MtDMI2) or SYMBIOSIS RECEPTOR-LIKE KINASE in *L. japonicus* (LjSYMRK), which facilitates the signal transduction between plasma membrane receptors and calcium channels (Wais et al., 2000; Endre et al., 2002; Stracke et al., 2002; Oldroyd, 2013). A potassium permeable calcium cation channel (known as MtDMI1 or LjCASTOR and LjPOLLUX), localized in the nuclear membrane, is essential for the calcium oscillation (Ane et al., 2004; Peiter et al., 2007; Charpentier et al., 2008; Capoen et al., 2011). *M. truncatula dmi1* mutants are defective in Nod-factor induced calcium spiking (Imaizumi-Anraku et al., 2005; Oldroyd and Downie, 2008). It is suggested that DMI1 controls the calcium influx into the nucleus (Oldroyd, 2013). Afterwards the activation of a nuclear calcium- and calmodulin dependent protein kinase (MtDMI3 or CCaMK) takes place (Levy et al., 2004; Mitra et al., 2004; Siciliano et al., 2007). DMI3 acts downstream of the calcium spiking and phopshorylates and interacts with a coiled-coil protein (MtIPD3 or LjCYCLOPS) (Levy et al., 2004; Messinese et al., 2007; Horvath et al., 2011). In *dmi3* mutants spontaneous nodulation was

observed in the absence of *Rhizobia*, indicating that DMI3 is functionally involved in organogenesis during the symbiosis (Mitra et al., 2004). Two members of the GRAS transcription factor family NODULATION SIGNALING PATHWAY 1 and 2 (NSP1 and NSP2) mediate the induction of symbiosis-related gene expression downstream of the common *sym* pathway (figure 3) (Kalo et al., 2005; Smit et al., 2005; Heckmann et al., 2006; Hirsch et al., 2009). Upon formation of a heterodimeric complex with NSP2, NSP1 binds to promoter *cis*-elements of target genes, such as *ETHYLENE RESPONSE FACTOR REQUIRED FOR NODULATION1* (*ERN1*) and promoters of the early nodulins *ENOD11* and *NIN* genes (Heckmann et al., 2006; Hirsch et al., 2009; Cerri et al., 2012).

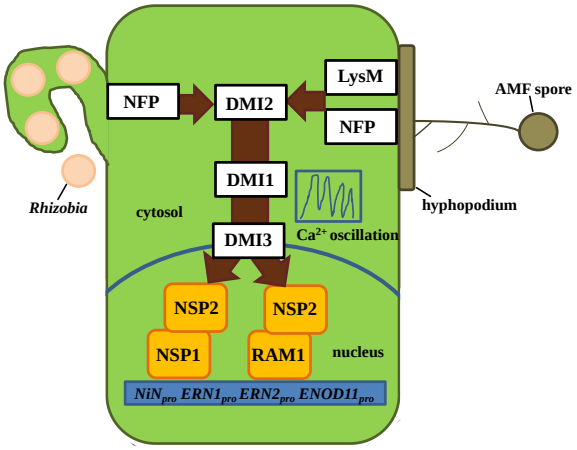

Figure 3: Root endosymbioses share a common signal transduction pathway (based on Oldroyd *et al.*, 2013). Signaling molecules, secreted by AMF spores and *Rhizobia* (Myc-and Nod-factors), are recognized *via* receptor-like kinases (NFP, LysM) in the plasma membrane of epidermal cells. Cytosolic calcium spiking is activated and decoded by the common *sym* pathway components leucine-rich repeat receptor-like kinase (DMI2), a calcium ion channel (DMI1) and a calcium-calmodulin kinase (DMI3). Downstream of the calcium spiking two GRAS transcription factors, NSP1 and NSP2, bind as heterodimer to the promoter *cis*-elements of *Nin* genes, *ERN1* and *ENOD11* to enable the symbiosis induced gene expression. During the mycorrhizal symbiosis NSP2 and REQUIRED FOR ARBUSCULAR MYCORRHIZATION 1 (RAM1) form a heterodimer to activate the RAM2 gene expression and force the hyphopodia formation.

Additionally, these GRAS TFs (NSP1 and NSP2) regulate strigolactone production thereby enhancing the reinfection of the plant (Liu et al., 2011). Analysis of *M. truncatula nsp1* has unraveled the nodulation specific function of NSP1. Delayed Nod-factor responses, like reduced nodulin gene expression and an impaired root hair deformation, were observed in *nsp1* mutants (Smit et al., 2005; Heckmann et al., 2006). But Myc-LCOs induced gene expression was not affected in the mutants (Olah et al., 2005; Maillet et al., 2011; Delaux et al., 2013). *nsp2* mutants displayed significantly reduced colonization intensities upon *Rhizobia* and mycorrhizal infection (Catoira et al., 2000; Oldroyd and Long, 2003; Mitra et al., 2004; Maillet et al., 2011). Accordingly, Maillet and co-workers suggested in 2011, that RN symbiosis recruits the signaling pathway of the AM symbiosis. Nevertheless, Gobatto and co-workers confirmed in 2012 an interaction of NSP2 with another GRAS transcription factor RAM1 during AM symbiosis (figure 3). RAM1 seems to be involved in hyphopodia formation, which is induced upon transcriptional activation of the glycerol acyltransferease (RAM2) (Gobbato et al., 2012). Taken together, both

root endosymbioses share a common signaling pathway, but downstream of the *sym* pathway different nodulation and mycorrhization responses can be observed (Oldroyd, 2013).

1.4 Regulation of gene expression *via* transcription factors and small RNAs

Plants are sessile organisms and complex regulatory systems are required to facilitate appropriate responses to environmental changes (light stress, nutrient and water availability, temperature changes, pests and diseases) (Libault et al., 2009). Transcription factors (TFs) and small RNAs regulate the expression of root endosymbiosis-related genes and mediate the reorganization of host root cells during the AM and RN symbioses (Boualem et al., 2008; Branscheid et al., 2010; Devers et al., 2011; Gaude et al., 2012; Lauressergues et al., 2012). TFs are defined as sequence specific DNA-binding proteins, that are able to activate or repress transcription (Udvardi et al., 2007). These proteins often interact with other transcriptional regulators (e.g. chromatin remodeling enzymes) to enable or to block the polymerase binding to DNA (Udvardi et al., 2007; Libault et al., 2009). Around 2000 TFs are encoded per genome, but less than one percent are characterized in the model legumes *M. truncatula* or *Lotus japonicus* so far (Udvardi et al., 2007). The identification of *M. truncatula* and *L. japonicus* TFs was facilitated by detection of sequence homologies to *Arabidopsis thaliana* TFs and characterization of mutants (Libault et al., 2009). They can be categorized based on their DNA binding domains into different families. During root endosymbioses members of the MYB, CAAT-box binding TF family, APETALA2/ETHYLENE-RESPONSIVE TRANSCRIPTION FACTORS (AP2/ERF) and GRAS TFs play essential roles (Combier et al., 2006; Andriankaja et al., 2007; Middleton et al., 2007; Hirsch et al., 2009; Cerri et al., 2012).

AP2/ERF TFs play key roles during RN symbiosis induced gene expression. ERN1, ERN2 and ERN3 modulate the expression of *ENOD11* upon Nod factor treatment (Andriankaja et al., 2007). These TFs bind to a “GCC” motifs in the promoter *cis*-elements of target genes (Gu et al., 2000) (Fujimoto et al., 2000; Chen et al., 2002; Onate-Sanchez and Singh, 2002; Brown et al., 2003; Lorenzo et al., 2003).

Apart from the transcriptional gene regulation *via* TFs, different classes of small RNAs, such as short interfering RNAs (siRNA), microRNAs (miRNAs) and piwi-interacting RNAs (piwiRNAs), mediate gene regulation in a posttranscriptional manner (Carthew and Sontheimer, 2009). The role of small RNAs during developmental processes, during abiotic or biotic stress responses and AM symbiosis was unraveled in the last decade *via* isolation and cloning of miRNAs as well as deep sequencing and miRNA microarray approaches (Reinhart et al., 2002; Sunkar and Zhu, 2004; Sunkar et al., 2005; Gu et al., 2010; Devers et al., 2011). Plant TFs are often targeted by miRNAs to control developmental and differentiation processes (Rhoades et al., 2002). The following examples describe miRNA regulated TFs with essential roles during root endosymbioses.

The CCAAT-box-binding TF family member MtHAP2-1 is essential for RN symbiosis and posttranscriptionally regulated by miRNA169 (Combier et al., 2006). Over-expression of miR169 results in a reduction of *MtHAP2-1* transcripts, delayed nodule development, arrested nodule growth and loss of nitrogen fixation ability (Combier et al., 2006). Accordingly, this regulation system seems to modulate nodule function and the elongation and differentiation of tissue around the meristematic zone of nodules (Combier et al., 2006). MtHD-ZIPIII is another TF playing a role in RN symbiosis. This TF regulates the induction of lateral root formation and vascular bundle differentiation in a symbiosis (RN symbiosis) and non-symbiosis dependent manner (Boualem et al., 2008). The TF transcript abundance is posttranscriptionally regulated by miRNA166. miRNA166 over-expression lines displayed significantly reduced lateral root density and lower number of nodules, indicating a function during organogenesis (Boualem et al., 2008). The combination of a MYB TF and miRNA-mediated gene regulation also plays an important role during phosphate homeostasis (Bari et al., 2006; Valdes-Lopez et al., 2008). MYB TFs are widely distributed in animal and plant kingdoms and are characterized by imperfect repeats in their protein structure (Lipsick et al., 2001). While animal MYB TFs include typical repeats (R1, R2, R3), MYB TFs in plants have only two imperfect repeats (R2 and R3) (Baranowskij et al., 1994). PHR1, a member of the MYB TF family induces the expression of miRNA399 in roots (Bari et al., 2006). This miRNA cleaves transcripts of the E2-ubiquitin-conjugase PHO2, which represses phosphate starvation-induced genes. Over-expression of miR399 leads to over accumulation of phosphate in the shoot (Bari et al., 2006; Branscheid et al., 2010).

GRAS TFs are involved in gibberellic acid signaling, root patterning and axillary meristem development (Di Laurenzio et al., 1996; Peng et al., 1997; Silverstone et al., 1998; Guether et al., 2009) The name of the TF superfamily is derived from the first identified family members GIBBERELLIC ACID INSENSITIVE (GAI), REPRESSOR OF GAI (RGA) and SCARECROW (SCR) (Di Laurenzio et al., 1996; Peng et al., 1997; Silverstone et al., 1998). As described earlier, members of the GRAS TF family play essential roles during RN and AM symbiosis-dependent signal transduction. NSP1, NSP2 and RAM1 mediate symbiosis induced gene expression upon heterodimer formation (Kalo et al., 2005; Smit et al., 2005; Heckmann et al., 2006; Hirsch et al., 2009; Gobbato et al., 2012). The targeting of *MtNsp2* transcripts by miR171h was predicted after deep sequencing of small RNAs from mycorrhizal and non-mycorrhizal *M. truncatula* roots (Branscheid et al., 2011; Devers et al., 2011). Cleavage of *MtNsp2* transcripts by miR171h was concluded from miRNA171h overexpressing lines, which disposed a reduced colonization intensity, but unaffected nodulation (Lauressergues et al., 2012). Taken together, miRNAs and TFs build up important regulation systems which play essential roles during the root endosymbioses.

1.5 *Medicago truncatula* mutants enable reverse genetic analyses

Several symbiosis-relevant proteins, such as DMI1, DMI2, DMI3, NSP2 and MtPT4 have been characterized by reverse genetic approaches (Wais et al., 2000; Oldroyd and Long, 2003; Mitra et al., 2004; Limpens et al., 2005; Javot et al., 2007b). These techniques are based on efficient generation of mutant populations. The *M. truncatula dmi3* (*does not make infection 3*) gamma-ray mutant was isolated and functionally characterized by transcript-based cloning (Mitra et al., 2004). The function of the AM symbiosis-specific phosphate transporter MtPT4 (Javot et al., 2007b) was determined in *M. truncatula* by target-induced-local lesions in genomes (TILLING) populations.

Mutants can also be obtained by homology dependent gene silencing, known as RNA-interference (RNAi). RNAi describes a posttranscriptional gene silencing mechanism in various organisms (plants, mammals, fungi) (Matzke et al., 2001). During the process, small double stranded RNA molecules 21-25 nt in length (siRNAs) are incoporated into a RNA-Induced Silencing Complex (RISC) in the cytosol, which enables the sequence specifically cleavage of homologous mRNA transcripts. This system is also useful for the functional characterization of genes by directly silencing their transcripts upon expression of RNAi constructs (Schweizer et al., 2000; Kumagai and Kouchi, 2003). For example, the role of the MtHAP2-1 TF in nodule development in *M. truncatula* was unravelled *via* RNAi-mediated gene silencing (Combier et al., 2006). But the system has the drawback, that RNAi-mediated gene silencing results in a variety of phenotypes, caused by different gene silencing levels (wild type, knock-down and knock-out) (Liu et al., 2002; Limpens et al., 2003; Wesley et al., 2003).

Saturation of genomes with transposon or retrotransposon element insertions is another method to establish mutant collections (d'Erfurth et al., 2003). Two types of transposons have to be distinguished. Class I transposons, known as retrotransposons, transpose *via* a “copy and paste” mechanism, the transposable element is transcribed into a mRNA intermediate, and upon reverse transcription a dsDNA is generated and integrated. In contrast to this, class II transposons transpose with the help of a DNA intermediate. In *A. thaliana* and *M. truncatula* the transposition is mostly activated upon biotic or abiotic stresses and during *in vitro* culture phases (Hirochika et al., 2000; Courtial et al., 2001; d'Erfurth et al., 2003). Retrotransposons are useful for insertional mutagenesis, because they transpose efficiently into genes and do not insert near to their integration site. The insertions are stable during the plant life cycle and they follow a mendilian segregation (d'Erfurth et al., 2003). Up to now, there are 9000 *M. truncatula* R108 *Tnt1* mutant lines available, including 4 to 30 insertions of tobacco retrotransposon elements (*Tnt1*) per plant (Samuel Roberts Noble Foundation) (Courtial et al., 2001).

2 Aim

The intracellular colonization of root cortex cells of terrestrial plants by arbuscular mycorrhizal fungi (AMF) requires a profound reprogramming of both, host plant and AM fungus. However, fungal root colonization during arbuscular mycorrhizal symbiosis is asynchronous with continuous reinfection events occurring. Additionally arbuscules, the intracellular structures, have a limited life-span of only a few days and a permanent formation and degradation of arbuscules takes place within mycorrhizal roots leading to the presence of both, arbuscule-containing and non-colonized cells in a root system. Thus, unraveling the reprogramming of root cells during the AM symbiosis, requires cell type-specific analyses. In this work, a transcriptome profiling with increased spatial resolution was achieved by coupling Laser Capture Microdissection with microarray analysis. For this purpose, arbuscule-containing (arb) cells and non-arbuscule-containing (nac) cells were sampled from *Rhizophagus irregularis*-inoculated *Medicago truncatula* roots. As control, cortex (cor) cells of non-mycorrhizal roots were analyzed. The transcriptome reprogramming of the two mycorrhizal cell types was analyzed with a particular focus on the transcriptional regulation of transcription factor (TF) encoding genes.

The transcriptional regulation of selected TF genes had to be confirmed by quantitative RT-PCR using RNA samples of the three cell types (arb, nac, cor). Also promoter-reporter fusions were applied to confirm the cell type-specific expression of selected TF genes.

To unravel the role of selected TF genes during AM symbiosis, expression perturbation experiments were carried out. For this purpose, gene knock-down experiments and analysis of *Tnt1* mutant phenotypes were conducted.

Further, alteration in diagnostic marker transcript levels, like the expression of a AM specific phosphate transporter, were investigated to achieve information about the influence of the TF knock-down on the AM symbiosis.

TF genes affecting the AM symbiosis development or functioning, had to be further characterized concerning their time course of gene expression and response to phosphate fertilization. Moreover, if applicable, upstream elements or downstream targets as well as putative interaction partner were identified.

Taken together, the aim of this approach was to obtain a cell type-specific expression data set of TF genes in mycorrhizal roots. Moreover, the detailed function of selected TF genes during AM colonization had to be unraveled.

3 Materials and Methods

3.1 Materials

3.1.1 Enzymes and Kits

Advantage® 2 Polymerase	*Clontech*, Heidelberg, Germany
DNA T4-Ligase Kit	*Promega*, Mannheim, Germany
Gateway® LR Clonase™ II Enzyme Mix	*Life Technologies*, Darmstadt, Germany
GoTaq® Flexi DNA Polymerase	*Promega*, Mannheim, Germany
InviTrap® Spin Plant RNA Mini Kit	*Stratec*, Berlin, Germany
Lysozym	*Carl Roth*, Karlsruhe, Germany
Maxima™ SYBR Green qPCR Master Mix	*Thermo Fisher Scientific*, Henningsdorf, *Germany*
MultiScribe™ Reverse Transcriptase	*Life Technologies*, Darmstadt, Germany
pENTR™/D-TOPO® Cloning Kit	*Life Technologies*, Darmstadt, Germany
Phusion® HF DNA-Polymerase	*Thermo Fisher Scientific*, Henningsdorf, Germany
Proteinase K	*Life Technologies*, Darmstadt, Germany
QIAshredder (50)	*Qiagen*™, Hilden, Germany
RevertAid™ Reverse Transcriptase	*Thermo Fisher Scientific*, Henningsdorf, Germany
RiboLock™ RNase inhibitor	*Thermo Fisher Scientific*, Henningsdorf, Germany
RNA 6000 Pico LabChip Kit	*Agilent*™, Berlin, Germany
RNase A	*Thermo Fisher Scientific*, Henningsdorf, Germany
RNeasy® MicroKit	*Qiagen*™, Hilden, Germany
Superscript® II Reverse Transcriptase	*Life Technologies*, Darmstadt, Germany
TURBO DNA-*free*™ Kit	TURBO DNA-*free*™ Kit
WGA Alexa Fluor® 488	*Life Technologies*, Darmstadt, Germany
Wizard® SV Gel Clean-Up System	*Promega*, Mannheim, Germany
WT-Ovation™_One-Direct amplification system	*NuGen*®, Leek, Netherlands

3.1.2 Antibiotics

All antibiotics were obtained from *Duchefa Biochemie B.V.* (Haarlem, Netherlands).

Table 1: Antibiotics

Antibiotic	Concentration	Target organism
Ampicillin	100 µg/ml	*Escherichia coli*
Carbenicillin	50 µg/ml	*Agrobacterium tumefaciens*
Kanamycin	25 µg/ml	*Medicago truncatula*
Kanamycin	50 µg/ml	*Escherichia coli*
Rifampicin	100 µg/ml	*Agrobacterium tumefaciens*
Spectinomycin	100 µg/ml	*Escherichia coli*
Streptomycin	600 µg/ml	*Agrobacterium rhizogenes*

3.1.3 Primer

Oligonucleotides were designed to generate RNA-interference (RNAi) constructs *via* restriction and ligation based cloning. For this purpose, the primers include restriction enzyme sites (highlighted in green). Overlapping primers (I and II or III and IV) were designed for the amplification of miRNA5204*, as described by Devers et al., 2013. The oligonucleotides contain the miRNA star strand sequence (III and IV) and the sequence complementary to the star strand (I and II) (labeled in red). All primers were ordered by *Eurofins MWG Operon*, Ebersberg, Germany as desalted oligonucleotides.

***MtGras8-RNAi* constructs:**

BamHI-MtGras8 3´UTR sense for	5´ATGGACGGATCCTTAGGATCACAGCGATTGGT
Acc65I-MtGras8 3´UTR sense rev	5´ATGCTGGGTACCGTCATCACTTTATTTCTGCTCC
MluI-MtGras8 3´UTR antisense for	5´TCAGGAACGCGTTTAGGATCACAGCGATTGGT
BspEI-MtGras83´UTR antisense rev	5´TGACTGTCCGGAGTCATCACTTTATTTCTGCTCC

Amplification of miRNA5204*:

amir backbone A:	5´CTGCAAGGCGATTAAGTTGGGTAAC
amir backbone B:	5´GCGGATAACAATTTCACACAGGAAACAG
Primer I:	5´GTTCCCTCAAAGGCTTCCAGTATAAATTGGACACGCGTCT
Primer II:	5´TTATACTGGAAGCCTTTGAGGGAACAAAAAGATCAAGGC
Primer III:	5´TTATACTGGAAGAATTTGAGGGCTCTAAAAGGAGGTGATAG
Primer IV:	5´TAGCCCTCAAATTCTTCCAGTATAATTAGGTTACTAGT

All other nucleotides are enlisted in the appendix (see chapter 9.4 table 13)

3.1.4 Plasmids

Table 2: Plasmids

Vector	Resistence bacteria	Resistence plants	Reference
pENTR™/D-TOPO®	Kanamycin	----------	*Life technologies*, Darmstadt, Germany
pCR2.1-TOPO® vector	Ampicillin	----------	*Life technologies*, Darmstadt, Germany
pGWB433	Spectinomycin	P_{NOS}:NPTII (kanamycin)	Nakagawa *et al.*, 2007b
pKDsRed-RNAi	Spectinomycin	P_{NOS}:NPTII (kanamycin)	Dr. Igor Kryvoruchko, Ardmore, Oklahoma, USA
pKDsRed-GFPi	Spectinomycin	P_{NOS}:NPTII (kanamycin)	Dr. Igor Kryvoruchko, Ardmore, Oklahoma, USA
pRED-UBQ3-exp	Spectinomycin/ streptomycin	P_{NOS}:NPTII (kanamycin)	AG Krajinski MPIMP, Golm 2011
pRED-Pt4-RNAi	Spectinomycin/ Streptomycin	P_{NOS}:NPTII (kanamycin)	AG Krajinski MPIMP, Golm 2011
pRED-Pt4-exp	Spectinomycin/ Streptomycin	P_{NOS}:NPTII (kanamycin)	AG Krajinski MPIMP, Golm 2011
pBluescriptSKII(+) including miRNA159b	lacZ	----------	*Agilent*™, Waldbronn, Germany
pE-SPYCE-GW	Ampicillin/ Carbenicillin	----------	(Walter et al., 2004)
pE-SPYCE-GW	Ampicillin/ Carbenicillin	----------	Walter et al., 2004

(Walter et al., 2004)

3.1.5 Buffer compositions

RNA isolation

RNA extraction buffer (adjusted to pH 7.0)	Guanidinium chloride	26.0 M
	EDTA	20 mM
	MES	20 mM

RNA gelelectrophoresis

Denaturation buffer	Formamide	100 µl
	Formaldehyde	38 µl
	10 x MOPS buffer	20µl
	H_2O DEPC	42 µl
Denaturating gel	Agarose	0.72 g
	DEPC treated H_2O	42 ml
	Formaldehyde	12 ml
	10 x MOPS buffer	6 ml
RNA-loading buffer	Bromphenol blue 6 x	99 µl
	EtBr 10 mg/ml	9 1 µl

Genomic DNA isolation

CTAB buffer (pH 8.0)	CTAB (N-Cetyl-N,N,N- Trimethyl- ammoniumbromid)	2.0 % [w/v]
	NaCl	1.40 M
	Tris-HCl (adjusted to pH 8.0)	10 mM
	EDTA (adjusted to pH 8.0)	20 mM
	PVP	1.0 %

Plasmid preparation

Solution I	Glucose	50 mM
	Tris-HCl (adjusted to pH 8.0)	25 mM
	EDTA (adjusted to pH 8.0)	10 mM
	Lysozym	5 mg/ml
Solution II	NaOH	20 mM
	SDS	1.0 % [w/v]
Solution III	Potassium acetate	3.0 M
	Acetic acid	5.0 M

Agarose gel electrophoresis

Agarose gel	Agarose	1.5 % [w/v]
		2.0 % [w/v]
EtBr bath	EtBr	0.01 %
	0.5 x TAE	50 ml
1 x TAE buffer (pH 8.0)	Tris-acetate	40 mM
	EDTA (adjusted to pH 8.0)	1mM

Gus staining

Gus staining buffer	Sodium phosphate buffer (pH 7.0)	100 mM
	$K_3[Fe(CN)_6]$	1 mM
	$K_4[Fe(CN)_6] \times 3H_2O$	1 mM
	EDTA (adjusted to pH 8.0)	10 mM
	25 mg X-Gluc dissolved in 250 µl NN-dimethyl formamide	0.5 mg/ml

Staining of fungal structures

wheat germ agglutinin (WGA) Alexa Fluor® 488 staining solution	50 µl WGA Alexa Fluor® 488 diluted in 10 ml 1x PBS	0.01 g/ml

Additional buffers

Citrate buffer (pH 6.5)	Citric acid anhydrous (1.92 mg/ml ddH_2O)	10 mM
DEPC-H_2O	Diethylpyrocarbonate (1µl/ml ddH_2O)	0.1 % [v/v]
MES-KOH buffer (pH 5.6)	19.5 g MES dissolved in 100 ml ddH_2O adjust pH to 5.6 by adding KOH	1 M
10 x MOPS buffer (pH 7.0)	3-(N-morpholino) propanesulfonic acid	400 mM
	NaOAc	100 mM
	EDTA	10 mM
1 x PBS buffer	NaCl	137 mM
	KCl	2.7 mM
	Na_2HPO_4	12 mM
TE buffer (pH8.0)	Tris-HCl	10 mM
	EDTA (adjusted to pH 8.0)	1 mM
Tris buffer (pH7.0)	Tris	50 mM
	NaCl	150 mM

3.1.6 Media

3.1.6.1 Bacterial growth media

AS medium (pH 5.6)	$MgCl_2$	10 mM
	MES-KOH buffer	10 mM
	Acetosyringone (dissolved in DMSO)	150 µM
LB medium (pH 7.0)	Bacto™Tryptone	10 g/l
	Yeast extract	5.0 g/l
	NaCl	10 g/l
	Bacto™ agar	15 g/l
YEB medium (pH 7.2)	Beef extract	5.0 g/l
	Yeast extract	1.0 g/l
	Peptone	5.0 g/l
	Sucrose	15.0 g/l
	Bacto™ Agar	15 g/l
	$MgCl_2$	0.5 g/l

3.1.6.2 Plant growth media and fertilizer

Fahraeus medium (Barker et al., 2006)

Macroelements: 0.5 mM MgSO4 x $7H_2O$, 0.7 mM KH_2PO_4, 0.8 mM Na_2HPO_4x H_2O, 1.0 mM Fe-EDTA, 0.5 mM NH_4NO_3, 1.0 mM $CaCl_2$; Microelements: $MnSO_4$ x H_2O, $CuSO_4$, $ZnSO_4$ x H_2O, H_3BO_3, Na_2MoO_4 x H_2O 1 mg/ml each

M-Medium (Becard and Fortin, 1988)

Macroelements: 3.0 mM $MgSO_4$ x $7H_2O$, 0.79 mM KNO_3, 0.87 mM KCl, 1.22 mM $Ca(NO_3)_2x4H_2O$, 35.0 µM KH_2PO_4, 21.7 µM NaFe-EDTA, 4.5 µM KJ, 30.3 µM $MnCl_2$ x $4H_2O$; Microelements: 9.2 µM $ZnSO_4$ x $7H_2O$, 24.0 µM H_3BO_3, 0.5 µM $CuSO_4$ x $5H_2O$, 0.01 µM Na_2MoO_4 x $2H_2O$; Vitamins: 40.0 µM Glycin, 0.3 µM Thiamin HCl, 0.5 µM Pyridoxin HCl, 4.0 µM Nicotinic Acid, 27 µM Myo-Inositol, 10 g/l Sucrose, 4 g/l Phytagel

0.5 x Hoagland´s solution (Hoagland and Arnon, 1950)

Macroelements: 2.5 mM $Ca(NO_3)_2$ x $4H_2O$, 2.5 mM KNO_3, 1.0 mM $MgSO_4$ x $7H_2O$, 20 µM KH_2PO_4, 50 µM NaFe-EDTA, 0.2 µM Na_2MoO_4 x $2H_2O$; Microelements: 10 µM H_3BO_3, 0.2 µM $NiSO_4$ x $6H_2O$, 1.0 µM $ZnSO_4$ x $7H_2O$, 2.0 µM $MnCl_2$ x $4H_2O$, 0.5 µM $CuSO_4$ x $5H_2O$, 0.2 µM $CoCl_2$ x $6H_2O$

3.1.7 Organisms

Table 3: Organisms

Organism	Cultivar /strain	Source
Agrobacterium rhizogenic	*ARqua1*	Quandt et al., 1993
Agrobacterium tumefaciens	*GV2260*	Deblaere et al., 1985
Allium schoenoprasum	*Forescate*	*Quedlinburger Saatgut*, Quedlinburg Germany
Dauctus carota incl. *Rhizophagus irregularis* T-DNA (root organ culture)	propagated from culture 'B' (IRBV'95)	*University of Guelph*, Ontario, Canada
Escherichia. coli	*DH5-α*	*Thermo Fisher Scientific*, Henningsdorf, Germany
Escherichia. coli	*TOP10*	*Thermo Fisher Scientific*, Henningsdorf, Germany
Medicago truncatula	Jemalong A17	*MPIMP*, Golm, Germany
Medicago truncatula	*R108*	*MPIMP*, Golm, Germany
Nicotiana benthamiana	*TW16*	*MPIMP*, Golm, Germany
Rhizophagus irregularis	*BB-E*	*Agrauxine*, Dijon, France

3.1.8 Software

Affymetrix annotations	NetAffyx™ Analysis Center	http://www.affymetrix.com/analysis/index.affx
Database of *Arabidopsis thaliana* transcription factors		http://datf.cbi.pku.edu.cn/browsefamily
EST and TC annotation software	DFCI-Plant Gene Indices	http://compbio.dfci.harvard.edu/tgi/plant.html
Identification of *M. truncatula* BACs	NCBI	http://www.ncbi.nlm.nih.gov/
Image processing software	Adobe Photoshop CS2	http://www.adobe.com/de/products/photoshop/family/
Laser microdissection software	P.A.L.M.® Robosoftware 1.2	*P.A.L.M Microlaser technologies*, Bernried, Germany
Medicago gene annotation software	Urmeldb	http://mips.helmholtz-muenchen.de/plant/medi/
M. truncatula expression data altas	Medicago Gene Expression Atlas	http://mtgea.noble.org
M. truncatula mutant data base	Noble Foundation	http://bioinfo4.noble.org/blast/
Phylogenetic analysis	Phylogeny.fr	http://www.phylogeny.fr
Phylogenetic analysis	TreeDyn198	http://www.phylogeny.fr/
Primer design	Perlprimer 1.1.21	http://perlprimer.sourceforge.net/
qRT-PCR software	SDS2.4 Software	*Life Technologies*, Darmstadt, Germany
Secondary structure prediction of small RNAs	UEA sRNA toolkit	http://srna-tools.cmp.uea.ac.uk/
Sequence analysis and alignment	Lasergene Core Suite 10	http://www.dnastar.com/t-products-lasergene.aspx

Statistical data analysis and graphs	SigmaPlot12®	http://www.sigmaplot.co.uk/products/sigmaplot/
Statistical microarray analysis	Robin®	http://mapman.gabipd.org/web/guest/robin
Visualization and categorization of microarray data in metabolic maps	MapMan®	https://gabi.rzpd.de/projects/MapMan/

3.2 Methods

3.2.1 Plant cultivation

3.2.1.1 Seed sterilization and cultivation of *Medicago truncatula*

Medicago truncatula seeds were incubated in concentrated H_2SO_4 for 14 min to crack the seed coat and were washed eight to ten times with ddH_2O. The seeds were surface sterilized in 1 ml of 6 % NaOCl solution for three minutes and washed three times with ddH_2O before they were plated on water agar plates. The germination was stimulated by incubation the seeds for two days at 4 °C in darkness, followed by one day at room temperature (in darkness).

A substrate consisting of equal amounts of sand (0.6-1.8 mm diameter), clay and vermiculite was used for greenhouse and phytotrone plant cultivation. Inoculation of plants with *R. irregularis* was enabled by adding substrate of an *A. schoenoprasum* culture in a 1:10 ratio. The seedlings were cultivated in green house (21 °C, 16 h light, 8 h darkness and 60 % humidity). Two times per week the plants were fertilized with half strength Hoaglands solution (containing 20 µM phosphate) (see chapter 3.1.6.2). After 21 days, the plants were harvested. Fresh root material was used for staining of fungal structures and establishment of cryosections (see chapter 3.2.2, 3.2.3), while RNA samples were prepared from roots that were immediately frozen in liquid nitrogen.

For seed production of *M. truncatula* R108 tobacco retrotransposon (*Tnt1*) mutants were cultivated in the green house for 3 months (21 °C, 16 h light, 8 h darkness and 60 % humidity). Homozygous mutant lines were obtained after two selfing generations. Each generation was screened for homozygous or heterozygous plants by PCR (chapter 3.2.12.1). The seeds of homozygous and heterozygous plants were harvested separately. For phenotypic analyses, 20 homozygous *Tnt1* mutant and 20 wild type plants (carrying a *Tnt1* insertion not in the *MtErf2* gene) were cultivated for 21 days, as described above, and fertilized with half strength Hoaglands solution containing 250 µM phosphate. Half of the plants were inoculated with *R. irregularis*. Roots and shoots were separately harvested to determine their fresh weights. The roots were divided in two representative parts required for RNA extraction and wheat germ agglutinin (WGA) Alexa Fluor® 488 staining (chapter 3.1.5) to verify the abundance of fungal structures, as described by Trouvelot et al., (1986).

3.2.1.2 Cultivation of *Nicotiana benthamina* for leave infiltration

Nicotiana benthamiana cv. TW16 plants were grown in the phytotrone (22 °C, 16 h day / 8 h night conditions and 60 % humidity) for six weeks. The opening of the stomata was conducted by watering the plants directly before leaf infiltration.

3.2.2 Visualization of fungal structures *via* WGA Alexa Fluor® 488 staining

The staining of fungal structures with WGA Alexa Fluor® 488 is enabled by binding a wheat germ agglutinin coupled fluorophore to the chitin elements in the fungal cell walls (Peters and Latka, 1986). Fresh root material was incubated in 10 % KOH solution at 90 °C for 7 min and neutralized by washing the material with 1 x PBS buffer. Afterwards the roots were covered with WGA Alexa Fluor® 488 staining solution (see chapter 3.1.5) and stored over-night at room temperature in darkness. After washing the roots with ddH_2O, 30 root fragments were mounted on microscope slides (*Paul Marienfeld GmbH&CoKG*, Lauda-Königshofen, Germany). The abundance of fungal structures was verified, as described by Trouvelot et al., (1986) using an epifluorescence microscope (Olympus BX51TF-5, Olympus, Hamburg, Germany) and a wavelength excitation of 488 nm.

3.2.3 Establishment of cryosections from *Medicago truncatula* roots

For Laser Capture Microdissection (LCM) approaches, cryosections from three-week-old mycorrhizal and non-mycorrhizal *M. truncatula* A17 roots were established using the Leica CM1950 cryostat (*Leica*, Wetzlar, Germany). The glassware was baked at 180 °C over-night and washing solutions were prepared with DEPC treated water to inactivate RNases.

Longitudinal sections of 35 µm of thickness were generated by freezing 1 cm long root fragments in TFM™ tissue freezing medium (*Science Service*, Munich, Germany) at -22 °C, as described by Gaude et al., (2012). The sections were mounted on UV-treated Poly-L-lysine covered microscope slide (*Poly-Prep Slides*, *Sigma-Aldrich*, Seelze, Germany). The sticky surface of Poly-L-lysine residues prevents the loss of sections during the following washing steps. LCM is hampered by trace amounts of tissue freezing medium. Accordingly, the slides were washed in three steps. First, the slides were incubated in 70 % ethanol (DEPC treated) for 2-3 min before the embedding medium was washed out with ddH_2O for 30 min. Upon incubation the sections in 96 % ethanol for 2-3 min, the ethanol was evaporated by storing the slides on a heating plate (Präzitherm, *Störk-Tronic*, Stuttgart, Germany) at 37 °C for 30 min. Afterwards the slides were stored in slide boxes (*Carl Zeiss Micro Imaging*, Bernried, Germany) at –80 °C.

3.2.4 Laser Capture Microdissection of *Medicago truncatula* cortical cells

To prevent water condensation and RNA degradation processes, microscope slides were thawed stepwise thawed from -80 °C (4 °C for 30 min, followed by incubation at room temperature for 30 min). *Via* the P.A.L.M.® Robosoftware 1.2 (*P.A.L.M Microlaser technologies*, Bernried, Germany) the laser function "Auto-LPC" was choosen for microdissection, as described by Gaude et al., (2012). With this laser function, the cells were dissected by applying numerous of defocused laser spots on one cell. Although the cell structures were destroyed, the nucleic acids, proteins and metabolites were not negatively influenced, because the UV-laser ablation wavelength does not correspond to the absorption wavelength of the analytes (see chapter 1.2). Dissected cells were catapulted *via* the photon-pressure of a laser beam into the lid of a collection tube (adhesive caps 500 clear, *Carl Zeiss Micro Imaging*, Bernried, Germany) (P.A.L.M.® Microbeam manufacturer´s manual-02027, 2003).

This method enabled the sampling of arbuscule-containing cells (arb cells) and non-arbuscule-containing cortical cells (nac cells) from *R. irregularis* inolucated *M. truncatula* roots. As control, cortical cells from non-inoculated *M. truncatula* roots (cor cells) were isolated. Around 10000 cells were sampled per cell type and directly lysated by adding a mixture of 350 µl RLT buffer (Qiagen RNeasy® Micro, *Qiagen*™, Hilden, Germany), 8.75 µl RiboLock™ RNase inhibitor (40 U/µl) and 3.5 µl ß-mercaptoethanol. The cells were mixed for 1 min at room temperature, centrifuged (12000 rpm for 2 min) and lysated at 56 °C for 5 min. After repeating the centrifugation step, the cell lysate was stored at -80 °C.

3.2.5 RNA isolation methods

RNA was isolated from LCM samples using the Qiagen RNeasy® Micro Kit (*Qiagen*™, Hilden, Germany). Cell lysate samples were thawed on ice, mixed for 1 min and centrifuged at 12000 rpm for 1 min. To enrich and stabilize the RNA, 5 µl Carrier RNA (4 ng/µl) was added to each sample (RNeasy® Micro Kit, manufacturer´s manual). After 2 min incubation on ice, the cell lysate was transferred to QIAshredder columns (*Quiagen*™, Hilden, Germany) and was centrifuged, as described in the manual to separate cell walls from nucleic acids. After RNA isolation with the Qiagen RNeasy® Micro Kit, a DNA digest (with DNAseI) was performed, as described in the manufacturer´s manual (*Qiagen*™, Hilden, Germany). The RNA was eluted in 12-14 µl of RNase free water.

For the RNA extraction from whole roots, up to 100 µg root material was transferred into 2 ml tubes, containing a metal bowl. The samples were frozen in liquid nitrogen and the roots were grinded using a retch mill (Retsch® MM 200, *Retsch*®, Haan, Germany).

RNA of whole *M. truncatula* A17 roots was used as control for the cell type-specific qRT-PCR analysis. The RNA was isolated with the InviTrap® Spin Plant RNA Mini Kit (*Stratec*, Berlin, Germany), as described in the manufacturer´s manual and eluted in 40 µl elution buffer.

In case of guanidinium chloride (GdmCl)-based RNA extraction *via* the grinded root material was mixed with 500 µl RNA extraction buffer (see chapter 3.1.5) to prevent RNA degradation. Cell fragments were pelleted upon centrifugation at full speed for 10 min in a precooled centrifuge (4 °C). The supernatant was transferred into a new tube and was mixed with 450 µl Roti®- Phenol/Chloroform/Isoamyl alcohol solution (*Carl Roth*, Karlsruhe, Germany). After centrifugation in a precooled centrifuge at 3000 rpm for 10 min, the aqueous phase was transferred into a new tube and was mixed with 0.1 volume of 1 M acetic acid as well as 0.7 volumes of 96 % ethanol. The RNA was precipitated at room temperature for 30 min and pelleted by centrifugation at full speed for 30 min. Afterwards, 500 µl 70 % ethanol was added to wash the pellet. The remaining ethanol was removed by pipetting. Finally, the pellet was dried at 37 °C for 7 to 10 min, before the RNA was resuspended in 40 µl of nuclease free water and stored at – 80 °C.

3.2.6 RNA quantification and quality control

3.2.6.1 Quantification of whole root RNA samples *via* NanoDrop® analysis

RNA from whole roots was quantified by spectral photometric analysis using the NanoDrop® ND-1000 (*NanoDrop® products*, Willington, Delaware, USA), as described in the manufacturer´s manual. As a blank, the appropriate elution buffer or nuclease free water was used.

3.2.6.2 RNA-gel electrophoresis

A denaturating RNA gel (100 ml) was prepared, as described in chapter 3.1.5. The RNA was denaturated by incubating 3 µl denaturation buffer and 3 µl RNA at 65 °C for 10 min. The samples were chilled on ice for 1 min, before 1 µl RNA-loading buffer was added. Afterwards the gel was running for 30 min at 100 Volt in 1 x MOPS running buffer.

3.2.6.3 Quantification of cell type-specific RNA by microfluid chip analysis

Quantification of cell type-specific RNA was performed by microfluid chip analysis using the Agilent™ 2100 Bioanalyzer (*Agilent™*, Berlin, Germany). The method utilizes a voltage dependent separation of macromolecules based on their molecule size. The system consists of a chip, containing channels filled with a gel matrix. Fluorescence intensity of the dye correlates with the RNA concentration of specific size (Schroeder et al., 2006). As an indicator for the RNA quality, the proportion of degraded RNA in relation to total RNA concentration is given as a RNA Integrity Number (RIN) (numbers between 1 and 10). While a RIN of 1 represents totally degraded RNA, a RIN of 10 indicates an intact RNA sample (Schroeder et al., 2006). For this

work a "RNA 6000 Pico LabChip Kit" (*Agilent™*, Berlin, Germany) was used, which enables the separation of RNA in 50-5000 pg concentrations and the "RNA 6000 ladder" consisting of a mixture of RNA transcripts (0.2, 0.5, 1.0, 2.0, 4.0 and 6.0 kb length) (*Agilent™*, Berlin, Germany). After denaturation of the ladder and RNA samples (70 °C for 2 min), the measurements were performed, as described in the manufacturer´s manual.

3.2.7 DNAse digest of whole root RNA *via* TURBO DNA-*free*™ Kit

The DNAse digests were performed in a 20 µl volume at 37 °C for 25 min, according to the manufacturer´s instructions (TURBO DNA-*free*™ kit, *Life Technologies*, Darmstadt, Germany).

3.2.8 Affymetrix GeneChip® Medicago genome array hybridization

Up to three RNA samples were pooled per cell type to achieve a concentration of 50-100 ng. Atlas Biolabs (Berlin, Germany) performed the linear-isothermal amplification and cDNA synthesis with the WT-Ovation™_One-Direct amplification system (*NuGen®*, Leek, Netherlands). Finally, around 3 µg defragmentated and biotin-labeled cDNA were obtained per cell type and applied to the microarray hybridization. Two microarray hybridizations were performed per cell type, as described by Gaude et al., (2012).

3.2.9 Reverse transcription of whole root and cell type-specific RNA

Upon RNA isolation of 20000 cells (two pooled samples), 11 µl RNA (50-100 ng) were reverse transcribed into cDNA by using the Superscript II™ Kit (*Life Technologies*, Darmstadt, Germany). The cDNA synthesis was performed in a 20 µl volume, as described in the manufacturer´s manual. As control 50 ng of DNAse digested whole root RNA was reverse transcribed into cDNA, as described in the following.

The RevertAid™ Reverse Transcriptase Reverse mediated the reverse transcription of 1 µg DNAse digested RNA obtained from whole roots (*Thermo Fisher Scientific*, Henningsdorf, Germany). The reaction was performed in a 20 µl volume, as described according to the manufacturer´s manual.

Stem-loop cDNA synthesis of 1 µg DNAse digested RNA was performed *via* MultiScribe™ Reverse Transcriptase (*Life Technologies*, Darmstadt, Germany) in a 25 µl volume, as described by Devers et al, (2011).

3.2.10 qRT-PCR analysis

The qRT-PCR analysis was performed in 10 µl reactions. In the case of whole root cDNA samples, the cDNA was diluted 1:10 and the gene expression was measured in two technical and three biological replicates.

Cell type-specific cDNA samples were not diluted. These samples derived from cells from different roots and cryosections and were analyzed in two technical replicates.

For the analysis of microRNA (miRNA) expression levels stem-loop qRT-PCR primers were designed, as described by Devers et al., (2011).

Maxima™ SYBR Green qPCR Master Mix (2x) (*Thermo Fisher Scientific*, Henningsdorf, Germany) was used as detector agent for qRT-PCR measurements. The cDNA mastermix included 4 µl of Maxima™ SYBR-Green qPCR Master Mix (2x) (*Thermo Fisher Scientific*, Henningsdorf, Germany) per 1 µl cDNA, and the primer mastermix consisted of 4 µl of 0.5 µM gene specific primers and 1 µl Maxima™ SYBR-Green qPCR Master Mix (2x) (*Thermo Fisher Scientific*, Henningsdorf, Germany). For the measurements, 5 µl of each mastermix were pipetted into a 384 well plate (MicroAmp® Optical 384 well reaction plate, *Life Technologies*, Henningsdorf, Germany). The qRT-PCR was carried out as described in table 4 with the ABI PRISM R 7900 HT fast Real-Time PCR system (*Life Technologies*, Darmstadt, Germany) including the SDS2.4 Software (*Life Technologies*, Darmstadt, Germany).

Table 4: PCR conditions for qRT-PCR measurements

Step	Temperature (°C)	Time (min)	
Initial denaturation	95	10	
Denaturation	95	15 seconds	40 cycles
Annealing	60	1	

A detection threshold of 0.2 was set. The relative expression values of target genes ($2^{-\Delta Ct}$ values) were calculated by normalization of the Ct values (Ct_{gene}) to the reference gene index (Ct_{HK}), representing a mean of *MtPdf2*, *MtEf1-α*, *MtUbiquitin*, and *MtGapdh* (Kakar et al., 2008) Ct values.

$$\Delta Ct = Ct_{gene} - Ct_{HK}$$

$$\text{relative expression} = 2^{-\Delta Ct}$$

The amount of genomic DNA in the cDNA samples was assessed using primers binding to an intron sequence of *MtUbiquitintron*. Additionally, the *MtPt4* transcript abundance gave an indication of the fungal colonization efficiency (Harrison et al., 2002) (see chapter1.1).

3.2.11 Preparation of constructs for plant transformation

3.2.11.1 Transformation of chemical competent *E. coli*

Aliquots (50 µl) of competent *E. coli TOP10* or *DH5-α* cells were thawed on ice for 10 min, before 3 µl of the appropriate destination vector were added. The bacteria were incubated on ice for 30 min, followed by a heat shock (42 °C for 45 sec) applied in a water bath. Immediately after the heat shock 250 µl LB medium without antibiotics was added. The bacteria were grown for 1.5 h at 37 °C shaking 200 rpm and 100 µl were transferred on LB medium with the appropriate selection agents.

3.2.11.2 Transformation of electrocompetent *Agrobacteria*

Competent *A. rhizogenes ARqua1* (Quandt et al., 1993) aliquots were thawed on ice for 10 min. The bacteria and 1-3 µl destination vector were transferred into a precooled electroporation cuvette (*PeqLab*, Erlangen, Germany) and incubated for 30 min on ice. For the electroporation an electric potential of 2500 Volt was applied for 5 seconds (Electroporator 2510, *Eppendorf*, Hamburg, Germany), before the bacteria were dissolved in 500 µl YEB medium without antibiotics and transferred into a fresh 1.5 ml tube. The bacteria were incubated at 28 °C on a shaker (>200 rpm) for 2 h, before 200 µl were transferred on YEB medium containing the appropriate antibiotics. Afterwards the cultures were grown at 28 °C for 2 days.

3.2.11.3 Preparation of standard Polymerase-Chain-Reactions (PCR)

Twenty microliter PCR reactions including GoTaq® Flexi DNA Polymerase (*Promega*, Mannheim, Germany) were prepared, as described in the manual to verify the *E. coli* and *Agrobacteria* colonies. The PCR was carried out as shown in table 5. In case of colony PCRs, a pipette tip was dipped into a bacteria colony and placed into the PCR reaction tube. Afterwards the pipette tip was transferred into 5 ml liquid media with the appropriate selection agents to enable the subcultivation of the bacteria at 37 °C (for *E. coli*) over-night or at 28 °C for 2 days (for *Agrobacteria*).

The amplification of promoter regions, untranslated regions (UTR) and full length genes as well as the *Tnt1* mutant screening was enabled by preparing 20 µl Advantage® 2 Polymerase reactions (*Clontech*, Heidelberg, Germany) as described in the manual. As template, 1 µl of 50 ng cDNA from mycorrhizal roots was added to each reaction.

The amplification was carried out as described in table 5 and the amplicons were verified by agarose gel electrophoresis, using a 1.5 % agarose a 1 kb Plus DNA Ladder (*Thermo Fisher Scientific*, Henningdorf, Germany).

Table 5: Standard PCR conditions. ^Elongation temperature for GoTaq® Flexi DNA Polymerase, ^^elongation temperature for Advantage® 2 Polymerase.

Step	Temperature (°C)	Time (min)	
Initial denaturation	95	2	
Denaturation	95	0.5	30 cycles
Annealing	55-62	1-3	
Elongation	^68 / ^^72	1min/1 kb	
Final elongation	^68 / ^^72	3	

3.2.11.4 Plasmid preparation from *E. coli* and *Agrobacteria*

Bacteria of a 5 ml liquid over-night culture were pelleted by centrifugation for 5 min at 8000 rpm. After discarding the medium and repeating the centrifugation step, the pellet was resuspended in 100 µl Solution I and 5 µl RNase A (10 mg/ml). The samples were incubated at room temperature for 5 min (in case of *Agrobacteria* 15 min), before 200 µl Solution II was added. After inverting the tubes and incubation on ice for 5 min, the lysates were mixed with 150 µl Solution III. After storing the samples on ice for 5 min, a centrifugation step at 13000 rpm for 10 min followed to separate the DNA from the cell fragments. The supernatant was transferred into a new tube, including 1000 µl of 96 % ethanol and 40 µl of 3 M sodium acetate (NaOAc). The plasmid DNA was precipitated at -20 °C for 30 min and pelleted by centrifugation for 5 min at 13000 rpm. After discarding the ethanol, the pellet was resuspended in 40 µl ddH_2O.

3.2.11.5 Genomic DNA isolation

Three leaves of four week old plants were harvested in a 1.5 ml tube containing glass pearls. The leaves were grinded after adding 1000 µl CTAB buffer and incubated in a thermomixer at 65 °C for 10 min. Afterwards 400 µl chloroform was added, the tubes were mixed and centrifuged at full speed for 5 min. The supernatant was transferred into a new tube, containing 700 µl isopropanol. After 10 min incubation on ice, the DNA was pelleted by centrifugating the samples at full speed for 5 min. The pellet was washed with 70 % ethanol, and resuspended in 50 µl nuclease free water.

3.2.11.6 *Agrobacteria*-mediated root transformation

Electrocompetent *A. rhizogenes ARqua1* (Quandt et al., 1993) were used to transform the roots of 2 day old *M. truncatula* seedlings, as described by (Boisson-Dernier et al., 2001). After cultering *Agrobactreria* in a liquid culture they were subcultured at 28 °C for 2 days on solid YEB medium, containing the appropriate antibiotics. Fourty seedlings were transformed per construct by dipping the wounded root tip into the *Agrobacteria* lawn (Boisson-Dernier et al., 2001). The *Agrobacteria* infected seedlings were incubated for two days on water agar plates at 24°C in darkness. Afterwards they were transferred to Fahraeus medium including 25 µg/ml kanamycin as selection

agent. The seedlings were grown in a climate chamber for three to four weeks (25 °C, 8 h day and 16 h night rhythm), before they were potted, as described in chapter 3.2.1.1. After additional three to four weeks the fluorescence marker gene expression of transgenic roots was verified by stereo microscopic analysis (Stereo microscope M37, *Leica*, Wetzlar, Germany).

3.2.11.7 Establishment of root organ cultures

Hairy roots obtained from *A. rhizogenes*-mediated root transformation can be subcultured in root organ cultures (ROCs) (Becard and Fortin, 1988). After the selection phase on Fahraeus medium (incl. 25 µg/ml kanamycin), hairy roots were identified by detection of fluorescence marker gene expression *via* stereo microscopy (*Leica*, Wetzlar, Germany) and were transferred on M-Medium plates (Becard and Fortin, 1988) containing 200 µg/ml β-Bactyl and 25 µg/ml kanamycin. Different roots obtained from one plant represent independent transformation events and were therefore subcultured as biological replicates. After two passages on M–Medium including selection agents the roots were transferred to M-Medium without antibiotics. The inoculation was carried out with *R. irregularis* spores, obtained from *D. carota* root organ cultures propagated from culture 'B' (IRBV'95) (*University of Guelph*, Ontario, Canada). Three months after inoculation colonized ROCs were harvested. The roots were washed with citrate buffer (pH 6.5) to remove the medium and divided into two representative samples. A sample of each ROC was frozen in liquid nitrogen for RNA isolation and the other part was sampled for trypan blue staining to monitor the abundance of fungal structures as described by Trouvelot et al., 1986.

3.2.11.8 Establishment of expression vectors with the Gateway® Cloning system

The establishment of promoter::*uidA* fusion constructs, RNAi constructs and expression vectors for the Bimolecular Fluorescence Complementation (BiFC) was mediated by the Gateway® Cloning system. Target sequences (promoters and UTR) were amplified by Advantage®2 Polymerase, as described in the manual (*Clontech*, Heidelberg, Germany). pENTR™/D-TOPO® vectors were established by using the pENTR™/D-TOPO® Cloning Kit (*Life Technologies*, Darmstadt, Germany), according to the manufacturer´s instructions. The clones were verified by PCR with gene specific primers and sequenced using "M13" and "SeqL-E" sequencing primers (*LGC* genomics, Berlin, Germany). Gateway® LR Clonase™ II Enzyme Mix reaction were performed, as described in the manufacturer´s instructions (*Life Technologies*, Darmstadt, Germany) to enable the recombination of positive entry clones with the destination vectors (e.g. pGWB433, pE-SPYNE-GW pE-SPYCE-GW and pKDsRed-RNAi). The expression vectors were verified by PCR. Expression of the constructs in *M. truncatula* roots was facilitated by *Agrobacteria*-mediated root transformation, as described in chapter 3.2.11.6.

3.2.11.9 Localization promoter GUS activity of transcription factors in mycorrhizal roots

Significantly, differentially expressed transcription factors (TFs) were identified upon Affymetrix GeneChip® Medicago genome array hybridization and MapMan® annotation. Twenty microliter Advantage® 2 Polymerase (*Clontech*, Heidelberg, Germany) was used to amplify promoter sequences of 1 kb length, located upstream of the start codons. One microgram of *M. truncatula* A17 genomic DNA was used as template. The recombination of the entry vectors with the pGWB433 expression vector (Nakagawa et al., 2007) was carried out with the Gateway® Cloning system. Transformed *M. truncatula* seedlings were grown for 28 days in the phytotrone (see chapter 3.2.1.1). GUS activity was visualized in mycorrhizal roots after incubation in GUS-staining buffer (see chapter 3.1.5) over-night. Roots with strong GUS activity were embedded in 4 % agarose and 50 µm longitudinal vibratome sections were obtained using the vibrating blade vibratome (Leica VT 1000S, *Leica*, Wetzlar, Germany). The root sections were incubated for 30 min in WGA Alexa Fluor® 488 staining solution and washed in ddH_2O, before they were mounted on microscope slides. Fungal structures were analyzed by epifluorescence microscopy (Olympus BX51TF-5, *Olympus*, Hamburg, Germany). WGA Alexa Fluor® 488 fluorescence was induced by using an excitation wavelength of 488 nm and the GUS activity was observed in the bright field channel. To enable the co-localization of arbuscules and GUS activity, overlay images were created with the Photoshop CS2 software (http://www.adobe.com/de/products/photoshop/family/).

3.2.11.10 Bimolecular Fluorescence Complementation

The protein-interactions of MtGRAS8 and MtNSP1, MtNSP2 with MtRAM1 were verified by Bimolecular Fluorescence Complementation (BiFC) analysis. The protein-interaction between MtNSP1 and MtNSP2 as well as the interactions of two *Arabidopsis thaliana* TCP transcription factors, AtTCP11 (At5g51910) and AtTCP19 (At5g08330) (provided by Jozefus Schippers, MPI of Molecular Plant Physiology, Potsdam, Germany) were used as positive controls (Hirsch et al., 2009; Arabidopsis Interactome Mapping, 2011). As a negative control, the E2-ubiquitin conjugase MtPHO2 was fused to either a C-terminal or N-terminal portion of Yellow Fluorescence Protein (YFP). Full length sequences of MtGRAS8, MtNSP1, MtNSP2, MtRAM1 and MtPHO2 (Medtr2g013650.1) were amplified *via* Phusion® HF DNA-Polymerase (*Thermo Fisher Scientific*, Henningsdorf, Germany), as described in the manufacturer´s instructions. For this purpose cDNA from mycorrhizal and nodulated *M. truncatula* A17 roots was used as template. Upon establishment of pENTR™/D-TOPO clones, a C-terminal fusion of the target genes to C-terminal or N-terminal portion of the YFP sequence was enabled by recombination of the clones with the Gateway® compatible pE-SPYCE-GW and pE-SPYNE-GW vectors (Walter et al., 2004) (see figure 4).

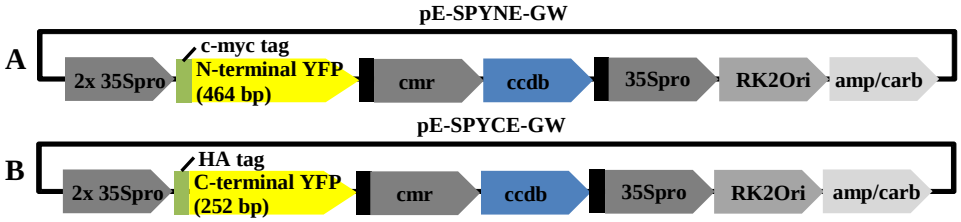

Figure 4: Scheme of A) pE-SPYNE-GW and B) pE-SPYCE-GW vectors (based on Walter *et al.*, 2004). 2x35Spro: double *35S* promoter, 35Spro: *35S* promoter, cmr: chloramphenicol resistance, ccdb: ccdb gene RK2 Ori: origin of replication for *Agrobacteria*, amp: ampicillin resistance, carb: carbenicillin resistance.

Transformed *E. coli* were selected on LB medium containing 100 µg/ml ampicillin. Positive clones were identified by colony PCR with target gene specific primers and sequencing, using a forward primer binding in the Yellow Fluorescence Protein (YFP) sequence and a reverse primer binding in the target gene sequence. The expression vectors were transformed into electrocompetent *A. tumefaciens* GV2260 (see chapter 3.2.11.2) to enable the transient expression in *Nicotiana benthamiana* leaves.

3.2.11.10.1 Agrobacterium tumefaciens-mediated tobacco leaf infiltration

A liquid culture consisting of 10 ml YEB medium (incl. 100 µg/ml rifampicin and 50 µg/ml carbenicillin) and 80 µl of *A. tumefaciens* GV2260 containing the BiFC constructs was grown at 28 °C over-night, before the bacteria were prepared, as described by Yang *et al.*, (2001). The bacteria were pelleted by centrifugation for 15 min at 4000 rpm and diluted in fresh AS-medium (see chapter 3.1.6.1) until an OD_{600} of 1.0 was achieved. Before the leaf infiltration was started the bacteria were grown for 2-3 h at room temperature. For the co-infiltrations the appropriate bacteria solutions (table 6) were mixed in a 1:1 ratio. Around 500 µl were injected *via* a sterile 1ml syringe (1ml NORM-JECT®, *Henke-Sass, Wolf GmbH*, Tuttlingen, Germany) into leaves (abaxial) of six-week-old well watered *N. benthamiana* plants. Three days after the infiltration the YFP fluorescence was monitored *via* confocal microscopy (Leica TCP SP5 confocal microscope, *Leica*, Wetzlar, Germany) using a wavelength excitation of 514 nm (argon laser).(Yang et al., 2001)

Table 6: Co-infiltration of BiFC constructs in *Nicothiana benthamina* leaves

SPYNE	SPYCE
**YFP^{N} -TCP1*	**YFP^{C} -TCP2*
**YFP^{N} -TCP2*	**YFP^{C} -TCP1*
**YFP^{N} -MtNSP1*	**YFP^{C} -MtNSP2*
**YFP^{N} -MtNSP2*	**YFP^{C} -MtNSP1*
YFP^{N} -MtGras8	*YFP^{C} -MtNSP2*
YFP^{N} -MtNSP2	*YFP^{C} -MtGras8*
YFP^{N} -MtGRAS8	*YFP^{C} -MtNSP1*
YFP^{N} -MtNSP1	*YFP^{C} -MtGras8*
YFP^{N} -MtRAM1	*YFP^{C} -MtNSP2*
YFP^{N} -MtNSP2	*YFP^{C} -MtRAM1*
***YFP^{N} -MtPHO2*	***YFP^{C} -MtGras8*
***YFP^{N} -MtGras8*	***YFP^{C} -MtPHO2*
***YFP^{N} -MtPHO2*	***YFP^{C} -MtNSP2*
***YFP^{N} -MtNSP2*	***YFP^{C} -MtPHO2*
***YFP^{N} -MtPHO2*	***YFP^{C} -MtRAM1*
***YFP^{N} –MtRAM1*	***YFP^{C} -MtPHO2*

(*) positive controls and negative controls (**) are labeled.

3.2.11.11 Expression of *35S* promoter-driven RNA-interference constructs

The functional characterization of *MtGras8* was mediated by expression of a RNA-interference (RNAi) construct under the control of a *35S* in *M. truncatula* roots. For this purpose, the Gateway® compatible pKDsRed-RNAi vector (Dr. Igor Kryvoruchko, Ardmore, Oklahoma, USA) was used. The vector contains a DsRed fluorescence marker gene (obtained from pRedRoot vector), which is N-terminally fused to the RNAi cassette, as well as resistance genes for selection in bacteria (streptomycin and spectinomycin resistance) and for plant selection (*nptII*) (see figure 5). An intron sequence of an *A. thaliana* chalcone synthase gene located between the sense and antisense orientated 3´UTRs enables the formation of a hairpin structure. The vector control contained a 327 bp long fragment of the GFP gene (pCAMBIA1302) (Dr. Igor Kryvoruchko, Ardmore, Oklahoma, USA).

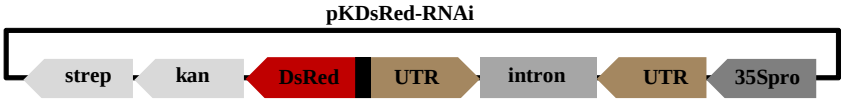

Figure 5: Scheme of pKDsRed-RNA-interference vector. strep: streptomycin and spectinomycin resistance, kan: kanamycin resistance, DsRed: DsRed visible marker originated from pRedroot, 35Spro: *35S* promoter, UTR: untranslated region of appropriate gene Intron: intron of an *A. thaliana* chalcone synthase gene, black bars represent terminators (Dr. Igor Kryvoruchko, unpublished).

Advantage® 2 Polymerase (*Clontech*, Heidelberg, Germany) facilitated the amplification of the 3´untranslated region (UTR) of *MtGras8*. cDNA of mycorrhizal *M. truncatula* A17 roots was used as template. pENTR™/D-TOPO® vectors were established and recombined with the pKDsRed-RNAi vector expression vector, as described in chapter 3.2.11.8. The bacteria were selected on spectinomycin (100 µg/ml) containing LB medium (see chapter 3.1.6.1). The appropriate orientation of the UTR sequence was confirmed by PCR and sequencing, using a combination of gene specific primers and intron specific primers (*LGC genomics*, Berlin, Germany). Afterwards the RNAi constructs were expressed in *M. truncatula* roots and root organ cultures were established, as described in chapter 3.2.11.6 and 3.2.11.7.

3.2.11.12 Restriction and ligation based cloning by using the DNA T4-Ligase

The establishment of *Mtpt4*-promoter-driven constructs (e.g. RNAi- and artificial microRNA constructs) was based on a classical restriction and ligation-based cloning. Target sequences (e.g. full length genes, UTRs) were ligated into pCR2.1-TOPO® vector, as described in the manufacturer´s manual (*Thermo Fisher Scientific*, Henningsdorf, Germany). Equal concentrations (3 µg) of pCR2.1-TOPO-TA and the destination vectors (pRED-Pt4-RNAi, pRED-Pt4-exp, pRED-UBQ3-exp) were digested (at 37 °C for 30 min) with the same or compatible restriction enzymes. The digest was verified by agarose gel electrophoresis. Extraction of the appropriate bands of the insert and linearized destination vector was perfomed with the Wizard® SV Gel and PCR Clean-Up System, according to the manufacturer´s instructions (*Clontech*, Mannheim, Germany). Afterwards the DNA quantity and quality was checked by agarose gel electrophoresis. The ligation of the target sequence and the destination vector, *via* their compatible restriction enzyme sites, was mediated by DNA T4-Ligase (*Promega*, Mannheim, Germany). Ten microliter reactions were prepared, as described in the manufacturer´s instructions. *E. coli* TOP10 bacteria were transformed with 3 µl of the ligation reactions and were grown on LB medium including spectinomycin (100 µg/ml) as selection agents (see chapter 3.1.6.1). Clones were verified by PCR and sequencing with sequence specific primers (*LGC genomics*, Berlin, Germany). *Agrobacteria*-mediated root transformation (as described in chapter 3.2.17) enabled the expression of the destination vectors in *M. truncatula* roots. As negative control empty destination vectors were expressed in roots. Regenerated plants were inoculated for three weeks with *R. irregularis* (see chapter 3.2.1.1) and transgenic roots were identified upon stereo microscopy (stereo microscope

M37, *Leica*, Wetzlar, Germany). One portion of the transgenic root material was frozen in liquid nitrogen for the guanidinium chloride-based RNA preparation (see chapter 3.2.5) and another portion of the fresh root material was stained with WGA Alexa Fluor® 488 to determine the abundance of fungal structures, as described by Trouvelot et al., (1986). The arbuscule morphology was examined by confocal microscopy (Leica TCP SP5 confocal microscope, *Leica*, Wetzlar, Germany), using a wavelength excitation of 488 nm (argon laser). Maximum projections were generated from 20-30 opitcal sections taken in 3 µm intervals.

3.2.11.13 Establishment of *MtPt4* promoter-driven RNA-interference constructs

Gene silencing of *MtGras8* in arbuscule-containing cells should be enabled by expression of a RNAi construct under the *MtPt4* promoter, using the pRED-Pt4-RNAi vector.

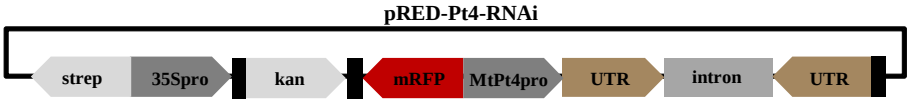

Figure 6: Scheme of the pRED-Pt4-RNA-interference vector. strep: streptomycin and spectinomycin resistance, kan: kanamycin resistance, mRFP: visible marker, 35Spro: *35S* promoter, MtPt4pro: *MtPt4* promoter, UTR: untranslated region; intron: intron of Δ12-desaturase (*A. thaliana*), black bars represent terminators.

The *MtPt4* promoter-driven RNAi cassette of the pRED-Pt4-RNAi vector consisted of the sense and antisense orientated 3´UTR sequence of *MtGras8*, divided by an intron sequence (figure 6). In the pRED-Pt4-RNAi vector backbone a *mRFP* gene (as visible marker gene), streptomycin and spectinomycin resistance genes for bacteria selection and kanamycin resistance gene for plant selection are encoded.

Due to a lack of compatible restriction enzyme sites of the destination and the pCR2.1-TOPO® vector, primers including restriction enzyme sites and a 6 bp linker sequences were used for the amplification of the UTR sequences (figure 7). cDNA samples from mycorrhizal *M. truncatula* A17 roots were used as template. Ligation reactions were performed with DNA T4-ligase, as described in the manual (*Promega*, Mannheim, Germany). First, the sense orientated UTR sequence was ligated with the destination vector, as described in chapter 3.2.11.12. Afterwards the vector was sequenced, digested again and the ligation of the antisense orientated UTR was performed (see figure 7). To confirm the accurate orientation of the sense and antisense orientated UTR sequences, PCR and sequencing was carried with a combination of intron specific and UTR specific primers.

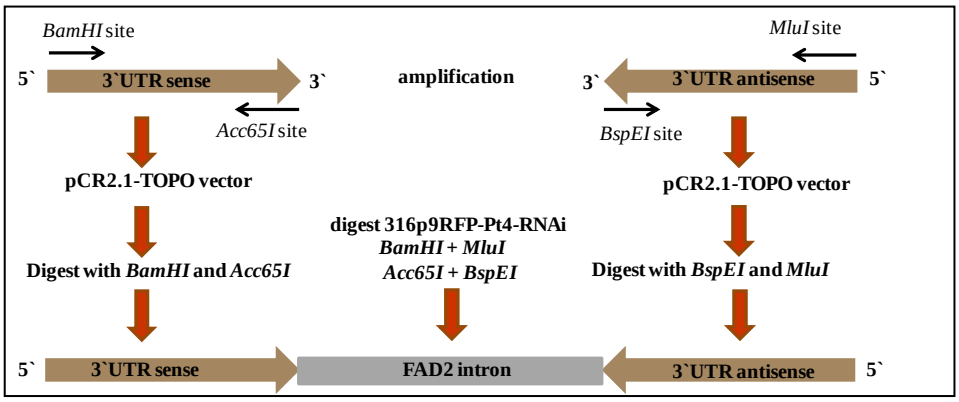

Figure 7: Cloning strategy for pRED-Pt4-RNAi constructs.

Upon amplification of the 3`UTRs of the appropriate genes with primers including restriction enzyme sites, the amplicons were ligated with the pCR2.1-TOPO® vectors. Equal concentrations of the pCR2.1-TOPO® vector containing the sense orientated UTR sequence and the destination vector (pRED-Pt4-RNAi vector) were digested with the same enzymes. After ligation *via* DNA T4-Ligase reaction at 4 °C over-night the clones were verified by PCR and sequencing. Positive destination vectors were digested again to ligate the antisense orientated UTR sequence. FAD2 intron: intron of *A. thaliana* Δ12-desaturase.

3.2.11.14 *MtPt4* promoter-driven expression of miRNA5204*

For the amplification of the miRNA5204* a pBluescript SKII(+) vector containing the miRNA159b precursor (Devers et al., 2013) was used as template.

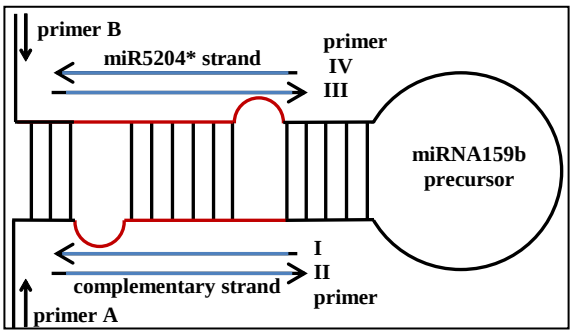

Figure 8: Amplification of miRNA5204* using the pBluescript SKII(+) vector including the miRNA159b precursor (Schwab et al., 2006 , modified).

Four miRNA specific primers facilitated the amplification of miRNA5204* (I-IV). Two primers with overlapping sequences, including the miRNA star strand (III and IV) and the complementary sequence were designed (I and II). Additional primers (A and B) are binding to the pBluescriptSKII+ vector backbone.

Normally, the mature miRNA159b sequence was replaced by the destination miRNA sequence (miRNA5204*) using an overlapping PCR system, as described by Schwab et al., 2006. All primers are enlisted in chapter 3.1.3.

In the case of miRNA5204*, the star strand was inserted at the position of mature miR159b in the miRNA159b backbone. Instead of the miRNA159b* strand, a complementary sequence was inserted complementary to the miRNA5204* strand (figure 8). Advantage® 2 DNA polymerase reactions (50 µl) consisted of 33.5 µl H_2O, 5 µl 10x Advantage® 2 buffer, 5 µl of 2 mM dNTP´s and 0.5 µl Advantage® 2 Polymerase. Per 46 µl aliquot, 4 µl of the appropriate primer mix (10 µM) and 2 µl template DNA (miRNA159b in pBluescript SKII(+) 1:10000 dilution) were added. The PCR reaction was performed under the following conditions (table 7).

Table 7: PCR conditions for first round amplification of miRNA5204*

Step	Temperature (°C)	Time (min)	
Initial denaturation	95	2	
Denaturation	95	0.5	24 cycles
Annealing	55	0.5	
Elongation	68	40 seconds	
Final elongation	68	7	

The amplicons (200 bp length) were verified by agarose gel electrophoresis (2 % agarose gel) and purified with the Wizard® SV Gel and PCR Clean-Up System (*Clontech*, Mannheim, Germany), as described in the manufacturer´s instructions. In the final PCR reaction, full length constructs were generated with primer A and B (figure 8), using a mix of equal amounts of the amplicons (1:100 diluted) as template. Advantage® 2 DNA polymerase reactions (50 µl) were prepared as described for the first round amplification. Two microliter of the PCR products obtained from the first round amplification (1:100 diluted) were used as template, before the PCR was carried out as described in table 8.

Table 8: PCR conditions for second round amplification of miRNA5204*

Step	Temperature (°C)	Time (min)	
Initial denaturation	95	2	
Denaturation	95	0.5	35 cycles
Annealing	52	0.5	
Elongation	68	40 seconds	
Final elongation	68	7	

The amplicons were analyzed by gel electrophoresis and cloned by using the TOPO-TA cloning Kit (*Thermo Fisher Scientific*, Henningsdorf, Germany), according to the manufacturer´s instructions. Subsequently, plasmids were verified by restriction analyses using restriction enzymes cleaving at both sites of the artificial microRNA (amiR) sequence (*SpeI* and *MluI*). Inserts of plasmids with correct restriction enzyme pattern were sequenced using the "M13" forward primer. A correct folding of amiR sequences was verified by using the fold prediction program UEA sRNA toolkit (http://srna-tools.cmp.uea.ac.uk/). Inserts with correct sequence were digested and ligated *via* the *SpeI* and *MluI* restriction enzyme sites, as described in chapter 3.2.11.12. pREDPt4-exp vector / RED-UBQ3-exp vector (figure 9).

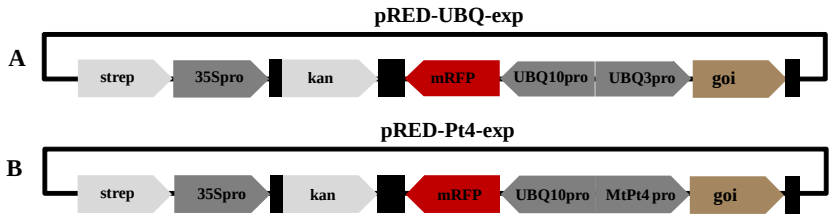

Figure 9: Scheme of the pRED-UBQ3-exp vector and pRED-Pt4-exp vector.
Scheme of the pRED-UBQ3-exp vector (A) and the pRED-Pt4-exp vector (B). strep: streptomycin and spectinomycin resistance, kan: kanamycin resistance, mRFP: visible marker, UBQ3pro: *A. thaliana* UBQ3 promoter, UBQ10: *A. thaliana* UBQ10 promoter, 35Spro: *35S* promoter, MtPt4pro: *MtPt4* promoter, GOI: gene of interest.

Upon Agrobacterium-mediated root transformation the RNA was extracted from three-week-old mycorrhizal plants with the guanidinium chloride protocol (see chapter 3.2.6). After DNaseI digest (see chapter 3.2.9) the stem-loop cDNA synthesis (see chapter 3.2.10) followed. The over-expression of miRNA5204* was confirmed by using stem-loop qRT-PCR analysis with miRNA5204* stem-loop primers, as described by Devers et al., (2011).

3.2.12 Analysis of tobacco retrotransposon insertion mutant plants

Functional characterization of the *MtErf2* TF was mediated by analyzing *M. truncatula R108* plants containing tobacco retrotransposon insertions (*Tnt1)*, provided by Samuel Roberts Nobel Foundation. A *M. truncatula* R108 *Tnt1* mutant line carrying a tobacco retrotransposon insertion in the locus of the *MtErf2* gene was identified by data base search (http://bioinfo4.noble.org/blast/blast.html). A sequence flanking the *Tnt1* insertion (FST sequences) of each mutant line was identified by sequence alignments using the CDS of *MtErf2* TF as query.

3.2.12.1 PCR based screening of homozygous *Tnn1* mutant plants

Advantage® 2 PCR based screening allowed for the identification of homozygous plants containing a *Tnt1* insertion in the *MtErf2* gene. Primers were designed to bind in front and behind the *Tnt1* insertion. The presence of the *Tnt1* insertion (5000 bp) in the *MtErf2* gene was confirmed by amplification of the *MtErf2* wild type band (711 bp) under standard PCR conditions (60 °C annealing temperature and one minute elongation time). Advantage® 2 (*Clontech*, Heidelberg, Germany) PCR reactions (20 µl volume) were prepared, as described in the manufacturer´s instruction. As template, 50 ng genomic DNA obtained from *Tnt1* mutant plants (see chapter 3.2.11.5) and wild type plants (*M. truncatula A17* and *M. truncatula R108*) were used. Amplicons were visualized by agarose gel electrophoresis using a 2 % agarose and a 1 kb Plus DNA Ladder (*Thermo Fisher Scientific*, Henningdorf, Germany).

3.2.13 Software applications for data analyses

3.2.13.1 Microarray data analysis with the Robin® Software

The statistical algorithm MAS5.0 facilitated the identification of present and absent calls per probe set in the Affymetrix GeneChip® Medicago genome array data set. The Affymetrix expression Console™ enabled the background correction and summarizing of the probe sets to generate "CEL files" (Gaude et al., 2012). Afterwards the "CEL files" were imported into the Robin® Software, which represent a Java based GUI R/Bioconductor function (Lohse et al., 2010). For the data normalization the Robust Multiplechip Average analysis (RMA) was used (Irizarry et al., 2003). Significantly differential expressed genes were identified by using the linear model based "limma" package (Smyth, 2004), using a Student´s t-test with a Benjamini-Hochberg corrected *p*-value of 0.05 (Gaude et al., 2012).

The results of the statistical analysis were summarized in an Excel data sheet ("result-table"), which enabled the data import into the MapMan® Software (Usadel et al., 2005). This data sheet consists of a list with all log 2-fold changes in gene expression in each comparison and includes flags. While the flag 0 marks not significant differentially expressed genes, the flag 1 marks significantly up-regulated and -1 marks significantly down-regulated genes. This enables the filtering of the microarray data upon their significant differential expression in the MapMan® Software (Usadel et al., 2009; Lohse et al., 2010).

3.2.13.2 Gene annotation and classification with the MapMan® Software

The MapMan® Software (Thimm et al., 2004) allows a visualization of transcriptomic datasets in metabolic pathways. Three types of data are necessary for the data visualization. A "mapping file" includes a unique identifier for each parameter (e.g. Affymetrix identifier), a text annotation and a numeric code of the functional category to enable the classification of measured parameters (gene represented on the microarray) into hierarchical functional categories (BINS, subBINS and enzymes). Further imported metabolic diagrams ("maps") and the experimental data set as "result table" (imported from Robin®) are required to display the data in metabolic pathways (Thimm et al., 2004). The results were given as "XML file" (Thimm et al., 2004). Since 2007 the software enables the display of Mt16kOligo1Plus microarray data. The annotations of *M. truncatula* genes were based on similarity to *A. thaliana* genes (blast search against Arabidopsis Information resource 6.0 database). TC´s, which were not classified could be annotated *via* TIGR 7.0 annotation (Tellström et al., 2007). Since 2009 the analysis of Affymetrix GeneChip® data was enabled by adding additional "mapping files" including Affymetrix annotations for *M. truncatula* (personal communication Axel Nagel MPIMP Golm, 2009), as described in Gaude et al., 2012.

3.2.13.3 Phylogenetic analysis

Amino acid sequences of *A. thaliana* GRAS and ERF TF family were obtained from the Database of *Arabidopsis thaliana* transcription factors (http://datf.cbi.pku.edu.cn/browsefamily). Highly similar sequences were identified by blastp search at the NCBI data base (e-value cutoff = 0) (http://blast.ncbi.nlm.nih.gov). Amino acid sequences of the remorin protein family members *MtSYMREM2* (XM_003611074.1), *MtSYMREM1* (JQ61257.1) and *LjSYMREM1* (BT148930.1) (Raffaele et al., 2007) were aligned to study the sequence similarities. For the alignments of GRAS and AP2/ERF TF sequences the amino acid sequences of MtGRAS8 (XM_003608835.1), MtERF2 (XM_003589108.1), MtNSP1 (AJ972473.1 and AJ972978.1), MtNSP2 (AJ832138.1), MtRAM1 (JN572683.1), MtERN1 (EU38802.2), MtERN2 (EU38803.2) and MtERN3 (EU38804.1) were obtained from the NCBI data base (http://www.ncbi.nlm.nih.gov/). The sequences were used to build a multiple amino acid sequence alignment and construction of a phylogenetic tree *via* the "A la Carte" mode of the Phylogeny.fr platform (http://www.phylogeny.fr) (Dereeper et al., 2008). The analyses included a multiple amino acid sequence alignment based on the ClustalW algorithm (Thompson et al., 1994), followed by the removing of ambiguous regions with Gblocks (version 0.91) (Castresana, 2000) and the establishment of an maximum likelihood based phylogenetic tree *via* the PhyML software (version 3.0 aLRT) (Guindon and Gascuel, 2003). The robustness of the phylogentic tree was statistically verified using the approximate likelihood ratio test (Anisimova and Gascuel, 2006), before the tree was visualized in the TreeDyn software (version 198.3) (Chevenet et al., 2006). The given branch length, values between 0.0 and 1.0 are proportional to the average probability of a change of the character (amino acid). A value of 1.0 indicates one change per character.

4 Results

4.1 Cell type-specific transcriptome analysis

Combining Laser Capture Microdissection (LCM) and Affymetrix GeneChip® Medicago Genome array hybridization enabled a cell type-specific transcriptome analysis of three different cortical cell types. From three-week-old *Rhizophagus irregularis* inoculated *Medicago truncatula* roots arbuscule-containing cells (arb cells) and non-arbuscule-containing cells (nac cells) were isolated from longitudinal root cryosections *via* LCM. As a control, cortex cells of non-mycorrhizal roots (cor cells) were selected. Ten thousand cells of each cell type were collected and were subjected to RNA isolation. The RNA quality and quantity was verified by Bioanalyzer measurements (figure 10). Around 50-100 ng RNA could be extracted from the cell lysate samples upon Laser Capture Microdissection. RNA samples with a RIN number larger than 6 were sent to Atlas Biolabs (Berlin, Germany) for Affymetrix GeneChip® Medicago genome array hybridization. After an amplification step around 3 µg of cDNA were obtained per cell type and applied for the hybridization.

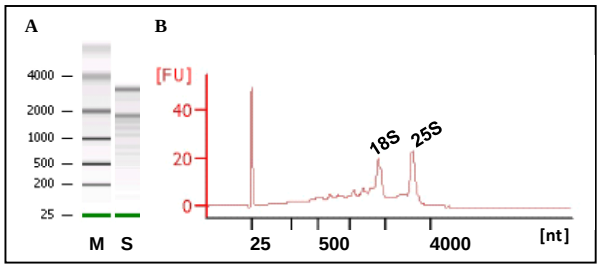

Figure 10: Data output of an Agilent™ 2100 Bioanalyzer measurement.

A) The gel picture displays the ladder (M) and a RNA sample obtained from laser capture microdissected cortex cells (S). B) Based on the 18S rRNA and 25S rRNA peaks, shown in the electropherogram, a RIN number (in this case RIN 7.3) is calculated. On the x-axis the detected fluorescence and on the y-axis the number of nucleotides depicted.

The results of two microarray hybridizations per cell type were submitted as so-called "CEL files". These "CEL files" were imported into Robin® Software for statistical analyses. Result tables containing the Robin® read-outs were imported into MapMan® Software to display the significantly regulated transcripts in functional categories (see chapter 3.2.13.1 and 3.2.13.2).

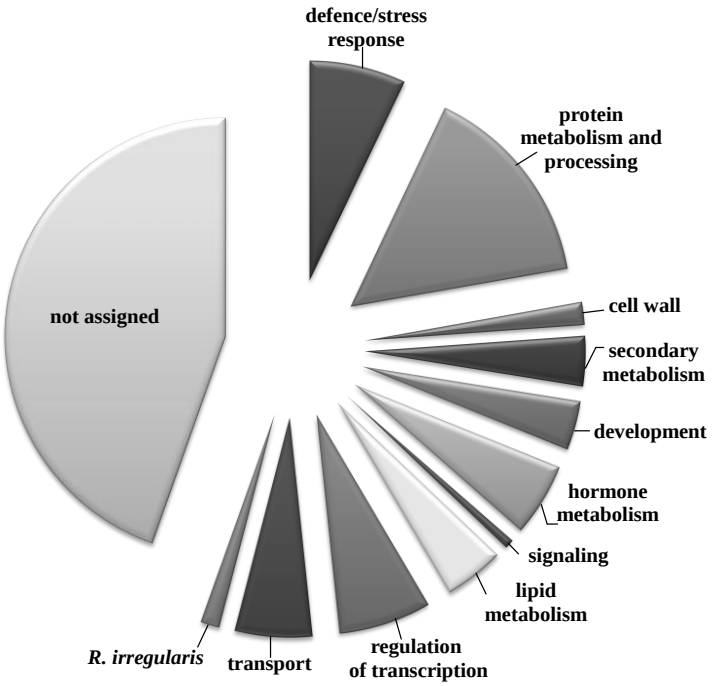

Figure 11: Categorization of differentially expressed genes to functional classes.
Genes with significant differential expression in arbuscule-containing cells compared to cortical cells of non-colonized roots (log2 fold change >2 or <-2) were categorized into functional categories using the MapMan® Software package into BINS re-presenting functional categories.

MapMan® Software enabled a categorization of differentially regulated transcripts into functional categories. A high proportion of significantly regulated genes could not be assigned to MapMan® BINS. Around 25 % of the assigned transcripts encoded proteins playing a role in protein-, RNA-, lipid- and secondary- metabolism as well as in signaling, transport and developmental processes. Only a low number of *R. irregularis* transcripts was detected, as compared to previous transcriptome analyses of whole mycorrhizal roots and *R. irregugularis* tissues (Hohnjec et al., 2005; Gomez et al., 2009; Hogekamp et al., 2011; Tisserant et al., 2012). A remarkable number of transcription factor (TF) genes were identified and numerous of transcripts encoded enzymes related to the lipid metabolism (figure 11).

In total, 1951 differentially expressed transcripts with a log 2-fod change higher than 1 or less than -1 were detected (figure 12A). In comparison to a transcriptomic analysis of whole mycorrhizal and non-mycorrhizal *M. truncatula* roots (i.e. 652 significantly regulated transcripts published by Gomez et al., 2009), the cell type-specific data set included a three times higher number of significantly regulated transcripts. Additionally, a high proportion of down-regulated genes was detected by the cell type-specific expression profiling. While the majority of differentially regulated genes between nac and cor cells was up-regulated in nac cells, only a few down-

regulated genes were detected in this cell type (figure 12A left circle). Interestingly, 283 arb cell-specifically expressed transcripts were identified, but more than 576 genes were coinduced in the arb and nac cells (figure 12A center). Furthermore, a numberous of down-regulated genes (252) were detected in arb cells (figure 12A right circle).

As described in chapter 1.4, the reprogramming of root cortex cells for the upcoming colonization is likely to be mediated by TFs. This cell type-specific data set included a remarkable number of significantly regulated TFs (figure 11). Overall, 68 TF genes were found to be significantly differentially expressed (log 2-fold change higher than 2 and less than -2).

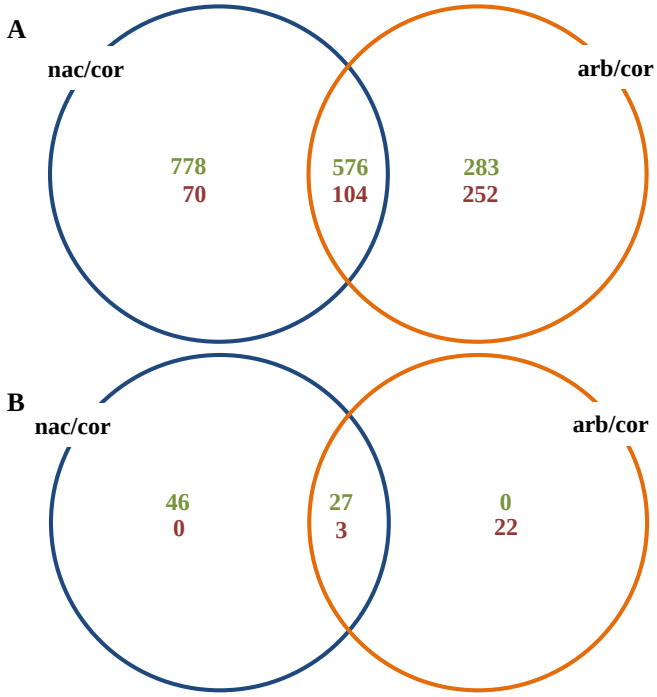

Figure 12: Venn diagrams of differentially regulated transcripts and transcription factors. Venn diagrams were established by using the Robin® Software. Significantly differentially regulated genes were ascertained by a Student´s t-Test (*p*-value <0.05). arb: arbuscule-containing cells, nac: non-arbuscule-containing cells from mycorrhizal roots, cor: cortex cells from non-mycorrhizal roots. Green numbers represent genes with significantly increased transcript abundances and red numbers symbolize significantly down-regulated transcripts. A) Overall number of differentially expressed transcripts (log2 fold change larger than 1 and less than -1). B) The number of differentially regulated TF genes (log2 fold change larger than 2 and less than -2).

The majority of differentially regulated TF genes (46) displayed elevated expression levels in the nac cell population during AM symbiosis.

In contrast to nac cells, most of the TF genes were down-regulated in arb cells. Further, no arb cell-specific induced TFs could be identified. Remarkably, all TFs with elevated expression in arb cells were also induced in the nac cell population (figure 12B center).

4.2 Cell type-specific expression of mycorrhizal marker genes

In order to confirm the transcriptional regulation observed after Affymetrix GeneChip® Medicago genome array hybridization, a qRT-PCR system for microdissected cells was developed. As first proof of concept, the expression of well known mycorrhizal marker genes was verified by cell type-specific qRT-PCR analysis (see chapter 3.2.9, 3.2.10). For the cDNA synthesis, two RNA samples from microdissected cortical cells were pooled per cell type (see chapter 3.2.9). As a control, RNA obtained from whole *M. truncatula* roots was reverse transcribed into cDNA. In case of the controls, the transcript abundances were measured in three biological and two technical replicates. Therefore, cell type-specific cDNA samples derived from cells of different root cryosections and plants.

Symbiosis-related induction of plant-derived nutrient transporter genes is well described in arbuscule-containing cells (Gianinazzi-Pearson et al., 1995; Harrison, 1999; Bago et al., 2000; Harrison et al., 2002; Krajinski et al., 2002). Further, previous cell type-specific analysis confirmed the constitutively expression of *GintPT*, a phosphate transporter of *R. irregularis*, in arbuscule-containing cells (Fiorilli et al., 2013).

In this study, the elevated expression of a phosphate transporter (*MtPt4*) and a putative copper transporter gene (Medtr2g07990.1) was confirmed in arb and nac cells and in mycorrhizal roots (figure 13A, B). Also a higher transcript abundance of a protease inhibitor (Medtr8g146780.1) was confirmed in the nac cell population (figure 13C). Another symbiosis marker gene encodes an expansin (Medtr5g013580.1), which might facilitate the entering of epidermis cells by fungal hyphae (Balestrini et al., 2005). The expression of this gene was confirmed in arb cells, mycorrhizal roots and cortical cells of non-mycorrhizal roots (figure 13D).

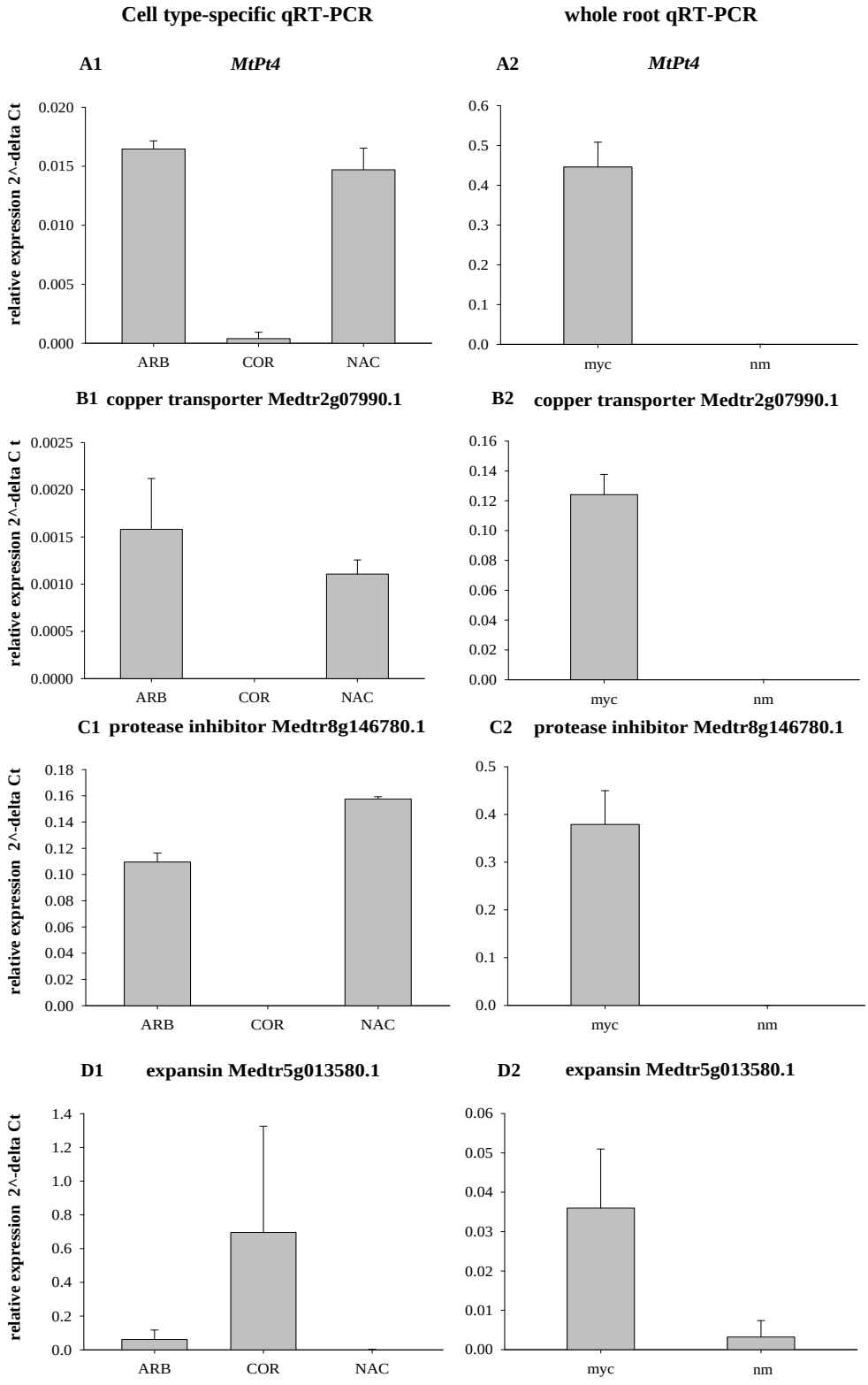

Figure 13: Confirmation the transcription of known symbiotic marker genes by qRT-PCR.

The left panel represents mean values of two technical replicates of cell type-specific qRT-PCR analysis. Mean values of three biological replicates of a whole root qRT-PCR measurement are displayed in the right panel. RNA obtained from 20000 cells or 50 ng of whole-root RNA was reverse transcribed into cDNA. The expression data were normalized to the *M. truncatula* housekeeping genes *MtEf1-α* and *MtGapdh* (Kakar et al., 2008). ARB: arbuscule-containing cells, NAC: non-arbuscule-containing cells of mycorrhizal roots, COR: cortex cells of non-mycorrhizal roots. myc: mycorrhizal roots, nm: non-colonized roots.

4.3 Candidate transcription factors selected from the cell type-specific data set

The differential expression of selected TFs should be confirmed by cell type-specific qRT-PCR and expression of promoter::*uidA* fusion constructs in *M. truncatula* roots. As shown in table 9, eleven TF candidates were selected from the Affymetrix GeneChip® data set, based on their significant transcriptional regulation (log 2-fold change larger than 2 and less than -2) in arb and nac cells. Transcripts with strongly increased abundances in arb and nac cells encoded members of the MYB TF family, CAAT-box binding TFs (*MtCbf2* and *MtCbf1*) and a GRAS TF family member. A moderately induced transcription in arb and nac cells was observed in case of Zinc finger proteins, Homeobox TFs and AP2/ERF TFs. Additionally, the elevated expression of a Homeobox family member (*MtHomeobox40*) in nac cells was verified by qRT-PCR analysis on cell type-specific level.

Table 9: Candidate transcription factors selected from the Affymetrix GeneChip® data set

Name	Medtr no (3.0)	Medtr no (3.5)	annotation UrmelDB (3.0)	LFC		
				arb-cor	arb-nac	nac-cor
MtMyb1	Medtr7g11170.1	Medtr7g093030.1	MYB family TF	9.22	1.07	8.15
MtCbf2	Medtr2g095980.1	Medtr2g081600.1	CAAT-box binding TF	8.89	1.14	7.74
MtCbf1	Medtr2g095930.1	Medtr2g081630.1	CAAT-box binding TF	8.20	1.73	6.47
MtGras8	Medtr8g109760.1	Medtr4g104020.1	GRAS TF	7.75	2.20	5.55
MtSYMREM2	Medtr5g010750.1	Medtr5g010590.2	Remorin protein	4.60	1.48	3.13
MtAba1	Medtr4g141530.1	Medtr8g092460.1	AP2/ERF TF	4.23	1.41	2.82
MtSWIRM1	Medtr3g159850.1	Medtr3g116120.1	SWIRM-domain protein	3.23	1.52	2.34
MtZinc1	Medtr159770.1	Medtr8g102580.1	Zinc finger TF	2.82	0.48	2.34
MtHomeobox1	Medtr3g130470.1	Medtr3g109800.1	HD-ZIP TF	2.60	1.84	0.76
MtErf2	Medtr1g024100.1	Medtr1g019110.1	AP2/ERF TF	2.58	0.60	1.98
MtHomeobox40	Medtr5g019580.1	Medtr5g019680.1	Homeobox protein 40	-1.32	-4.52	3.20

Candidate transcription factors with a graeater than log 2-fold change in their expresssion >2 or <-2 in different cell-types are listed in the table. Annotations and identifiers related to *M. truncatula* genome version 3.0 and 3.5 are indicated. arb: arbuscule-containing cells, nac: non-arbuscule-containing cells of mycorrhizal roots, cor: cortex cells of non-mycorrhizal roots, TF: transcription factor.

4.3.1 Cell type-specific qRT-PCR confirmed the expression of transcription factors

As shown in figure 14, the cell type-specific expression of eight TF genes was confirmed by qRT-PCR. According to the Affymetrix GeneChip® data, the majority of differentially expressed TF genes was coinduced in arb and nac cells of mycorrhizal roots. In these cell types, strongly mycorrhizal-induced gene expression of *MtMyb1, MtCbf2, MtGras8* and *MtErf2* TFs was observed (figure 14A1, B1, D1, G1). Moderately elevated transcript levels of *MtCbf1* TF and *MtSYMREM* TF were detected in arb and in arb and nac cells, respectively (figure 14C1, E1). Furthermore, nac cell-specific expression of the *MtHomeobox40* TF was verified by qRT-PCR analysis (figure 14H). The Affymetrix GeneChip® hybridization revealed that *MtSWIRM1* is co-expressed in the arb and nac cell population. However, a higher transcript abundance of *MtSWIRM1* was detected in nac cells and in non-mycorrhizal roots by qRT-PCR analysis (figure 14F). For several TFs a mycorrhizal-specific transcription was confirmed using whole mycorrhizal roots (figure 14A2-H2). Due to the presence of RNA from non-colonized cells in mycorrhizal roots, higher expression levels were determined in cell type-specific samples, as compared to whole roots (e.g. *MtGras8*, *MtSWIRM1* and *MtHomeobox40* (figure 14D, F, H).

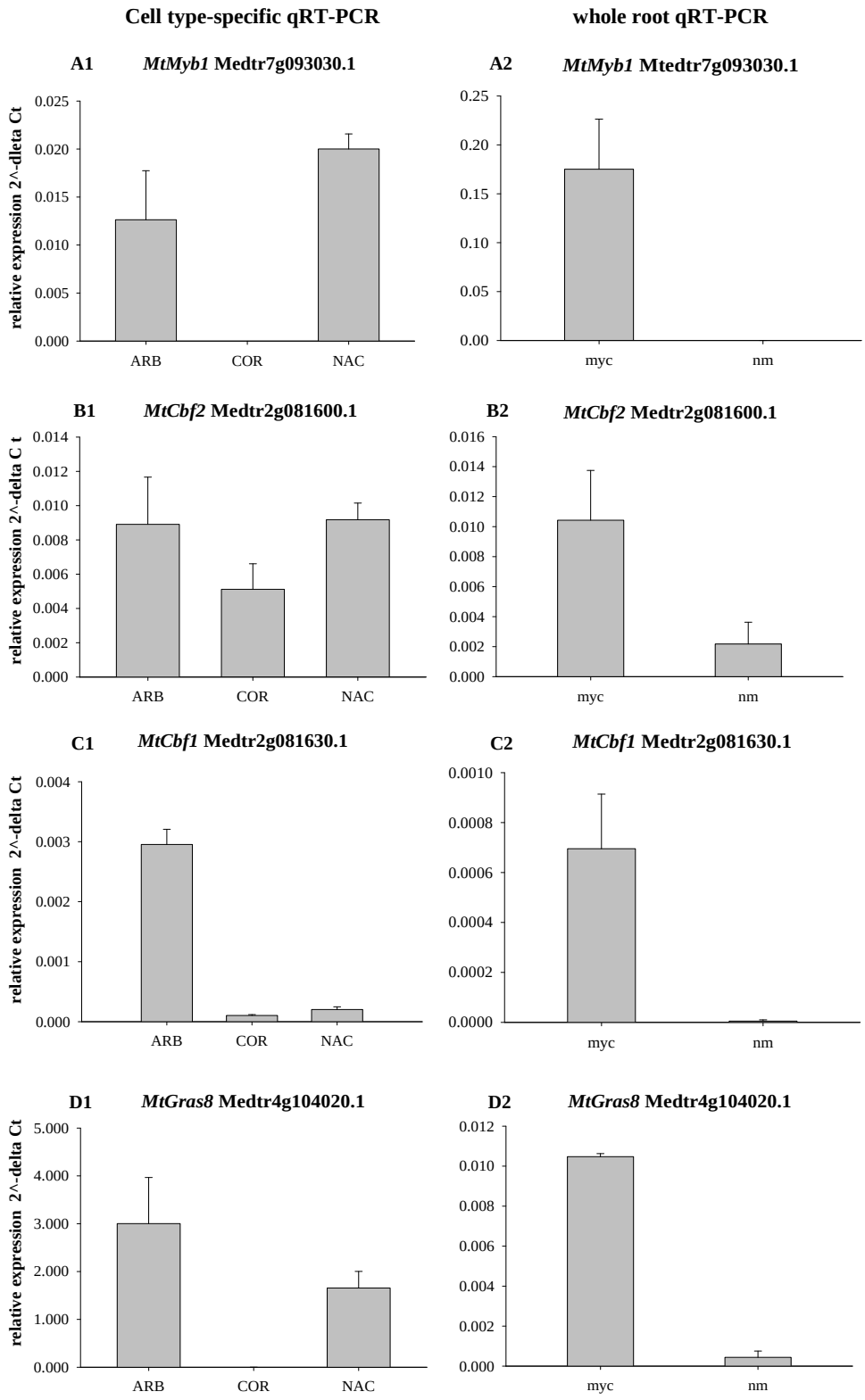

Figure 14: qRT-PCR analysis of candidate transcription factors.

For cDNA synthesis the RNA obtained from 20000 cells or 50 ng whole root RNA was used. The relative expression values were normalized to the reference genes *MtEf1-α* and *MtGapdh* (Kakar et al., 2008). The left panel shows mean values of two technical replicates of cell type-specific expression data. The right panel represents mean values of three biological replicates measured in whole roots. ARB: arbuscule-containing cells, NAC: non-arbuscule-containing cells of mycorrhizal roots, COR: cortex cells of non-mycorrhizal roots. myc: mycorrhizal roots, nm: non-colonized roots non-colonized roots.

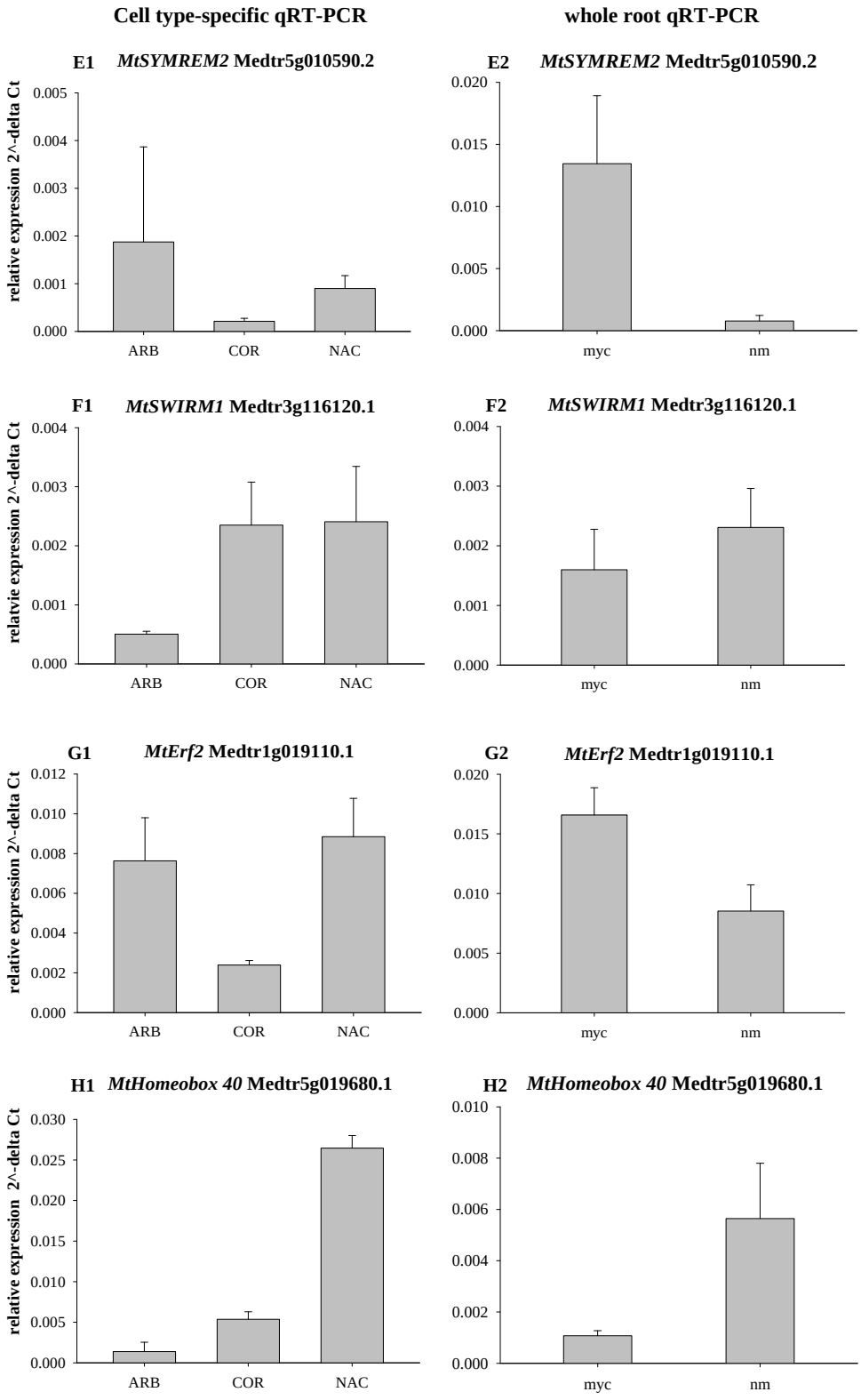

Continuation of figure 14: qRT-PCR analysis of candidate transcription factors.

4.3.2 Localization of transcription factor promoter activities

To further confirm the transcriptional regulation of selected TFs, promoter::*uidA* fusion constructs were established. For this approach, a 1 kb region upstream of the start codon of the appropriate TF was amplified and was cloned *via* Gateway® Cloning system into the pGWB433 vector. Three weeks post inoculation fresh root material was stained to visualize the GUS activity. Subsequently, longitudinal vibratome sections were generated and stained with WGA Alexa Fluor® 488 to visualize fungal structures (see chapter 3.2.2, 3.2.11.9).

The promoter activity of eight TFs (e.g. *MtMyb*, *MtCbf2*, *MtGras8*, *MtSYMREM2* and *MtErf2*) was confirmed in arb cells (figure 15). In accordance with the Affymetrix GeneChip® and qRT-PCR results, the promoter activity of *MtMyb1*, *MtGras8*, *MtAba1* and *MtZinc1* TFs was observed in arb and nac cells. Additionally, a weak basal promoter activity in cor cells could be observed for *MtMyb1*, *MtCbf2 MtSYMREM2* and *MtZinc1* TFs.

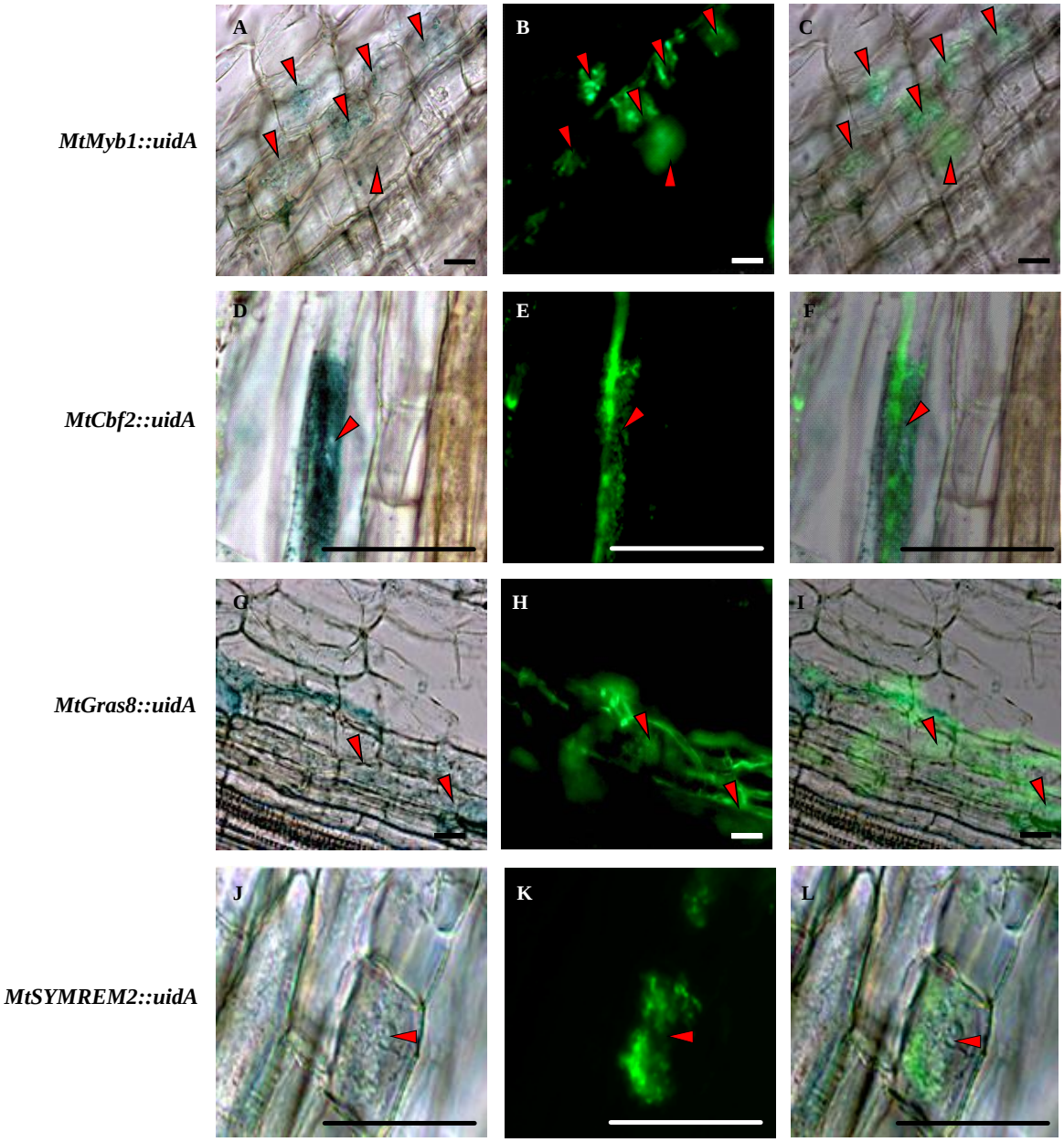

Figure 15: **Co-localization of promoter activity and fungal structures in *M. truncatula* root cells.**
Roots were histochemically stained for GUS activity, and subsequently 50 µm longitudinal sections were produced and co-stained with WGA Alexa Fluor® 488. The sections were analyzed by epifluorescence microscopy, using an excitation wavelength of 488 nm. The co-localization of promoter activity and fungal structures was determined by fusion of bright field (A, D. G, J) and fluorescence (B, E, H, K) images to create overlay images (C, F, I, L). Arbuscules are labeled with red arrows. The scale bars represent 50 µm.

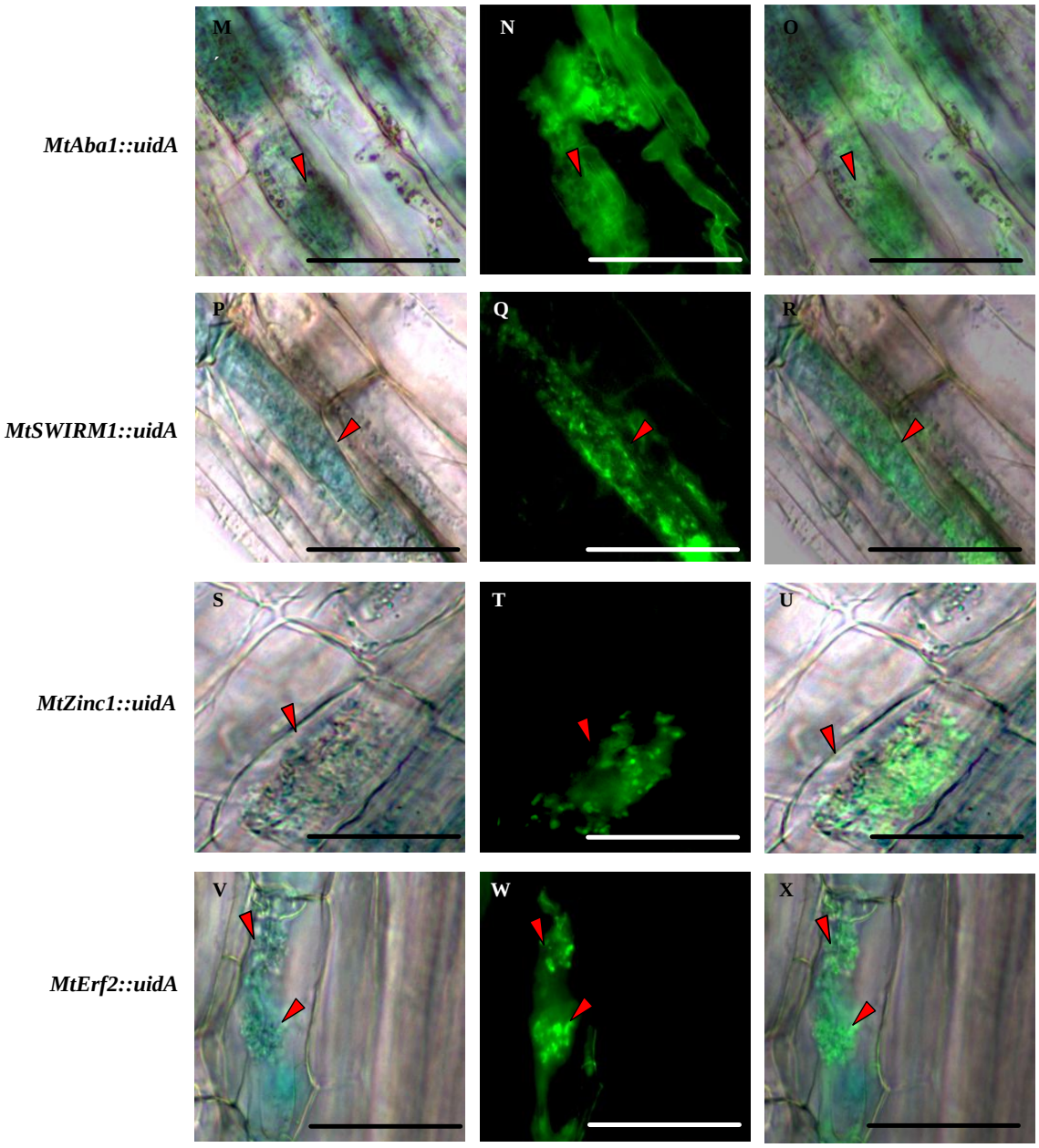

Continuation of figure 15: Co-localization of promoter activity and fungal structures in *M. truncatula* root cells. The fusion of bright field (M, P, S, V) and fluorescence (N, Q, T, W) images enabled the co-localization of GUS activity and arbuscules in overlay images (O, R, U, X).

4.3.3 Phylogenetic analysis of symbiosis-related transcription factor families

Multiple amino acid sequence alignments were performed with the ClustalW algorithm (see chapter 3.2.13.3) to investigate the sequence similarity of MtGRAS8, MtSYMREM2 and MtERF2 to functionally described members of these TF families.

GRAS TFs share a highly conserved C-terminus and a highly variable N-terminus (Pysh et al., 1999; Bolle, 2004; Tian et al., 2004). While two leucine-rich repeat domains facilitate protein-protein- interactions, a VHIID domain mediates the DNA binding (Bolle, 2004). GRAS superfamily members can be subdivided upon their C-terminal domain structure in the following seven subfamilies: DELLA, SCR, Ls branch, HAM branch, PAT branch, SHR branch and SCL branch. Phylogenetical studies of GRAS TF family members should unravel the relationship of MtGRAS8 to GRAS family members involved in the root endosymbiosis-related signal transduction, such as NSP1, NSP2 and RAM1 (Kalo et al., 2000 Catoira et al., 2000, Cerri et al., 2012; Stracke et al., 2002; Hirsch et al., 2009; Gobbato et al., 2012).

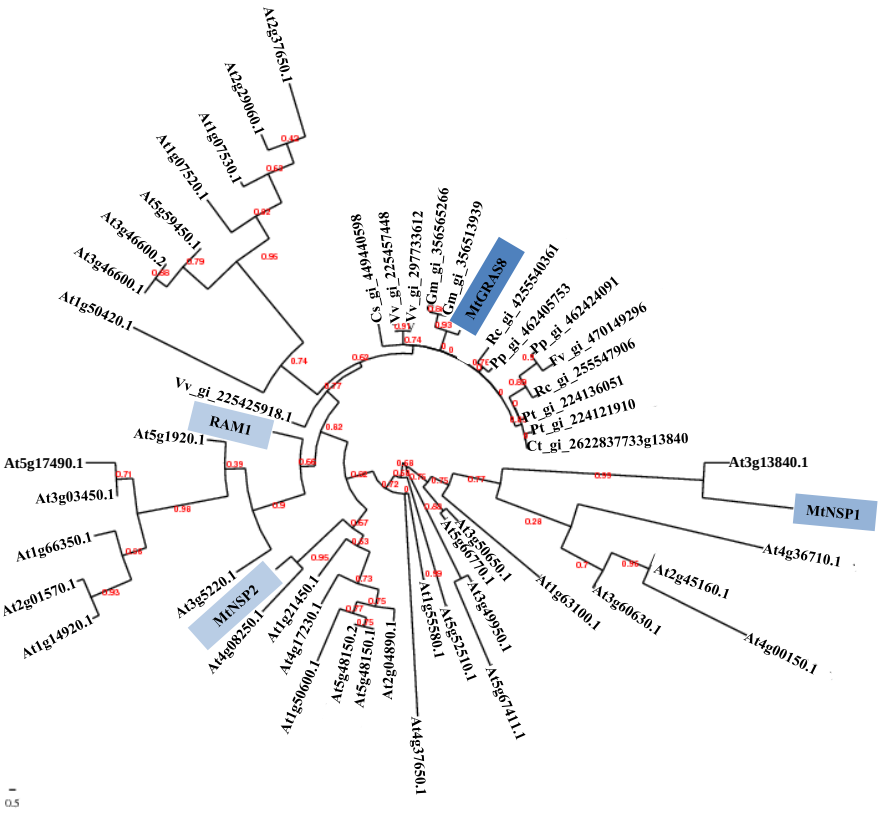

Figure 16: Unrooted phylogenetic tree of GRAS transcription factors closely related to MtGRAS8

The amino acid sequences of orthologous GRAS TF sequences in legumes and non-legumes, all GRAS TFs from *Arabidopsis thaliana*, as well as MtNSP1, MtNSP2 and MtRAM1 were applied to a multiple amino acid sequence alignment. The amino acid sequence alignment was performed with the Phyldeny.fr platform. (http://www.phylogeny.fr) including a ClustalW algorithm. An unrooted phylogenetic tree was built *via* the PhyML software using the maximum likelihood algorithm. Branch lengths are indicated by red numbers. The scale bar indicates the number of amino acid substitution per character.

Orthologous sequences of MtGRAS8 encoding DELLA protein family members (GIBBERELLIC INSENSITIVE (GAI) and REPRESSOR OF GIBBERELLIG INSENSITIVE-like) in legumes, (i.e.*Glycine max*) and *Fragaria vesca subsp. Vesca* (strawberry) (figure 16) as well as in non-legumes, such as *Ricinus communis, Populus trichocarpa* and *Vitis vinifera*. Also MtRAM1, which regulates the expression of a glycerol acyltransferase (MtRAM2) (Gobatto et al., 2012), is highly conserved in legume and non-legume species and closely related to DELLA proteins. Like MtRAM1, MtGRAS8 does not seem to have an ortholog in the non-mycorrhizal plant *A. thaliana*. While MtRAM1 and MtGRAS8 share 34 % sequence identity, weaker sequence similarity (25- 30 %) was detected between MtGRAS8 and NSP1 and NPS2 as well as SCARECROW family members of *A. thaliana*.

Remorins are so far not described as TFs *per se*, they are plant specific proteins that comprise multi-gene family and can be regarded as marker proteins for membrane domains (Raffaele et al., 2009; Lefebvre et al., 2010). These filamentous proteins are known to be involved in signal transduction, secretory processes and root endosymbioses (Bariola et al., 2004; Colebatch et al., 2004; El Yahyaoui et al., 2004; Raffaele et al., 2009; Ivanov et al., 2010). In this work, the symbiosis-related transcriptional induction of MtSYMREM2 in arb and nac cells was shown. MtSMREM2 shares 99.3 % identical amino acids with MtREM2.1. Upon a blastp search MtSYMREM2 was identified as an alternative splice product of MtREM2.1, a member of the group 2 remorins, such as MtSYMREM1 and LjSYMREM1 (Lefebvre et al., 2010; Toth et al., 2012). Members of this remorin family, such as MtSYMREM1 are known to be involved in the *Rhizobia* infection processes (Fedorova et al., 2002; Wienkoop and Saalbach, 2003; El Yahyaoui et al., 2004). While MtSYMREM2 shares around 44 % identical amino acids with MtSYMREM1, weaker sequence similarity was detected between MtSYMREM2 and LjSYMREM1 (39.3 %).

The APETALA2/ETHYLENE-RESPONSIVE TRANSCRIPTION FACTOR (AP2/ERF) family represents one of the largest TF families in plants (Nakano et al., 2006) (Nakano et al., 2006). These TFs can be subdivided, upon the number of AP2/ERF domains in the AP2- subfamily including two AP2/ERF domains, the ERF-subfamily containing one AP2/ERF domain and the RAV-subfamily (proteins related to ABI3 /VP1) including one AP2/ERF domain and one B3 domain (Riechmann et al., 2000; Kizis and Pages, 2002; Sakuma et al., 2002; Nakano et al., 2006). The 60-70 amino acid long AP2/ERF domains facilitate the binding of the TFs to ethylene responsive elements in the promoter region of their target genes (Riechmann and Meyerowitz, 1998). The elevated transcription of two AP2/ERF TFs (*MtAba1* and *MtERF2*) in arb and nac cells was detected in this work.

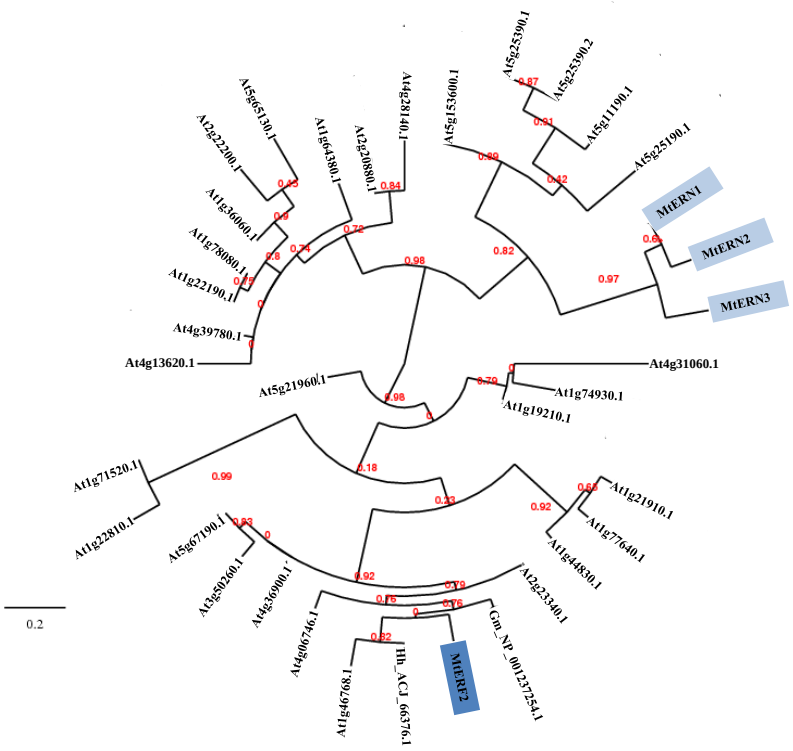

Figure 17: Unrooted phylogenetic tree of ERF transcription factors closely related to MtERF2.
A multiple amino acid sequence alignment of orthologous ERF sequences in legumes and non-legumes, *A. thaliana* ERF TFs, as well as MtERN1, MtERN2 and MtERN3 sequences was performed *via* the ClustalW algorithm (http://www.ebi.ac.uk/Tools/msa/clustalw2/) and an unrooted phylogenetic tree was built *via* the PhyML software using the maximum likelihood algorithm. Red numbers represent the branch lengths. The scale bar represents distance of 0.2 amino acid substitution per position.

Phylogenetic analyses of ERF TF family members from legumes and *A. thaliana* revealed that MtERF2 is closely related to DEHYDRATION-RESPONSIVE ELEMENT BINDING FACTOR (DREB) proteins of *Glycine max* and *Halimodendron halodendron*. Further, an orthologous sequence encodes a RAP2.1 TF (At1g46768) in *A. thaliana* (figure 17). Recently, two ERF TFs, ERN1 and ERN2, have been shown to be involved in the regulation of the symbiosis-related gene expression during root nodule symbiosis (Andriankaja et al., 2007; Middleton et al., 2007). Remarkably, weak sequence similarity (20-25 %) could be investigated between MtERF2 and MtERN1, MtERN2 and MtERN3.

4.3.4 Functional characterization of *MtErf2*

In the cell type-specific data set *MtErf2* displayed a moderately induced transcription in arb and nac cells (see chapter 4.3.1 figure 14). Functionally AP2/ERF TFs are involved in stress response reactions (Gutterson and Reuber, 2004), organ development and differentiation processes (Wilson et al., 2006). As mentioned earlier, TFs of the ERF subfamily, such as ERN1, ERN2 and ERN3 are essential for Nod factor signal transduction during root nodule symbiosis (Andriankaja et al., 2007; Middleton et al., 2007). While ERN1 and ERN2 activate the expression of *ENOD11* upon binding to the NF-box in the *ENOD11* promoter, another ERF TF (ERN3) acts as negative regulator of ERN1 and ERN2 (Andriankaja et al., 2007). Furthermore, ERN2 might also play a role during AM symbiosis related signal transduction (Andriankaja et al., 2007; Cerri et al., 2012).

4.3.4.1 Identification of homozygous *erf2-1/Tnt1* mutants

Indications for a probable function of this AP2/ERF TF family member during AM symbiosis should be gained from an analysis of a *M. truncatula* R108 *Tnt1* insertion mutant, obtained by Michael Udvardi (Samuel Roberts Noble Foundation, Ardmore, Oklahoma, USA).

The *M. truncatula* R108 *Tnt1* insertion mutant line NF5082 contains a ~5 kb long *Tnt1* insertion, located in reverse orientation in the exon of the *MtErf2* gene at position 362. Homozygous plants (with regard to the *Tnt1* insertion in the *MtErf2* gene) were generated by cultivation of two selfing generations. From here on homozygous *Tnt1* mutant plants are referred as *erf2-1/Tnt1* and homozygous wild type plants (with regard to the *MtErf2* gene) are described as *erf2-1/Wt*.

As shown in figure 18, the *Tnt1* insertion in the *MtErf2* gene could be confirmed with gene specific primers flanking the *Tnt1* insertions (see chapter 3.2.12.1). In case of the homozygous *erf2-1/Tnt1* plants the amplification of a 711 bp amplicon with *MtErf2* specific primers was hampered by the presence of a 5 kb *Tnt1* insertion (located in the *MtErf2* gene) (figure 18, lanes 1 and 2). In contrast to this, the amplification of the 711 bp fragment was successful if genomic DNA obtained from *erf2-1/Wt* plants and the *M. truncatula* A17 control was used as template (see figure 18 lanes 3-5).

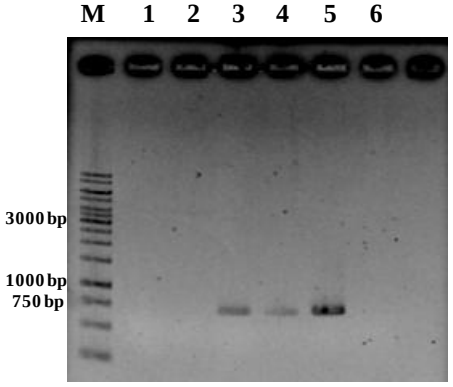

Figure 18: Confirmation the presence of the *Tnt1* insertion in the *MtErf2* gene *via* PCR. The PCR was performed with *MtErf2* specific primers. Genomic DNA of homozygous *erf2-1/Tnt1* mutant (lanes 1-2) and *erf2-1/Wt* plants (in regard to the *MtErf2* gene) was used as template (lanes 3-4). Control reactions were prepared with genomic DNA from *M. truncatula* A17 (lane 5) and H_2O (lane 6). M: 1 kb ladder.

4.3.4.2 Impact of the tobacco retrotransposon insertion on *MtErf2* transcription

The influence of the tobacco retrotransposon insertion (*Tnt1*) insertion on the transcription of the full length *MtErf2* gene was unraveled by PCR, using cDNA samples of four week old mycorrhizal roots as template. The PCR reactions were prepared with primers that enable the amplification and quantification of transcript fragments upstream (5´) or downstream (3´) of the *Tnt1* insertion. Additionally, the cDNA quality was verified by amplifying transcripts of the *M. truncatula* housekeeping gene *MtPdf2* (figure 19 lanes 11-14). The transcript fragments located 3´and 5´of the *Tnt1* insertion could be detected in case of the *erf2-1/Wt* plants (figure 19 lanes 1-10). *MtErf2* transcript fragments could be amplified from *erf2-1/Tnt1* cDNAs as well. Accordingly, the DNA-dependent RNA Polymerase II reads through the *Tnt1* insertion. Hence, it might be assumed that aberrant *MtErf2* transcripts are present in the mutants (figure19 lanes 7 and 8).

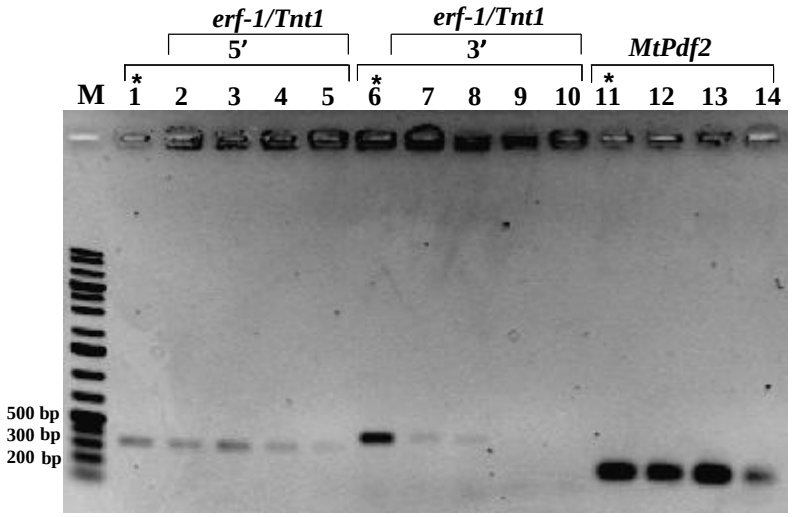

Figure 19: Detection of *MtErf2* transcripts in cDNA samples from *erf2-1/Tnt1* and *erf2-1/Wt* roots. The amplification of a transcript fragment located 5´ of the *Tnt1* insertion is shown in lanes 1-5 and amplified transcript fragments located 3' of the *Tnt1* insertion are displayed in lanes 6-10. cDNA obtained of *erf2-1/Tnt1* plants (lanes 2 ,3, 4, 5, 7, 8, 9, 10, 12, 13 and 14) and *erf2-1/Wt* plants (lanes 1, 6 and 11) was used as template (*). The cDNA quality was verified by using *MtPdf2* primers (lanes 11-14). M: 1kb plus ladder.

4.3.4.3 Effects of the *Tnt1* insertion on plant growth

Homozygous *erf2-1/Tnt1* plants and *erf2-1/Wt* plants were cultivated for four weeks upon inoculation. Half of the mutant and wild type plants were inoculated with *R. irregularis*. In general, development (germination, flowering time point) and morphology of mutant plants was not affected in mutant plants, as compared to wild type plants.

The influence of the *Tnt1* insertion on plant growth was estimated by determining the root and shoot fresh weights. The root and shoot fresh weights of mycorrhizal and non-mycorrhizal *erf2-1/Tnt1* mutants were not significantly altered in comparison to *erf2-1/Wt* plants (figure 20A and B).

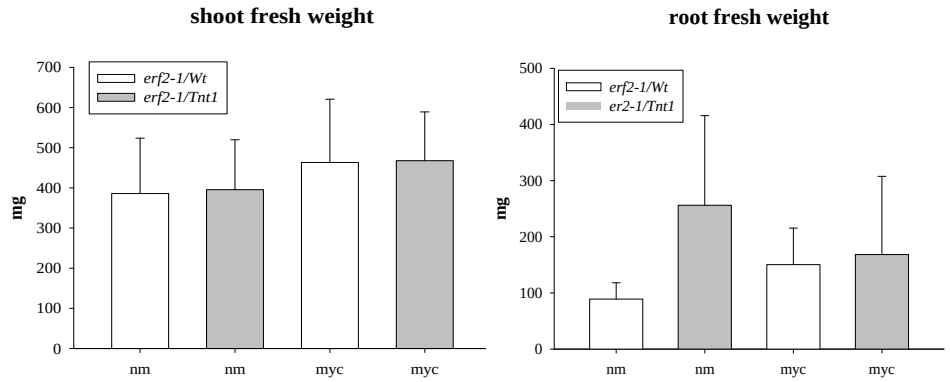

Figure 20: Shoot and root weights of *erf2-1/Tnt1* and *erf2-1/Wt* plants.
Fresh weights of four week old mycorrhizal and non-mycorrhizal plants were determined. Data represent mean values of ten biological replicates. Error bars represent the standard deviation. myc: mycorrhizal roots, nm: non-colonized roots.

4.3.4.4 *Erf2-1/Tnt1* mutants dispose a reduced arbuscule abundance

The fungal colonization of wild type and mutant plants was analyzed by WGA Alexa Fluor® 488 staining of mycorrhizal roots and counting of fungal structures. Roots of *erf2-1/Tnt1* plants and *erf2-1/Wt1* were fully colonized (frequency of colonization of 100 %). While the colonization intensity (M %) was not severely altered, a significantly lower arbuscule abundance per root system (A %) was observed in roots of the *erf2-1/Tnt1* mutant plants (figure 21A). No alterations of the arbuscule morphology could be observed *via* epifluorescence microscopy (figure 21B).

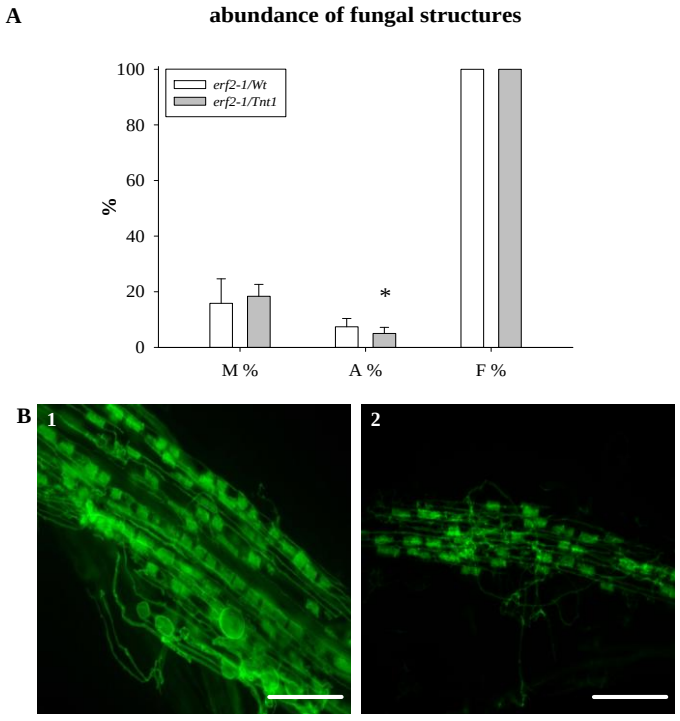

Figure 21: Phenotypical analysis of *erf2-1/Tnt1 and erf2-1/Wt* roots by WGA Alexa Fluor® 488 staining.
A) The abundance of fungal structures was calculated in ten biological replicates, four weeks post inoculation. M %: colonization intensity, A %: arbuscule abundance, F %: colonization frequency. B) Epifluorescence images of *erf2-1/Wt* (1) and *erf2-1/Tnt1* roots (2). The scale bar has a size of 200 µm. Asterisk: significance level ($p<0.05$) was calculated v*ia* Student´s t-Test.

4.3.4.5 Alterations in symbiosis marker gene expression in *erf2-1/Tnt1* roots

The influence of the *Tnt1* insertion on the AM symbiosis marker gene expression was investigated by qRT-PCR analysis. cDNA samples obtained from roots of four week old *erf2-1/Tnt1* and *erf2-1/Wt* lines were analyzed in two technical and up to four biological replicates. The presence of *MtErf2* transcripts in mutant plants and the read through the *Tnt1* insertion was shown. Nevertheless, a lower *MtErf2* transcript abundance was detected in *erf2-1/Tnt1* mutant plants, in comparison to the *erf2-1/Wt* lines (figure 22A). Reduced transcript levels were observed in *erf2-1/Tnt1* roots for genes encoding symbiosis-related nutrient transporters, such as an ammonium transporter (*MtAmt*), a phosphate transporter (*MtPt4*) and a proton ATPase (*MtHa1*) and TFs (e.g. *MtGras8*) (figure 22B, C, D, E). Also lower expression levels of fungal genes, like the. *R. irregularis* translation elongation factor, were observed (figure 22F). However, similar expression levels of the phosphate stress marker genes phospholipase D (Branscheid et al., 2010) and *Mt4* were observed in wild type and mutant plants (figure 22G, H).

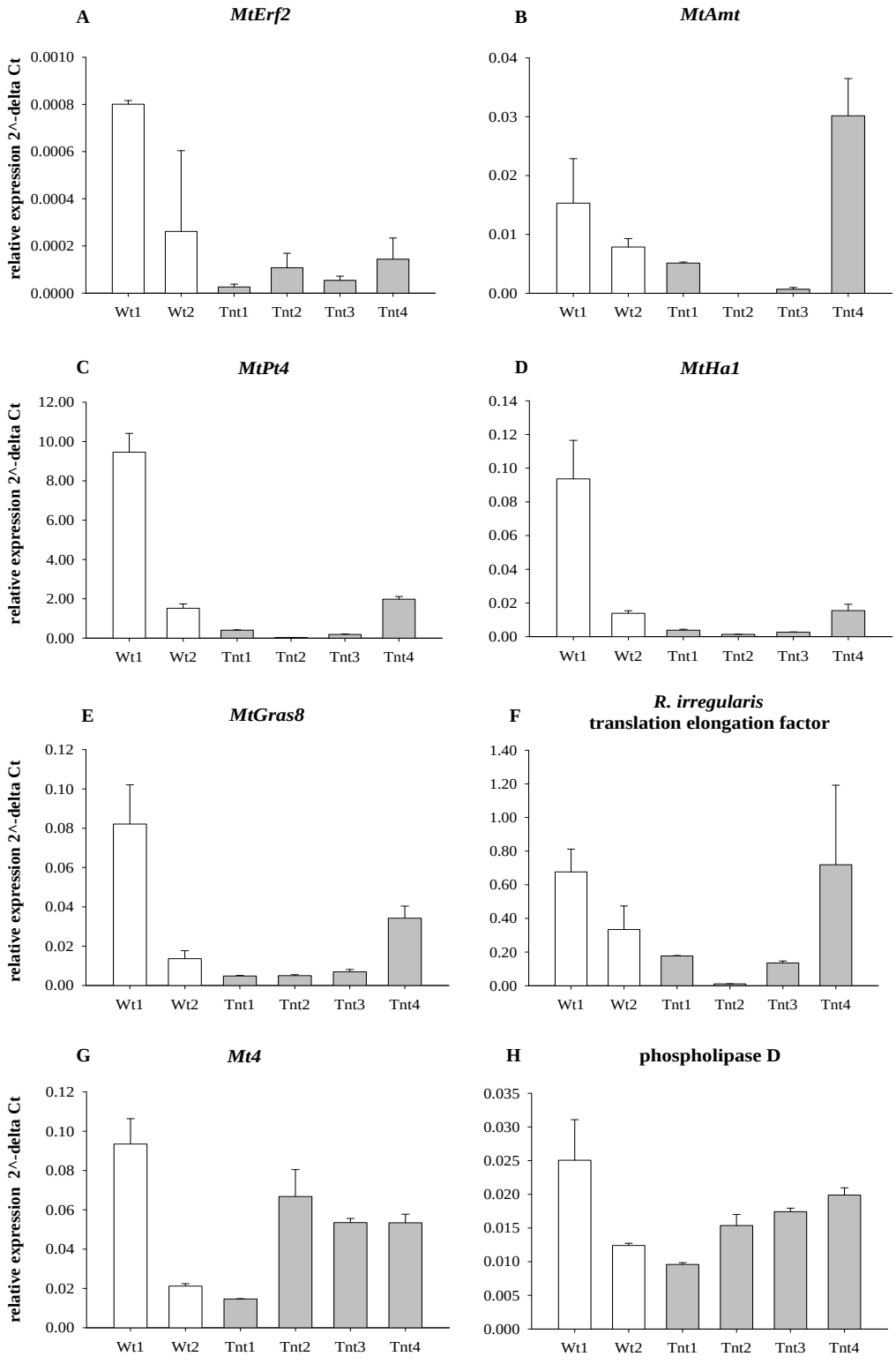

Figure 22: qRT-PCR analysis of *erf2-1/Tnt1* mutant and *erf2-1/Wt* plants.

cDNA samples obtained from four week old mycorrhizal roots were measured in two technical replicates. White bars represent *erf2-1/Wt* lines and grey bars display *erf2-1/Tnt1* lines. The expression data were normalized to the reference gene index, based on *MtPfdf2* and *MtEf1-α* (Kakar et al., 2008). Data represent two biological replicates of *erf2-1/Wt* plants and four biological replicates in case of *erf2-1/Tnt1* mutant lines.

4.3.5 Functional characterization of *MtGras8*

As described earlier, GRAS TFs, such as NSP1, NSP2 and RAM1, are essential for the signal transduction downstream of the common *sym* pathway during root endosymbioses (Catoira, 2000; Kalo et al., 2005; Hirsch et al., 2009; Cerri et al., 2012; Marsh et al., 2007; Gobbato et al., 2012; Delaux et al., 2013). Apart from that, GRAS TFs are involved in diverse developmental processes e.g. gibberellic acid signaling, root patterning and axillary meristem development (Di Laurenzio et al., 1996; Peng et al., 1997; Silverstone et al., 1998; Guether et al., 2009).

In our data set, a member of the GRAS TF family (*MtGras8*) displayed increased transcript abundance in arb cells and in whole mycorrhizal roots (see chapter 4.3.1 figure 14). Additionally, the posttranscriptional regulation of this TF by the phosphate dependent microRNA (miRNA). miRNA5204* was predicted recently (Devers et al., 2011). Accordingly, the phosphate-dependent regulation of *MtGras8* in regard to AM symbiosis should be investigated in this work.

4.3.5.1 Time course of miRNA5204* and *MtGras8* expression

To analyze the expression of miRNA5204* and *MtGras8* in response to the AM symbiosis, their transcript abundances were measured by qRT-PCR analysis in *M. truncatula* roots. Fungal colonization was estimated by determining expression levels of *MtPt4* and the *R. irregularis* translation elongation factor. The reverse transcription of RNA obtained from 1, 2, 3, 4, 5 and 6 week old mycorrhizal and non-mycorrhizal *M. truncatula* roots was performed with a mixture of an oligo-dT and miRNA5204* stem-loop primers.

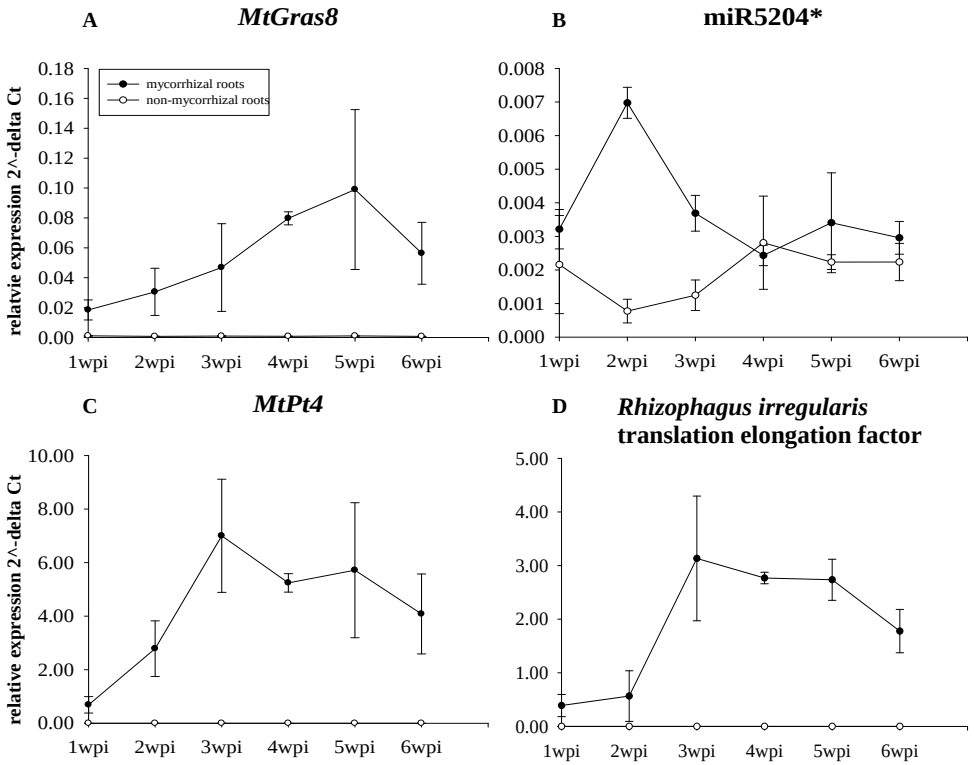

Figure 23: Time course of gene expression in mycorrhizal and non-mycorrhizal *M. truncatula* roots. Mean values of three biological and two technical replicates are displayed. The data were normalized to the expression levels of *M. truncatula* reference genes *MtPf2* and *MtEf1-α* (Kakar et al., 2008). Expression levels of the mature miRNA5204* were assessed by stem-loop qRT-PCR analysis (C). wpi: weeks post inoculation.

Similar expression patterns were observed for *MtGras8*, *MtPt4* and a *R. irregularis* translation elongation factor. Transcripts of these genes were exclusively detected in mycorrhizal roots (figure 23). A Spearman-rank correlation analysis confirmed a positive correlation between *MtGras8* and *MtPt4* expression levels. In contrast to the mycorrhizal marker genes, the highest miRNA5204* transcript levels were detected in two week old mycorrhizal roots (figure 23B).

4.3.5.2 Influence of the phosphate nutrition on *MtGras8* expression in mycorrhizal roots

The accumulation of *MtGras8* RNA and mycorrhizal marker genes was measured in five week old mycorrhizal roots of plants cultivated under different phosphate conditions. The cDNA samples were analyzed in three biological replicates *via* qRT-PCR measurements.

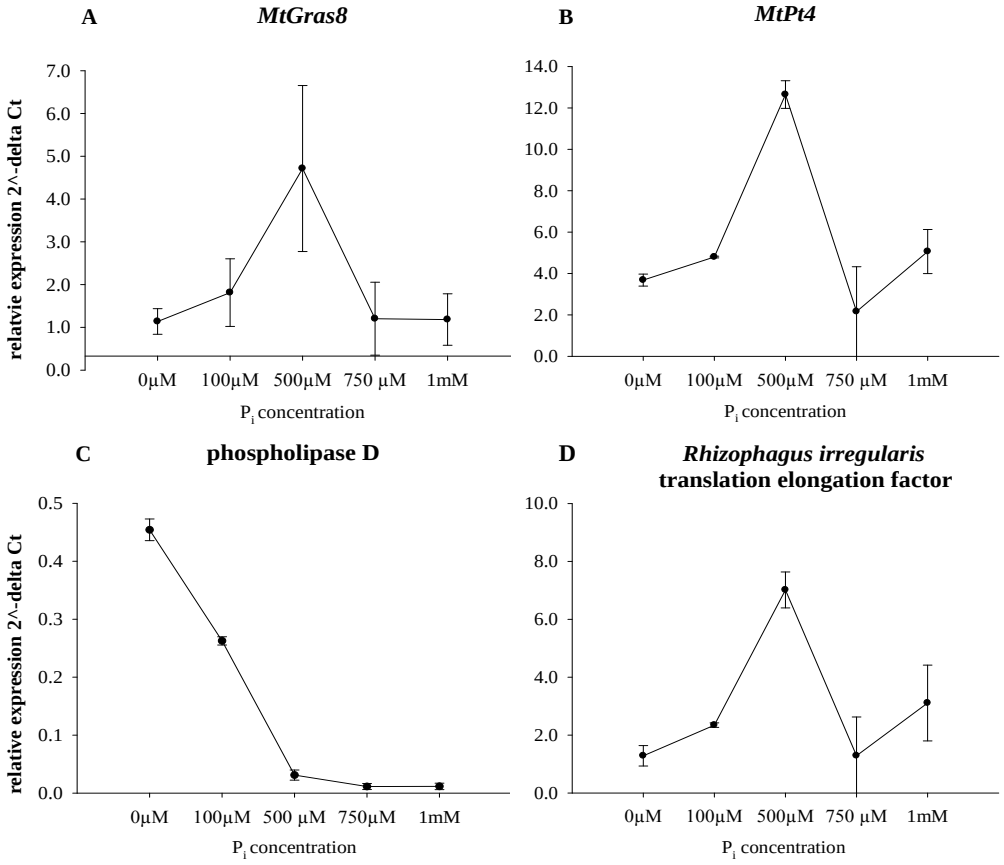

Figure 24: Expression data from *M. truncatula* A17 roots cultivated under different phosphate conditions.
The data represent mean values of three biological replicates. The expression data were normalized to the housekeeping gene index, based on *MtPf2* and *MtEf1-α* Ct values (Kakar et al., 2008). Phosphate concentrations are scaled on the x-axis.

MtGras8, *MtPt4* and the fungal translation elongation factor revealed similar expression patterns (figure 24A, B, D).The transcript levels of these genes increased up to 500 µM phosphate and declined at higher phosphate concentrations. This indicates that the *MtGras8* transcription levels are not directly affected by phosphate. As a control, the expression level of a phosphate starvation marker gene (phospholipase D) (Branscheid et al., 2010) was measured. As expected, phospholipase D expression decreased with increasing phosphate concentrations (figure 24C).

4.3.5.3 RNA-interference-mediated gene silencing of *MtGras8*

Due to a lack of an appropriate *M. truncatula Tnt1* mutant, RNA-interference (RNAi) constructs were expressed in *M. truncatula* roots under the control of two different promoters. The RNAi construct was expressed under a *35S* promoter to achieve an ubiquitous gene silencing in the whole root. A second experiment, more stringent gene silencing in mycorrhizal roots was achieved by cloning the RNAi constructs downstream of the promoter of the mycorrhizal induced phosphate transporter *MtPt4*.

4.3.5.3.1 MtGras8 gene silencing via 35S promoter-driven RNA-interference constructs

For the expression of RNAi constructs under *35S* promoter control, the 3`UTR sequence of the *MtGras8* gene was cloned in sense and antisense orientation in the pKDsRed-RNAi vector (Devers et al., 2013). As a control, a 327 bp long fragment of the GFP gene was cloned downstream of the *35S* promoter (Devers et al., 2013). Transgenic hairy roots, obtained by *Agrobacterium rhizogenes*-mediated root transformation, were subcultured as root organ cultures (ROCs) to obtain sufficient material for qRT-PCR analyses.

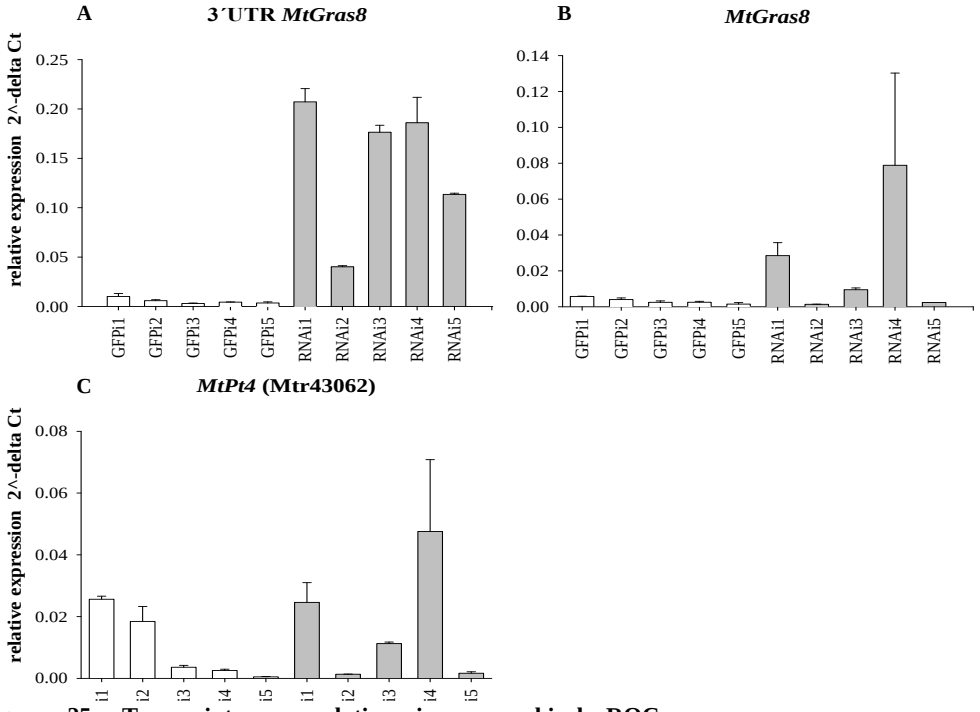

Figure 25: Transcript accumulation in mycorrhizal ROCs.

The data represent mean values of two technical replicates and were normalized to *MtEf1-α* and *MtGapdh* (Kakar et al., 2008). White bars display expression data of roots transformed with the $35S_{pro}$::*gfpi* vector control and grey bars represent the expression data of the $35S_{pro}$::*gras8-RNAi* lines**.**

Although the over-expression of the cDNA fragments used for the preparation of RNAi constructs (*MtGras8* 3´UTR) was confirmed in $35S_{pro}$::*gras8-RNAi* roots (figure 25A), endogenous *MtGras8*

transcript levels were not decreased in the RNAi lines. Also *MtPt4* and endogenous *MtGras8* transcript abundances were strongly correlated, indicating that the *35S* promoter-driven RNAi constructs did not affect the endogenous *MtGras8* transcript levels (figure 25B).

4.3.5.3.2 MtPt4 promoter-driven RNA-interference leads to a reduced MtGras8 transcript levels in mycorrhizal roots

Efficient gene silencing in mycorrhizal roots was achieved by cloning the 3´UTR sequence of *MtGras8* behind the mycorrhizal-specific *MtPt4* promoter. As a control, the full length *uidA* gene was cloned downstream of the *MtPt4* promoter. The RNAi construct ($MtPt4_{pro}$::*gras8-RNAi*) and the vector control ($MtPt4_{pro}$::*uidA*) were expressed in *M. truncatula* roots *via A. rhizogenes*-mediated root transformation. Roots were colonized with *R. irregularis* and harvested five weeks post inoculation. Mycorrhizal marker gene expression was determined by qRT-PCR.

The efficient gene silencing of *MtGras8* was confirmed by significantly reduced *MtGras8* transcript levels in $MtPt4_{pro}$::*gras8-RNAi* lines (figure 26A). Significantly lower *MtPt4* transcript abundances of *R. irregularis* transcripts (fatty acid desaturase (Gomez et al., 2009) and translation elongation factor (Helber et al., 2011) were detected, as compared to the control plants (figure 26B, E, F)

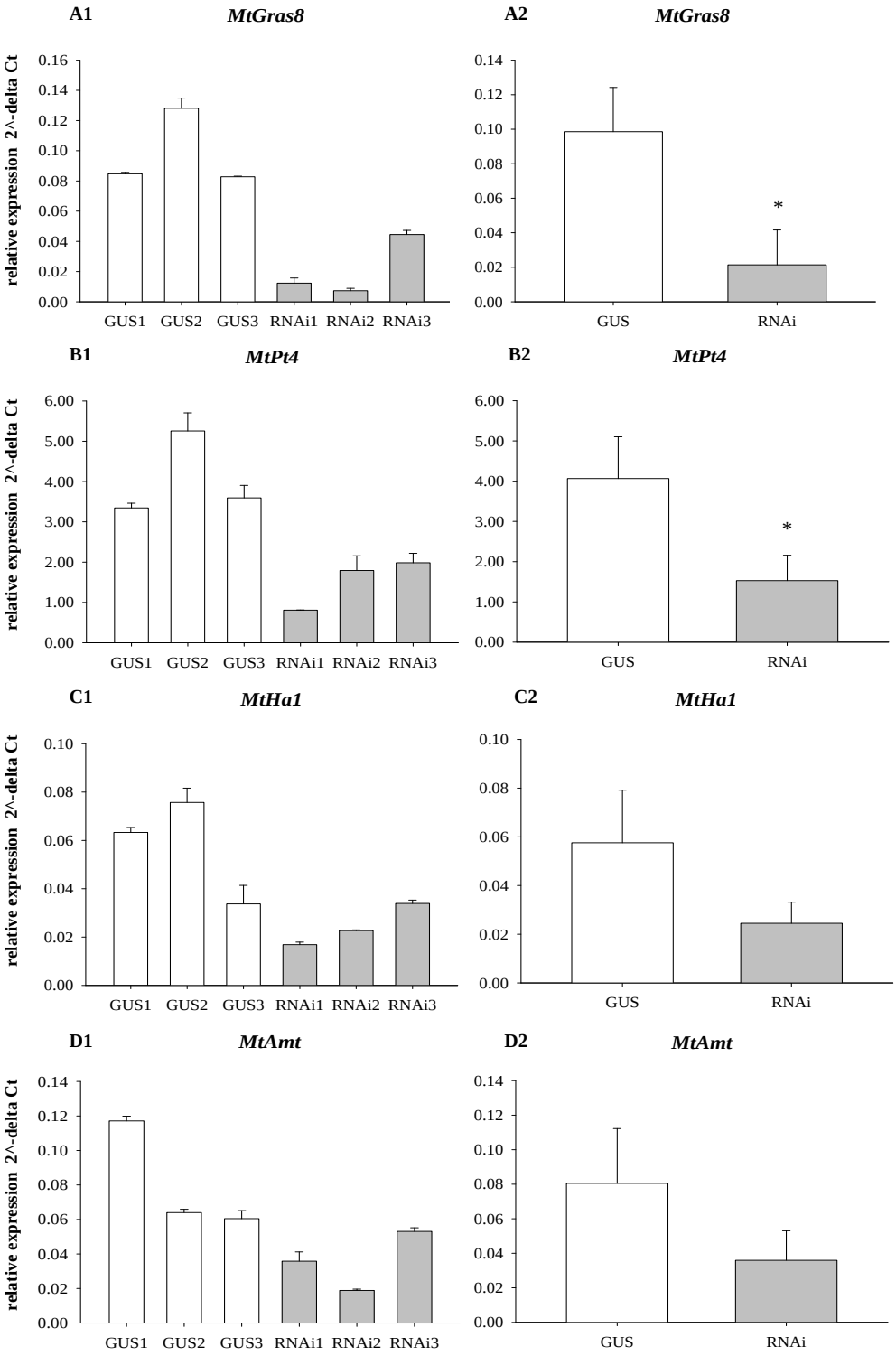

Figure 26: RNA accumulation in MtPt4$_{pro}$::*gras8-RNAi* and MtPt4$_{pro}$::*uidA* control roots. Mean values of two technical replicates are displayed in the left panel. In the right panel, mean values of three biological and two technical replicates are represented. The data were normalized to the reference genes index (*MtEf1-α*, *MtGapdh* and *MtPdf2*) (Kakar et al., 2008). White bars represent expression values measured in MtPt4$_{pro}$::*gus* control plants and transcript abundances of MtPt4$_{pro}$::*gras8-RNAi* lines are shown with grey bars. Asterisk: Student´s t-Test ($p < 0.05$). GUS: vector control including a *uidA* gene, GRAS: MtPt4$_{pro}$::*gras8-RNAi* line.

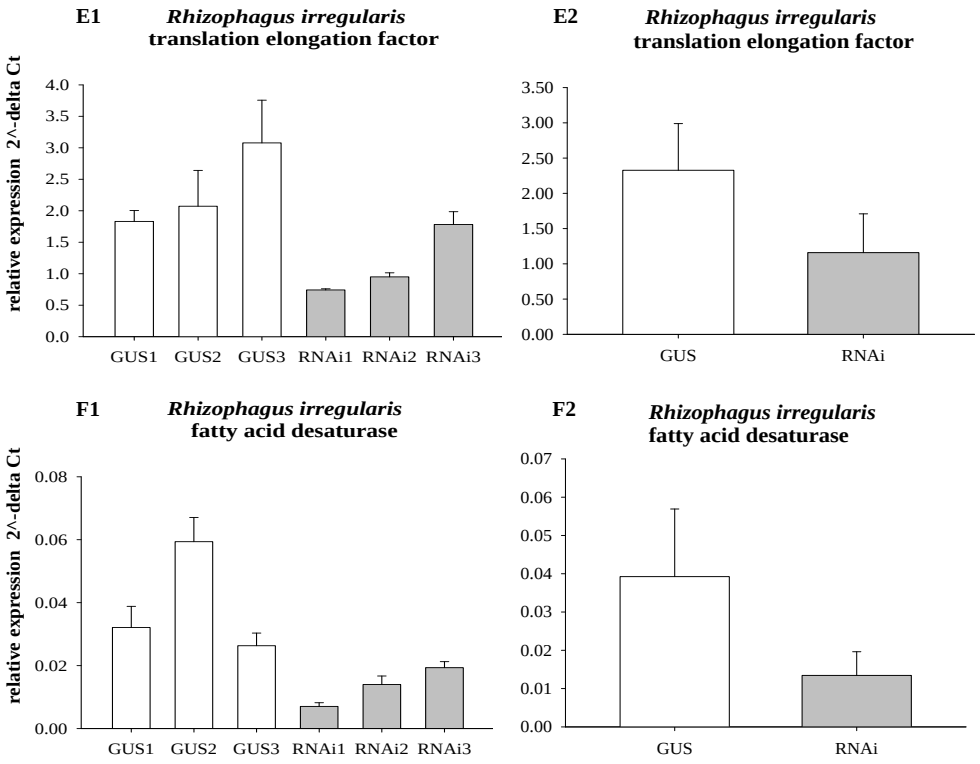

Continuation of figure 26: RNA accumulation in MtPt4$_{pro}$::*gras8-RNAi* and MtPt4$_{pro}$::*gus* control roots.

4.3.5.3.3 *MtPt4$_{pro}$::gras8-RNAi roots show altered arbuscule abundance and morphology*

The abundance of fungal structures in roots expressing the MtPt4$_{pro}$::*gras8-RNAi* and MtPt4$_{pro}$::*gus* constructs was verified upon WGA Alexa Fluor® 488 staining and epifluorescence microscopy. In general, silencing of *MtGras8* leads to a reduction in arbuscule abundance and colonization intensity.

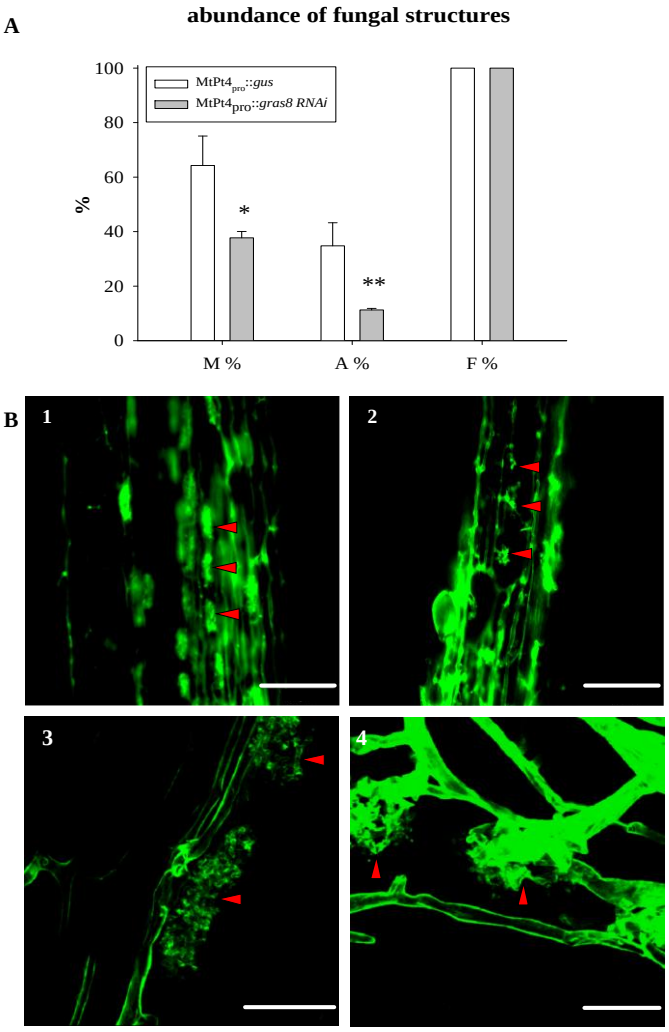

Figure 27: Estimation of fungal colonization and arbuscule morphology of MtPt4$_{pro}$::*gras8-RNAi* roots.
A) The abundance of fungal structures was analyzed in three biological replicates. M % colonization intensity, A % arbuscule abundance, F % colonization frequency. The significance levels were calculated *via* Student´s t-Test (*p*-value< 0.05 (*) and *p*-value< 0.01 (**)). B) The arbuscule morphology was examined by epi-fluorescence (1 and 2) and confocal microscopy (3 and 4) using 488 nm excitation wave length. 1 and 3 arbuscules of *MtPt4pro*::*gus* root. 2 and 4 arbuscules of the *MtPt4pro*::*gras8-RNAi* roots. The scale bars on epifluorescence images represent 100 µm. Confocal images represent a maximum projection of 20 optical sections on the z-axis taken at 3 µm intervals. The scale bars indicate a size of 25 µm.

Although the overall colonization frequency was unchanged, the arbuscule abundance and colonization intensity were significantly reduced in MtPt4$_{pro}$::*gras8-RNAi* roots (figure 27A). Numerous of deformed arbuscules were observed by epifluorescence microscopy. Around 70 % of the arbuscules in *MtPt4pro*::*gras8-RNAi* roots displayed an aberrant morphology, with less visible branches. Remarkably, only 20 % of the arbuscules in the control roots disposed a deformed phenotype. A detailed examination of the altered arbuscule morphology was mediated by confocal microscopy. Fully developed arbuscules were observed in roots transformed with the vector control (MtPt4$_{pro}$::*gus*). In contrast to this, the arbuscules of the MtPt4$_{pro}$::*gras8-RNAi* roots exhibited a dense round-shaped structure and did not fill-out the cell lumen (figure 27B2 and 27B4).

4.3.5.4 miRNA5204*-mediated posttranscriptional regulation of *MtGras8*

In order to investigate the role of miRNA5204*-mediated cleavage of *MtGras8* transcripts, a mis-expression of miRNA5204* was carried out in *M. truncatula* roots. Additionally, this approach should facilitate a specific gene silencing of *MtGras8.* The miRNA5204* was expressed under *MtPt4*- and an *A. thaliana* ubiquitin (*UBQ3*) promoter control in vectors containing an *mRFP* gene as visible marker. The $MtPt4_{pro}$::*miRNA5204** and UBQ_{pro}::*miRNA5204** constructs were assembled as earlier described by (Schwab et al., 2006) and expressed in *M. truncatula* roots *via A. rhizogenes*-mediated root transformation. Control plants were transformed with a *uidA* gene driven by the *MtPt4* promoter. Transgenic seedlings were harvested three weeks post inoculation with *R. irregularis*.

4.3.5.5 Stem-loop qRT-PCR analysis confirms the mis-expression of miRNA5204*

Transcript abundances of *MtGras8* and mycorrhizal marker genes were estimated by qRT-PCR, while the accumulation of the mature miRNA5204* was determined by stem-loop qRT-PCR, as described by Devers et al., (2011).

4.3.5.5.1 Expression of miRNA5204 under ubiquitin promoter control*

Expression miRNA5204* by the *UBQ3* promoter in mycorrhizal roots was confirmed by stem-loop qRT-PCR analysis in three of five UBQ_{pro}::*miR5204** lines (figure 28A). But miRNA5204* did not appear to affect *MtGras8* transcript levels. (figure 28).

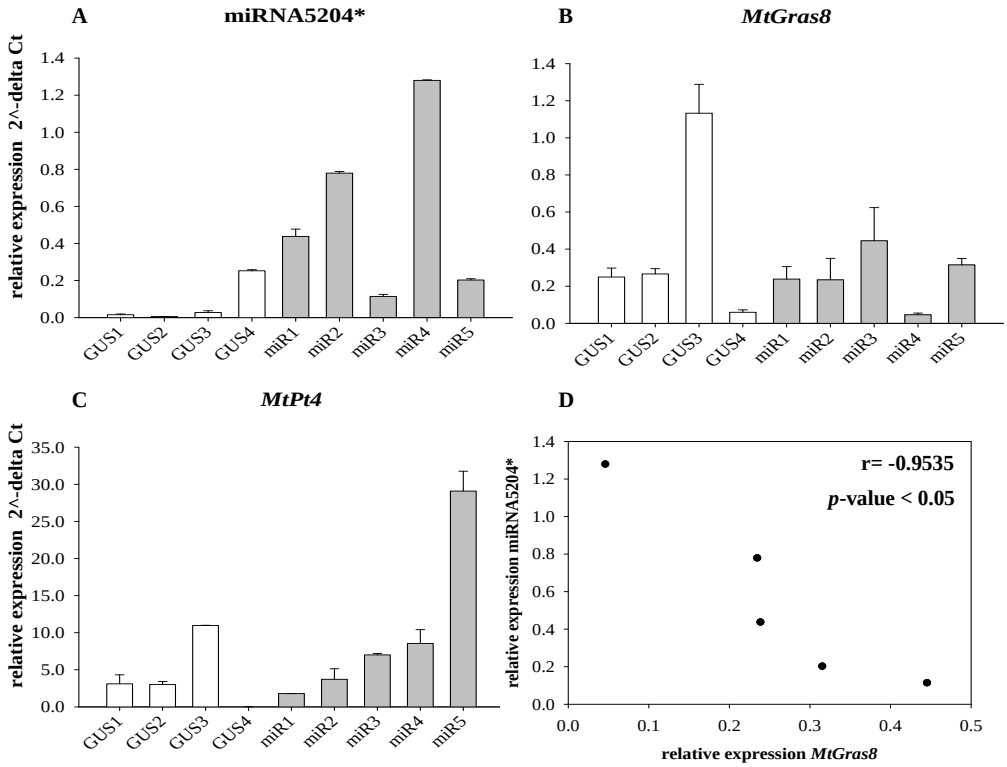

Figure 28: Stem-loop qRT-PCR analysis of UBQ_{pro}::*miR5204 roots.**

The cDNA samples were measured in two technical replicates. A) Transcript levels of mature miRNA5204* were measured by stem-loop qRT-PCR. B) and C) Expression levels of *MtGras8* and *MtPt4* were estimated by qRT-PCR analysis. All data were normalized to the reference genes *MtPdf2* and *MtEf1-α* (Kakar et al., 2008). White bars represent expression levels of control roots transformed with the empty destination vector and the transcript abundances of miRNA over-expression lines are displayed in grey bars. GUS: vector control, miR: miRNA5204* over-expression lines. D) Scatterplot of *MtGras8* and *miRNA5204** transcript abundances detected in UBQ_{pro}::*miRNA5204** lines. r= correlation coefficient, *p*-value of a Pearsson correlation analysis.

However, in the UBQ_{pro}::*miR5204** lines displaying a strong over-expression of miRNA5204* (such as in miR4) a lower *MtGras8* transcript abundance was found, in comparison to roots with weaker miRNA5204* transcription (such as in miR3 and miR5). Similar to the time course experiment (see chapter 4.3.5.1 figure 23), *MtGras8* and *MtPt4* seem to be co-regulated in roots of the control plants (figure 28B, C). Depicting the transcript levels of *MtGras8* and *MtPt4* measured in UBQ_{pro}::*miRNA5204** lines revealed a nearly linear relationship. Pearsson correlation analysis confirmed a negative, linear correlation (correlation coefficient r= -0.9535) of *MtGras8* and miRNA5204* transcript levels.

4.3.5.5.2 Mycorrhizal colonization of UBQ$_{pro}$::miRNA5204 roots*

The influence of the miRNA5204* mis-expression under *UBQ3* promoter control was unraveled by analyzing three-week-old mycorrhizal roots upon WGA Alexa Fluor® 488 staining. The analysis of fungal abundance in roots transformed with the UBQ$_{pro}$::*miRNA5204** construct revealed slightly, but non-significantly (Student´s t-Test *p*-value >0.05) reduced colonization (M %, A %, F %) (figure 29A).

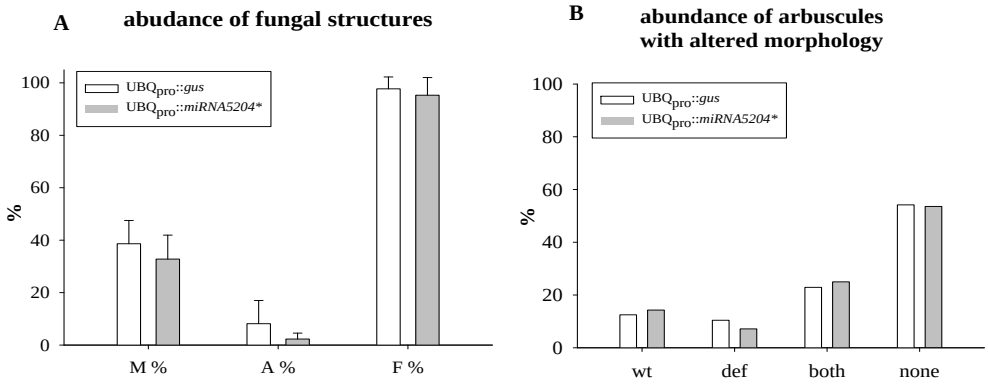

Figure 29: Alterations in fungal colonization and arbuscule morphology in UBQ$_{pro}$::*miRNA5204 roots.** A) The abundance of fungal structures was estimated in four biological replicates of three-week-old mycorrhizal roots, as described by Trouvelot et al., 1986. B) Number of root fragments with wild type (wt), deformed (def), both arbuscule types (both) and no arbuscules (none).

Additionally, arbuscule morphology was examined by epifluorescence and confocal microscopy. The arbuscules of UBQ$_{pro}$::*miRNA5204** roots had a similar morphology as arbuscules in the MtPt4$_{pro}$::*gras8-RNAi* roots. The arbuscules had a round-shaped structure, did not fill-out the whole cell lumen and seemed to be remarkably smaller than arbuscules observed in control plants. The quantification of deformed arbuscules was mediated by categorizing approximately 50 root fragments based on their arbuscule morphology in the following categories: wild type arbuscules, deformed arbuscules, both or no arbuscules. However, the number of root fragments containing deformed arbuscules was not statistically different in UBQ$_{pro}$::*miRNA5204** roots than from roots expressing the vector control (figure 29B).

4.3.5.5.3 Expression of miRNA5204 under MtPt4 promoter control*

In roots expressing miRNA5204* under the control of the *MtPt4* promoter, an elevated miRNA5204* transcript abundance was determined (figure 30A). But, *MtGras8* expression was not significantly altered in MtPt4$_{pro}$::*miRNA5204** lines compared to control plants. However, *MtGras8* expression level was found to be reduced in one MtPt4$_{pro}$::*miRNA5204** line (miR4), as compared to the roots of the control plants (figure 30B). Similar to the UBQ$_{pro}$::*miRNA5204** over-expression lines, the *MtPt4* transcription was not significantly affected by the miRNA5204* over-expression (figure 30C). A correlation between *MtGras8* and *MtPt4* transcript levels, as shown in the time course experiment (chapter 5.3.5.1 figure 23), could not be confirmed in this experiment (figure 30B and C).

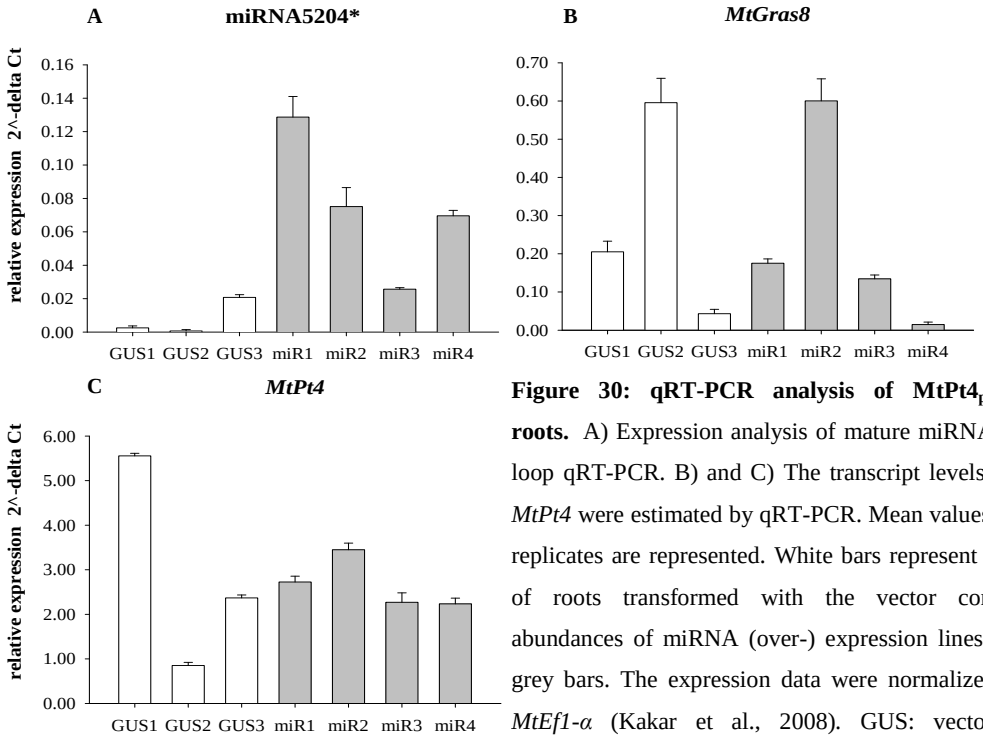

Figure 30: qRT-PCR analysis of MtPt4$_{pro}$::*miRNA5204 roots.** A) Expression analysis of mature miRNA5204* *via* stem-loop qRT-PCR. B) and C) The transcript levels of *MtGras8* and *MtPt4* were estimated by qRT-PCR. Mean values of two technical replicates are represented. White bars represent expression levels of roots transformed with the vector control. Transcript abundances of miRNA (over-) expression lines are displayed in grey bars. The expression data were normalized to *MtPdf2* and *MtEf1-α* (Kakar et al., 2008). GUS: vector control, miR: miRNA5204* over-expression line.

4.3.5.5.4 Mycorrhizal colonization of MtPt4$_{pro}$::miRNA5204 roots*

MtPt4 expression did not differ between MtPt4$_{pro}$::*miRNA5204** lines and the vector controls. Nevertheless, a significantly reduced colonization intensity and arbuscule abundance was observed (figure 31A). The arbuscule morphology was investigated by epifluorescence and confocal microscopy (figure 31C1-4). Remarkable smaller and round-shaped arbuscules were detected in the roots transformed with the MtPt4$_{pro}$::*miRNA5204** construct (figure 31C1, 2).

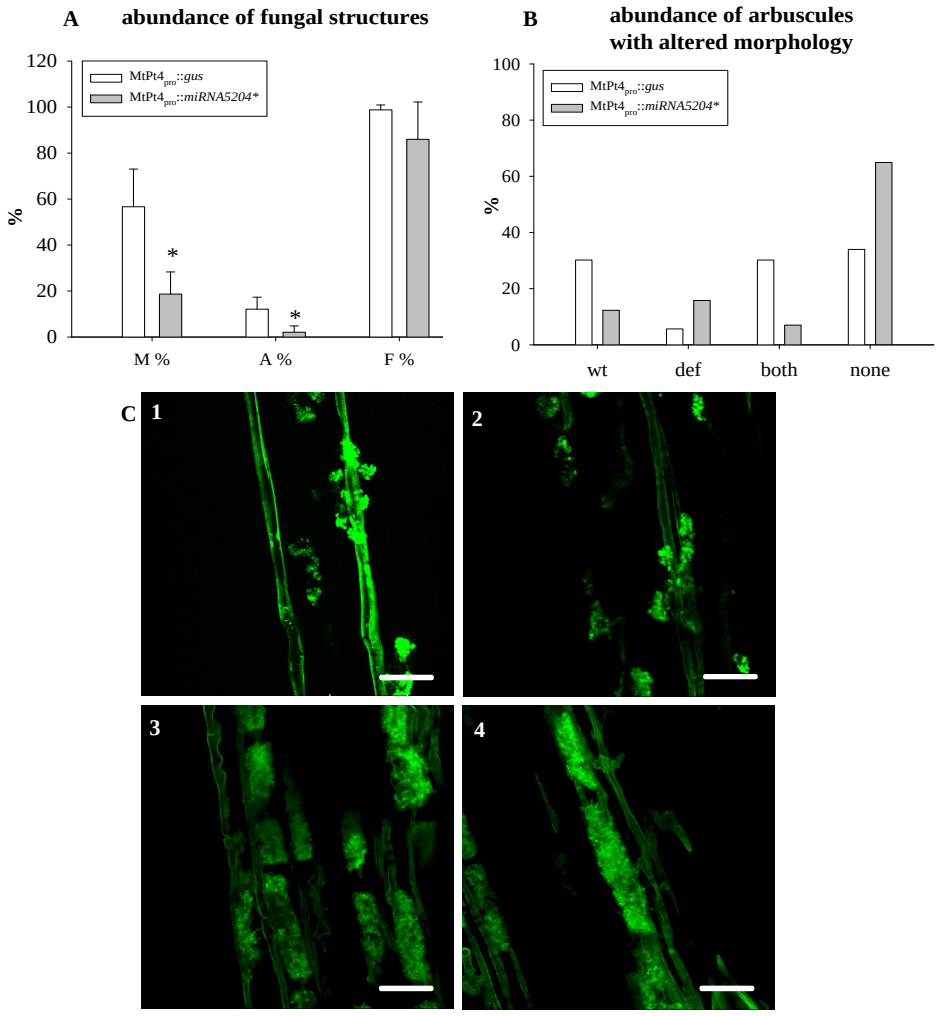

Figure 31: Fungal colonization and arbuscule morphology of MtPt4pro::*miRNA5204 roots.**
A) The abundance of fungal structures was determined in three to four biological replicates of three-week-old plants. Asterisk: Student´s t-Test (P<0.05). B) Number of root fragments with wild type (wt), deformed (def), both arbuscule types (both) and no arbuscules (none). B) Deformed arbuscules in three-week-old MtPt4$_{pro}$::*miRNA5204** roots were observed *via* confocal microscopy using a UV laser excitation of 488 nm (1 and 2). Fully developed arbuscules were detected in roots expressing the MtPt4$_{pro}$::*gus* constructs (3 and 4). Confocal images represent a maximum projection of 28 optical sections on the z- axis taken at 3 µm intervals. The scale bars represent 25 µm.

In contrast to the control roots, the arbuscules did not fill-out the cell lumen. The Arbuscules in MtPt4$_{pro}$::*miRNA5204** roots possessed a considerably smaller surface area and were less branched, in comparison to arbuscules observed in UBQ$_{pro}$::*miRNA5204** lines. Additionally, a three times higher number of deformed arbuscules and severely reduced number of wild type arbuscules were detected in MtPt4$_{pro}$::*miRNA5204**roots (figure 31B). In fact, no arbuscules were found in 65 % of the root fragments of the MtPt4$_{pro}$::*miRNA5204** lines (figure 31A). Overall, the arb cell-specific transcription of miRNA5204* revealed a more severe colonization phenotype than the expression of miRNA5204* under *UBQ3* promoter control.

4.3.5.6 MtGRAS8 forms heterodimers with MtNSP2 and MtRAM1

Possible protein-protein-interactions of GRAS8 and other known GRAS proteins are known to play essential roles during the root endosymbioses like MtNSP1, MtNSP2 and MtRAM1 were investigated *via* Bimolecular Fluorescence Complementation (BiFC) analysis. The full-length coding sequences (CDS) were fused to the C-terminal or N-terminal part of a Yellow Fluorescence Protein (YFP). *Agrobacterium tumefaciens* transformed with the corresponding constructs were co-infiltrated in *Nicothiana benthamiana* leaves. After three days the leaves were analyzed by confocal microscopy.

As a positive control, the interaction of two *A. thaliana* TCP TFs (AtTCP11 and AtTCP19) was confirmed (Arabidopsis Interactome Mapping, 2011) (figure 32A-C). As a negative control the E2-ubiquitin conjugase MtPHO2 (Medtr2g013650.1) was fused to the C- (^{C}) and N-(^{N}) terminal part of the YFP protein (figure 32G, M). Similar to previous BiFC analyses performed by Hirsch et al., 2009, the heterodimerization of MtNSP1 and MtNSP2 was observed (figure 32D-F). Co-infiltration of YFP^{C}-MtNSP2 and YFP^{N}-MtGRAS8 (figure 33H) revealed only weak YFP signals in the nucleus, but the co-expression of YFP^{C}-MtGRAS8 and YFP^{N}-NSP2 resulted in clear fluorescence signal (figure 32I). Nevertheless, no clear protein-protein-interaction could be confirmed in case of NSP1 and GRAS8 (figure 32K-L). Further, YFP fluorescence signals with nuclear localization could be observed after co-infiltration of YFP^{C}-MtGRAS8 and YFP^{N}-MtRAM1 (figure 32O). Similar to the interaction of GRAS8 and NSP2, no interaction could be detected upon co-expression of YFP^{C}-MtRAM1and YFP^{N}-MtGRAS8 in tobacco leaves. Taken together, a protein-protein-interaction of GRAS8 with NSP2 and RAM1 was shown.

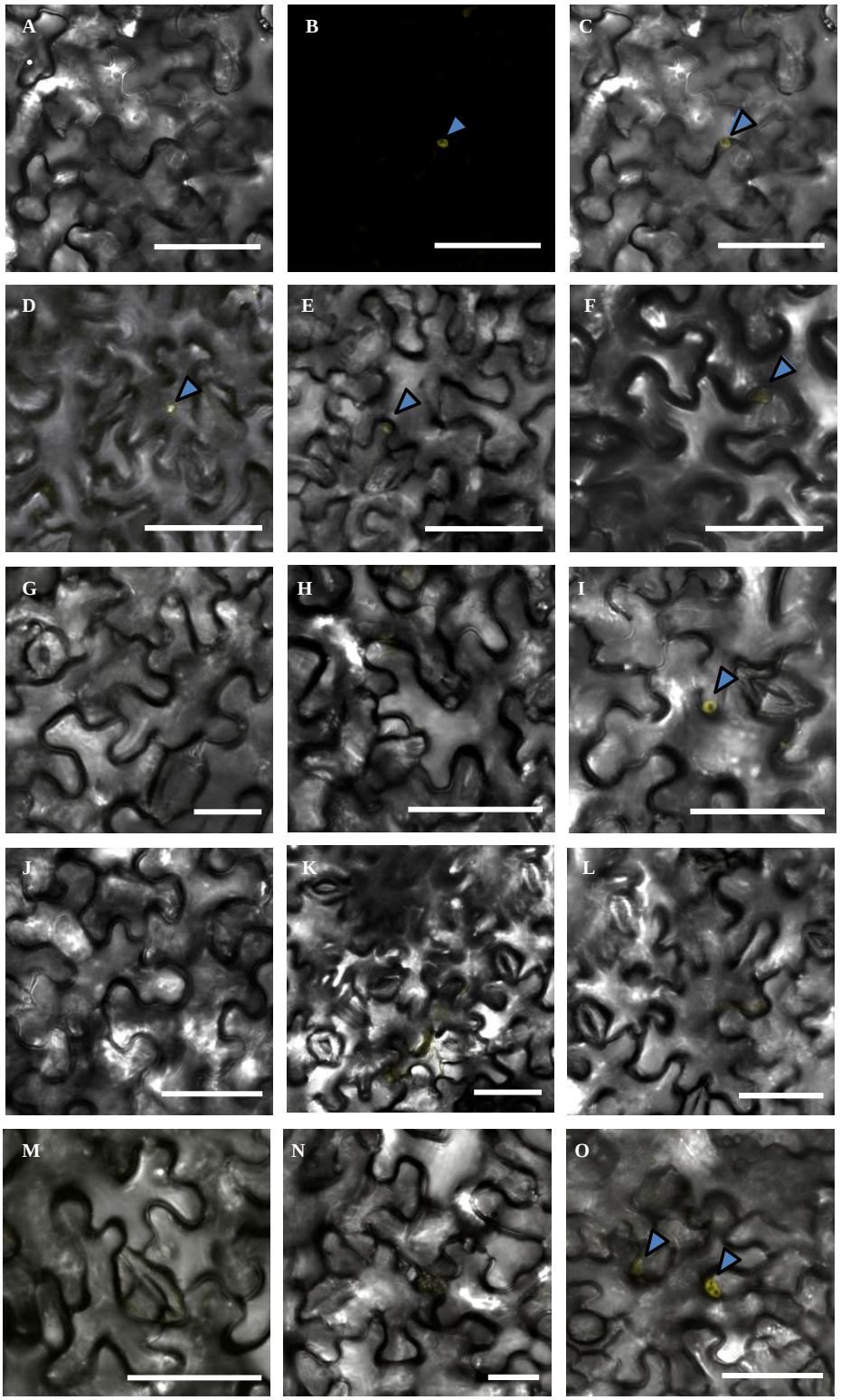

Figure 32: Bimolecular Fluorescence Complementation analysis. *A. tumefaciens* transformed with YFP-fusion constructs were co-infiltrated in six-week-old *N. benthamiana* leaves A)-C) YFP^C-AtTCP11 and YFP^N-AtTCP19 as a positive control, (A) overlay of YFP fluorescence picture (B) and bright field image (C). D)-F) MtNSP1::MtNSP2 heterodimer, D)-E) YFP^C-MtNSP2 and YFP^N-MtNSP1, F) YFP^C-MtNSP1 and YFP^N-MtNSP2, G) YFP^C-MtGRAS8 and YFP^N-MtPHO2, H) YFP^C-MtNSP2 and YFP^N-MtGRAS8, I) YFP^C-MtGRAS8 and YFP^N-MtNSP2, J) YFP^C-MtNSP1 and YFP^N-MtGRAS8, K)-L) YFP^C-GRAS8 and YFP^N-MtNSP1, M) YFP^C-MtPHO2 and YFP^N-MtRAM1, N) YFP^C-MtRAM1 and YFP^N-MtGRAS8, O) YFP^C-MtGRAS8 and YFP^N-MtRAM1. The scale bars have a size of 50 µm. YFP fluorescence in the nuclei was monitored using 514 nm excitation wavelength (blue arrows).

5 Discussion

5.1 Laser Capture Microdissection enables an analysis of transcriptomic changes at cell type-specific resolution

The arbuscular mycorrhizal (AM) symbiosis is formed between the majority of terrestrial land plants and arbuscular mycorrhizal fungi (AMF), which colonize the root cortex inter- and intracellularly. In the inner cortical root cells, arbuscules are formed, which are the site of nutrient transfer from the AMF to the host plant (Toth and Miller, 1984; Alexander et al., 1988; Alexander et al., 1989). During the arbuscule development a strong cellular reorganization takes place (Balestrini and Bonfante, 2005; Genre and Bonfante, 2005). In previous studies a massive reorganization of the cytoskeleton was observed in cortical cells harbouring arbuscules (Genre and Bonfante, 1997, 1998) and neighboring cells (Blancaflor et al., 2001). The arbuscules are surrounded by an extension of the plant plasma membrane, the periarbuscular membrane (PAM). Further, cell wall components are recruited for the arbuscule development (Balestrini and Bonfante, 2005) and microtubles as well as microfilaments arrange around the arbuscules (Genre and Bonfante 2002; Peterson et al., 2000). However, colonized and non-colonized cells are simultaneously present in mycorrhizal roots. Accordingly, an analysis of the genetic reprogramming of the root cells based on whole mycorrhizal roots is hindered by dilution effects, due to non-colonized cells or different symbiotic stages being present in one root system. These effects should be overcome by establishment of cell type-specific expression analysis. A combination of Laser Capture Microdissection (LCM) and Affymetrix GeneChip® Medicago genome array hybridization was applied to study the reprogramming of root cortical cells of *Rhizophagus irregularis* inoculated and non-inoculated *Medicago truncatula* roots with higher spatial resolution. Arbuscule-containing (arb) cells and non-arbuscule-containing (nac) cells were selected from *R. irregularis* inoculated roots. As a control, cortex (cor) cells of non-inoculated roots were analyzed.

As mentioned earlier, the tissue preparation for LCM is a critical step, because the morphological preservation and the extractability of the analytes (DNA, RNA, proteins or metabolites) have to be balanced (Kerk et al., 2003). Paraffin embedding enables a high quality tissue preservation (Goldsworthy et al., 1999; Gillespie et al., 2002; Kerk et al., 2003). But for paraffin embedding tissue fixation steps are required to preserve the tissue morphology. These fixatives negatively influence the extractability of the analytes (RNA) (Bustin, 2000; Gillespie et al., 2002; Kerk et al., 2003). In this work this problem was overcome by preparation of cryosections. In contrast to paraffin sections, a treatment with fixatives, such as formaldehyde and ethanol, is not required for cryosections (Asano et al., 2002; Casson et al., 2005; Schad et al., 2005). Due to high water content and huge vacuoles in plant tissues, the formation of ice crystals takes place during the

freezing process, which lead tissue disruption (Casson et al., 2005, Nakazono et al., 2003). Nevertheless, working at low temperatures hampers the RNase activity and enables the extraction of high quality RNA (Goldsworthy et al., 1999; Nakazono et al., 2003; Casson et al., 2005).

The establishment of cryosections enabled the extraction of RNA with sufficient quality and quantity for microarray hybridization. Similar to previous Laser Capture Microdissection experiments (Nakazono et al., 2003; Cai and Lashbrook, 2006; Balestrini et al., 2007), around 50-100 ng RNA could be obtained from 5000-10000 cells isolated from cryosections. The RNA quality and quantity was analyzed *via* Bioanalyzer measurements. As mentioned in chapter 3.2.7.3, the RNA Integrity Number (RIN) gives information about the RNA quality. While a RIN of 1 indicates totally degraded RNA, a RIN of 10 denotes intact RNA (Schroeder et al., 2006). In this work, only RNA samples with a RIN larger than 6 were pooled and successfully used after an amplification step for the Affymetrix GeneChip® Medicago genome array hybridization.

5.2 Transcription factors with differential expression in mycorrhizal root cells

As described in earlier, transcription factors (TFs) genes are assumed to play key roles in the reprogramming of root cortex cells during root endosymbioses. As mentioned in chapter 1.4, members of the GRAS, CAAT-box binding, as well as the AP2/ERF TF families have been shown to act as key regulators in root endosymbioses-related signal transduction (Combier et al., 2006; Andriankaja et al., 2007; Hirsch et al., 2009; Cerri et al., 2012). Sixty-eight significantly regulated TFs were detected in the cell type-specific data set represented here.

According to a previous transcriptome analysis of mycorrhizal roots, the elevated expression of a MYB TF family member, *MtMyb1*, was confirmed in arb and nac cells and mycorrhizal roots (Hogekamp et al., 2011; Hogekamp and Küster, 2013). The induced expression of *MtMyb1* in arb and nac cells was confirmed by promoter::*uidA* fusions in *M. truncatula* roots. In general, the induction of MYB TFs was observed upon transriptome analyses of whole mycorrhizal roots (Liu et al., 2003; Guether et al., 2009; Hogekamp et al., 2011). MYB TFs are known to play a role in secondary metabolism and regulation of the anthocyanin biosynthesis (Martin and PazAres, 1997; Jin and Martin, 1999; Endt et al., 2002; Peel et al., 2009). These findings are in line with an elevation of the secondary metabolism in mycorrhizal roots during the AM symbiosis (Harrison and Dixon, 1994; Fester et al., 2002; Strack et al., 2003). Especially chalcone synthase transcripts are highly abundant in arb cells, which is known to be regulated by MYB TFs (Harrison and Dixon, 1994). Recent studies described a mycorrhizal induced MYB TF, LjMAMI, which seems to be involved in the root branching and growth control and might play a role in mycorrhiza-independent phosphate starvation responses (Volpe et al., 2013). Additionally, MYB TFs seem to be required for the induction of nodule development upon nitrate starvation (Colebatch et al., 2004). These findings indicate that MYB TFs are important for both root endosymbioses. From

the co-induced expression of *MtMyb1* in arb and nac cells, a role of this TF in the reprogramming of both cortical cell types during the fungal colonization can be concluded.

An elevated expression of two CAAT box binding TFs, *MtCbf1* and *MtCbf2* in arb and nac cells detected, which is in line with previous cell type-specific studies (Hogekamp et al., 2011).

Also a member of the remorin family, MtSYMREM2, has been identified with strongly induced expression in arb and nac cells. These filamentous proteins are known to be involved in signal transduction, secretory processes and root endosymbioses (Fedorova et al., 2002; Wienkoop and Saalbach, 2003; El Yahyaoui et al., 2004; Ivanov et al., 2010; Lefebvre et al., 2010). Remorins can be subdivided in six groups upon their protein domain structure (Raffaele et al., 2007). While their C-terminus facilitates homo-oligomerization, their N-terminus is intrinsically disordered (Raffaele et al., 2007; Marin and Ott, 2012; Marin et al., 2012). The N-terminus can be phosphorylated, as it was described for AtREM1.3, and seems to regulate the strength of protein-protein-interactions mediated by the C-terminus (Marin and Ott, 2012; Marin et al., 2012). Ten remorins are known in *M. truncatula* genome (Raffaele et al., 2007).

Phylogenetic analysis revealed that MtSYMREM2 was identified as an alternative splice product of MtREM2.1, which is functionally not characterized so far and belongs to the group 2 remorins, such as MtSYMREM1 (Lefebvre et al., 2010). However, MtSYMREM1 showed only around 44.4 % sequence identity to MtSYMREM2 on amino acid level. It is supposed that SYMREM1 plays a role in cellular signal transduction, upon formation oligo- and heterodimers with symbiosis-related receptor-like kinases, such as NFP, LYK3, DMI3 and is involved in the polar growth of infection structures during root nodule symbiosis (Lefebvre et al., 2010; Jarsch and Ott, 2011; Popp and Ott, 2011; Toth et al., 2012). But MtSYMREM2 shares weaker sequence similarity (39.3 %) to another group 2 remorin, LjSYMREM1, which is known to be induced during the late stages of AM symbiosis in *Lotus japonicus* roots (Kistner et al., 2005; Toth et al., 2012). Interestingly, several members of group 1, 2, 5 and 6 remorins include in their N-terminal region putative phosphorylation sites (Marin and Ott, 2012). In case of LjSYMREM1 the symbiosis-related phosphorylation by NFR1 and SYMRK was confirmed *in vivo* (Toth et al., 2012). In general, remorins might play fundamental roles during infection processes as well as in both root endosymbioses, the root nodule and the AM symbiosis, respectively. A role of MtSYMREM2 during AM symbiosis related signal transduction is suggested.

Significantly elevated transcript levels of *MtSWIRM1* were detected in arb and nac cells. This TF belongs to the SWIRM protein family, which is named according to the first identified TFs of this family (SWI3P, RSC8P and Moira). SWRIM TFs have been found in several plant species, such an *Arabidopsis thaliana*, *M. truncatula*, *Oryza sativa* and *Zea maydis*. These TFs seem to be involved in developmental processes (flower development) and responses against abiotic stress

(like cold and heat stress) (Gao et al., 2012). However the role of SWIRM proteins during AM symbiosis was not described so far.

The cell type-specific transcriptome analyses identified also two Homeobox TF genes (*MtHomeobox1* and *MtHomeobox 40*) with induced expression in mycorrhizal roots. While *MtHomeobox1* is arb cell-specifically induced, *MtHomeobox40* seemed to be stronger accumulating in nac cells. Homeobox proteins contain a characteristic homeodomain (HD-domain) and are mostly expressed in shoot and root meristems. They are often involved in the control of lateral shoot and roots development, such as WUSCHEL, REVOLUTA, PHABULOSA, HB1 and NDX of *A. thaliana* (Talbert et al., 1995; Schoof et al., 2000; McConnell et al., 2001; Gronlund et al., 2003; Ariel et al., 2010). In *M. truncatula* a class III HOMEODOMAIN-LEUCINE ZIPPER TF, MtHD-ZIP III, is known to be involved in nodule development (Boualem et al., 2008).

Significantly elevated transcript levels of two AP2/ERF TFs, *MtAba1* and *MtErf2* were detected in arb and nac cells upon microarray hybridization. Phylogenetic analyses revealed that MtERF2 seems to belong to the ERF TF subfamily. Members of this subfamily activate the gene expression in ethylene-responsive manner *via* binding to a ”GCC” motif of their target promoters and seem to be involved in the pathogen responses (Ohmetakagi and Shinshi, 1995; Shinshi et al., 1995; Büttner and Singh, 1997). MtERF2 is closely related to TFs involved in drought stress responses, such as a *Glycine max, Halimodendron halodendron* and *A. thaliana* DEHYDRATION-RESPONSIVE ELEMENT BINDING PROTEIN (AtDREB), which belong to the sub group of the ERF TFs (Riechmann, 2000; Riechmann et al., 1998, Sakuma et a., 2002). DREB proteins contain a single AP2-domain and bind to dehydration responsive elements (DRE) of promoter *cis*-elements (Okamuro et al., 1997). DREB proteins are involved in salt and cold stress responses (Riechmann, 2000; Pradeep et al., 2006). On the other hand, MtERF2 disposed only weak sequence similarities (20-25 %) to ERF TFs involved in the Nod-factor signaling, like ERN1, ERN2 and ERN3 (Andriankaja et al., 2007; Middleton et al., 2007). Screening the *Medicago truncatula* Gene Expression Atlas for *MtErf2* transcript levels in *M. truncatula* also supports a putative function of MtERF2 under salt stress responses. Elevated *MtErf2* transcript levels were found in shoots and roots of *M. truncatula* plants cultivated under drought and salt stress conditions. These data indicate that MtERF2 might play a role in the stress responses rather than being directly involved in specific symbiosis-related signal transduction, as it was described for ERN1, ERN2 and ERN3. Further, orthologous sequences of MtERF2 in legumes (*Glycine max*) and non-legumes (*H. halodendron, A. thaliana*) imply that MtERF2 might be not only conserved in legume species. On the other hand, an elevated drought stress tolerance is well described in mycorrhizal roots (Auge, 2001; Auge et al., 2001; Ruiz-Lozano, 2003). Accordingly, due to the

mycorrhizal-specific transcription of MtERF2 (in arb and nac cells) this ERF TF might represent a link to the drought stress tolerance of mycorrhizal plants.

To investigate the role of *MtErf2* during the AM symbiosis, a homozygous *M. truncatula* R108 *Tnt1* mutant line was characterized. Unfortunately, *MtErf2* transcripts were still detectable in homozygous mutant plants suggesting a read through the *Tnt1* insertion. Furthermore, only slightly reduced *MtErf2* and diagnostic marker gene (*MtPt4*, *MtAmt1*, *MtHa1*) transcript levels were observed in mycorrhizal mutant plants, as compared to the wild type plants. However, a significant lower arbuscule abundance was observed in mycorrhizal mutant roots. But, neither mutant, nor wild type plants showed enhanced growth upon mycorrhizal colonization, which was due to a rather low fungal colonization of both plant lines. The *M. truncatula R108* background of the *Tnt1* mutant population shows a significantly different response to phosphate fertilization as the *M. truncatula* cultivar Jemalong (Devers et al., 2013). To promote growth of the *Tnt1* mutant lines, rather high phosphate concentrations (250 µM) were applied. It is well described, that upon a high phosphate concentration in the soil the AM symbiosis is repressed (Nagy et al., 2009; Branscheid et al., 2010). The cultivation of the plants under more stringent phosphate starvation conditions will reveal higher colonization levels, which will facilitate a detailed examination of the mutant phenotype.

A further TF gene with strongly increased expression in mycorrhizal roots showed strong sequence similarity to GRAS TF genes. As mentioned earlier, GRAS TFs are involved in several developmental processes, such as the gibberellic acid signaling, root patterning, axillary meristem development and play essential roles during root endosymbioses. SHORTROOT (SHR) activates the expression of SCARECROW (SCR) upon heterodimerization to regulates the root patterning (Nakajima et al., 2001; Sabatini et al., 2003; Cui et al., 2007). During the root nodule symbiosis (RN symbiosis) NSP1 and NSP2 form a heterodimer to bind to the "AATTT" motif of *ERN1*, *ENOD11* and *NiN* gene promoters (Hirsch et al., 2009; Cerri et al., 2012). During AM symbiosis another GRAS TF, RAM1, interacts with NSP2 to mediate the symbiosis-related gene expression of RAM2, which might promote the fungal infection (Gobbato et al., 2012). Recent studies proposed that NSP1 and NSP2 also regulate the AMF colonization during AM symbiosis (Maillet et al., 2011; Delaux et al., 2013).

A strong mycorrhizal induced expression of *MtGras8* was confirmed in this work in arb and nac cells by cell type-specific qRT-PCR and expression of promoter-reporter fusions. Previous microarray experiments revealed a strong mycorrhizal-specific expression of different GRAS TF genes, such as SCR3, SCR1, SCR-like, in *M. truncatula* and *L. japonicus* roots (Gomez et al., 2009; Guether et al., 2009; Hogekamp et al., 2011). An induction of *MtGras8* was also described in *Funneliformis mosseae*-inoculated *M. truncatula* roots (Hogekamp et al., 2011).

Screening the *Medicago truncatula* Gene Expression Atlas for *MtGras8* transcript accumulation across different *M. truncatula* tissues revealed that the highest transcript levels were observed in arb cells and whole mycorrhizal roots. Lower transcript levels were detected in non-mycorrhizal roots and in mycorrhizal *dmi3* mutant roots (figure 33).

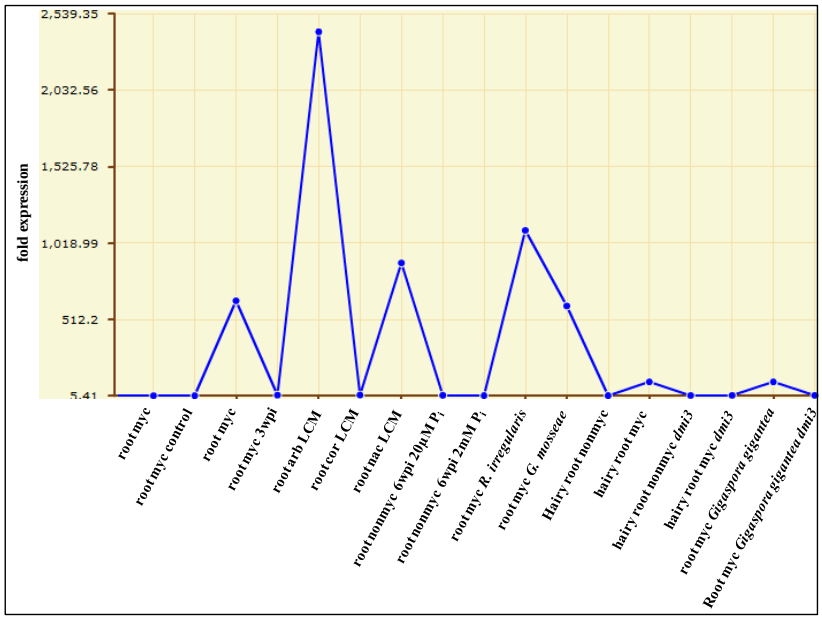

Figure 33: Expression pattern of *MtGras8* in *Medicago truncatula.*

The graphic displays *MtGras8* transcription levels in roots of *M. truncatula* wild type and mutants cultivated under different growth conditions. The data were obtained from the *Medicago truncatula* Gene Expression Atlas (http://mtgea.noble.org). arb: arbuscule-containing cells, cor: cortical cells of non-colonized roots, nac: non-arbuscule-containing cells of mycorrhizal roots, LCM: cDNA samples from cells isolated *via* Laser Capture Microdissection, myc: mycorrhizal roots, nonmyc: non-colonized roots, dmi3 myc: mycorrhizal roots of *M. truncatula dmi3* mutants.

Also in this work, *MtGras8* transcript accumulation was exclusively detected in mycorrhizal roots. Further, *MtGras8* seems to be co-regulated with symbiosis-specific phosphate transporter *MtPt4*.

Mycorrhizal colonization of plants and the efficiency of the AM symbiosis with regard to an improved phosphorous nutrition are strictly dependent on the soil phosphate content (Smith et al., 2003; Nagy et al., 2009; Branscheid et al., 2010). Therefore, the impact of phosphate on the symbiosis-related *MtGras8* expression was investigated in this work. Phosphate gradient experiments again showed a similar expression pattern of *MtPt4*, *R. irregularis* translation elongation factor and *MtGras8*. Their transcript levels increased drastically in mycorrhizal roots up to a phosphate content of 500 µM in the experimental system and declined at higher phosphate concentration. However, a clear correlation of *MtGras8*, *MtPt4* and *R. irregularis* translation elongation factor transcript levels propose that *MtGras8* are not directly affected by phosphate.

5.3 *MtGras8* plays a role during the arbuscule development and maintenance

Amino acid sequence alignments revealed that orthologous sequences of *MtGras8* represent DELLA proteins (GAI and RGL-like), which were exclusively found in many legume species, such as *Glycine max* and non-legumes such as *Populus trichocarpa*. But no strong sequence similarity to GRAS TF family members in *A. thaliana*, such as AtSCL3, could be detected. These findings indicate that MtGRAS8 is conserved in legumes and in non-legumes. DELLA proteins, such as GAI and RGA are known to be involved in the phosphate starvation responses (Eckardt, 2002; Jiang et al., 2007). These proteins facilitate the repression of the GA mediated growth promotion under phosphate depletion conditions. Under phosphate repletion conditions DELLA proteins are ubiquitinated to enhance the GA mediated growth induction (Jiang et al., 2007). Due to the improved phosphate status of the plant roots during the AM symbiosis, a similar function of MtGRAS8 is unlikely.

Further, MtGRAS8 shares a higher sequence similarity (34 %) to MtRAM1, than to MtNSP1 and MtNSP2 (25-30 %). MtNSP1 and MtNSP2 seem to be closely related to GRAS TFs of the SCARECROW family in *A. thaliana*. SCARECROW-like GRAS proteins form a different sub group of GRAS proteins. Like MtRAM1 (Gobbato et al., 2012), MtGRAS8 seems to be conserved in the whole plant kingdom. But, no orthologous proteins have been found in the non-mycorrhizal plant *A. thaliana*. This points to a specific function of both GRAS TF proteins during AM symbiosis. As mentioned earlier, RAM1 regulates the expression of a glycerol acyltransferase (RAM2). RAM2 might be involved in the phospholipid, lyso-phosphatidylcholin and cutin/suberin biosynthesis (Wang et al., 2012). It is suggested that RAM1and RAM2 are involved in the control of the hyphopodia formation (Gobbato et al., 2012).

Further clues about the symbiosis-related function of *MtGras8* should be obtained upon a homology-dependent gene silencing. A *35S* promoter-driven RNAi construct was overexpressed in *M. truncatula* roots, but the *MtGras8* and *MtPt4* transcript abundances were not significantly altered in the RNAi lines. The *35S* promoter has been shown to be only very weakly active in arbuscule-containing cells (Pumplin and Harrison, 2009). Therefore, it might be assumed that the RNAi construct was also only weakly expressed in arbuscule-containing cells and was thus not affecting *MtGras8* transcript levels.

As an alternative, the RNAi construct was driven by the *MtPt4* promoter, which mediates a strong transcription in arbuscule-containing cells were *MtGras8* transcripts are highly abundant (Harrison, 2005; Javot et al., 2007b). An efficient down-regulation of *MtGras8* and significantly lower *MtGras8* transcript levels were confirmed in $MtPt4_{pro}$::*gras8-RNAi* roots. Accordingly, the *MtPt4* promoter enabled a more efficient gene silencing than the *35S* promoter in mycorrhizal roots and presumably specifically in arbuscule-containing cells. From a reduced expression of

R. irregularis transcripts and mycorrhizal-specific nutrient transporter genes, such as *MtPt4, MtAmt* and *MtHa1* in MtPt4$_{pro}$::*gras8-RNAi* roots an affected fungal colonization and symbiosis function can be concluded.

A significantly reduced colonization intensity and significantly lower arbuscule abundance were observed in MtPt4$_{pro}$::*gras8-RNAi* roots. Additionally, the proportion of deformed arbuscules was increased, as compared to mycorrhizal control roots. Around 70 % of the arbuscules in Mtpt4$_{pro}$::*gras8-RNAi* roots disposed a remarkable reduced surface area and were less branched. Due to the reduced surface area, it can be assumed that a lower number of nutrient transporters might be localized in the PAM. Accordingly, the declined *MtPt4* expression in MtPt4$_{pro}$::*gras8-RNAi* roots might be the consequence of a reduced number of arbuscules, as well as a lower number of nutrient transporters per arbuscule. A similar phenotype was observed in roots of *mtpt4* mutants (Javot et al., 2007b). But it is unclear if the fungal structures identified in MtPt4$_{pro}$::*gras8-RNAi* roots are degenerated and not functional, similar to arbuscules observed in *mtpt4* mutants (Javot et al., 2007b). Due to permanent arbuscule formation and degradation processes in mycorrhizal roots, a basal level of degenerated arbuscules (20 %) was observed in the control roots. Accordingly, arbuscules with an aberrant morphology could not be distinguished from collapsing arbuscules (due to the arbuscule turn-over) in this study. To enable an efficient morphological analysis of the arbuscules detected in Mtpt4$_{pro}$::*gras8-RNAi* plants, the roots have to analyzed at an earlier time point to keep the basal level of degenerated arbuscules low. In case of *mtpt4* mutants the arbuscule morphology was studied six days post inoculation (Javot et al., 2007b).

Although, the functionality of the arbuscules observed in the MtPt4$_{pro}$::*gras8-RNAi* lines is not proven, *MtGras8* seems to have an impact on arbuscule morphology and abundance. It might be assumed that *MtGras8* is involved in the regulation of the arbuscule life-span, similar to *MtPt4* (Javot et al., 2007b). like *MtGras8, MtPt4* is strongly and specifically induced in arb cells and a strong correlation was found for the transcript level of both genes. The expression of the RNAi construct was driven by the arb cell-specific *MtPt4* promoter resulted in a decreased arbuscule abundance, which might be caused by previous arbuscule senescence and degeneration. This is in line with the increased abundance of deformed arbuscules. Assuming that MtGRAS8 might also act upstream of *MtPt4* induction during arbuscule development, additional functions of MtGRAS8 might be proposed. However, the here-observed lower arbuscule abundance with increased proportion of deformed arbuscules in MtPt4$_{pro}$::*gras8-RNAi* lines strongly suggests a role of MtGRAS8 during arbuscule development and maturation. MtGRAS8 might presumably required for sustaining the arbuscule morphology or functionality.

A posttranscriptional regulation of *MtGras8* transcripts by microRNA5204* (miRNA5204*) was previously described by Devers et al., 2011. Stem-loop qRT-PCR data showed a phosphate-dependent expression of miRNA5204* in *M. truncatula* roots (Devers, 2011; Devers et al., 2011). As shown in figure 34A, the miRNA5204* accumulation is elevated in mycorrhizal roots and in plants cultivated under full nutrition. At low phosphate conditions the miRNA accumulation remained low. Finally, the posttranscriptional regulation of *MtGras8* by miRNA5204* was supported *in vivo* in *M. truncatula* miRNA5204* precursor (pre-miRNA5204*) over-expression lines. The spearman-rank correlation analysis, showed a negative, non-linear correlation between *MtGras8* transcript and miRNA5204* transcript levels (figure 34B). These results indicate that the majority of *MtGras8* transcripts seemed to be cleaved after a threshold level ($2^{-\Delta}Ct=0.02$) of miRNA5204* accumulation is reached Devers 2011.

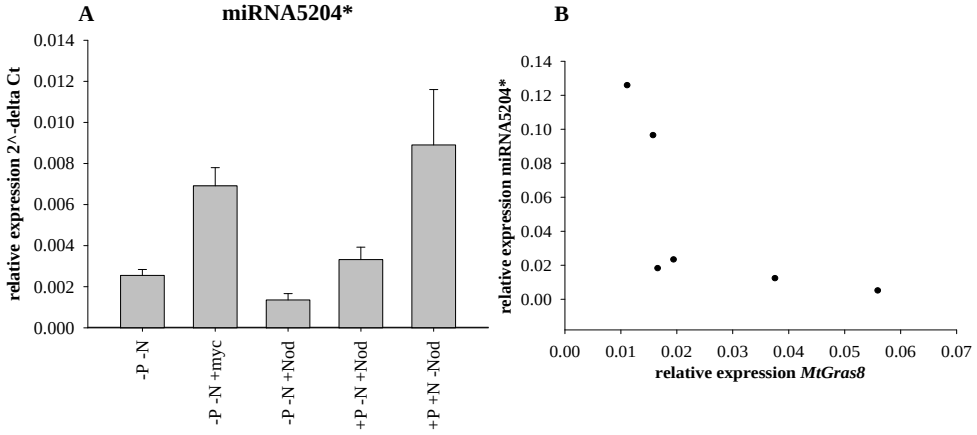

Figure 34: Expression analysis of miRNA5204* by stem-loop qRT-PCR and Spearman-rank correlation (Devers, 2011). A) Stem-loop qRT-PCR data represent mean values of three biological replicates. Three-week-old *M. truncatula* plants were either inoculated with *R. irregularis* (+myc) or *Sinorhizobium meliloti* (+Nod). Inoculated and non-inoculated plants were cultivated under different nutrient conditions. -P: 20 µM phosphate, +P: 1mM phosphate, -N: 0 µM nitrate, +N: 5 mM nitrate. B) Spearman-rank correlation of miRNA5204* and *MtGras8* expression levels (correlation coefficient r = -0.943, *p*-value = 0,0167). The transcript abundances of miRNA5204* and *MtGras8* were verified in three-week-old pre-miRNA5204 over-expression lines *via* stem-loop qRT-PCR.

5.4 miRNA5204* expression is increased in the first two weeks of the symbiosis

In this work the miRNA5204* accumulation was investigated in mycorrhizal *M. truncatula* roots by stem-loop qRT-PCR analysis. In contrast to mycorrhizal marker genes, the highest miRNA5204* accumulation was observed at two weeks post inoculation. Also *MtGras8* transcript level remained low in the first two weeks. At later time points, the miRNA5204* transcript level declined to levels of non-mycorrhizal roots (Branscheid, 2012). MiRNA5204* seems to have no global effect on the *MtGras8* transcript accumulation, because the strongly increase of the miRNA5204* expression in the first two weeks of the symbiosis seems to have no direct effect on the *MtGras8* transcript abundance. It can not be ruled out that the miRNA5204* and *MtGras8* are

located in different cell types. The arb cell-specific transcription of *MtGras8* was confirmed by cell type-specific qRT-PCR, but localization of miRNA5204* in mycorrhizal roots is still unclear. It can not be ruled out that miRNA5204* transcription is not restricted to arbuscule-containing cells. Similar phenomena are described for miRNA399. The phloem mobile miRNA399 seem to be translocated from the shoot to the roots of phosphate-starved plants (Pant et al., 2008; Branscheid et al., 2010).

5.5 Mis-expression of miRNA5204* confirms the regulation of *MtGras8* transcript levels *in vivo*

To investigate the role of miRNA5204*-mediated *MtGras8* transcript cleavage, mis-expression of mature miRNA5204* was driven by the *A. thaliana* ubiquitin (*UBQ3*) and *MtPt4* promoter. In case of UBQ_{pro}::*miRNA5204** lines, a strict negative, linear correlation confirmed the miRNA5204*-mediated transcript cleavage. These results are in line with previous results of pre-miRNA5204 over-expression lines, as shown in figure 34B (Devers, 2011). But due to different precursors used in the studies, different relationships of miRNA5204* and *MtGras8* transcript abundances were observed. In this work the expression of a miRNA159b precursor (figure 35) resulted in a linear negative correlation of miRNA5204* and *MtGras8* transcript abundances. In contrast to this the expression of the native precursor revealed a non-linear negative correlation of miRNA5204* and *MtGras8* transcript levels. Accordingly, the expression levels and processing can vary between these experiments and lead to differences in the silencing efficiencies.

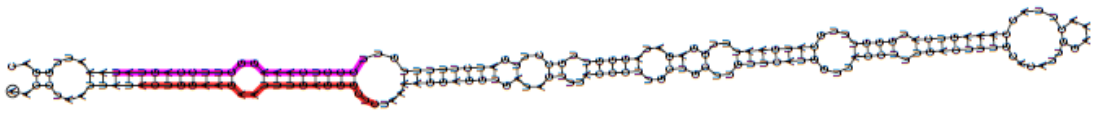

Figure 35: Secondary structure prediction of miRNA5204* in the miRNA159b precursor. The miRNA star strand is marked in pink and the complementary miRNA strand is labeled in orange. The miRNA precursor folding and small RNA prediction was performed with the UEA sRNA toolkit (http://srna-tools.cmp.uea.ac.uk).

In case of $MtPt4_{pro}$::*miRNA5204** lines a negative correlation of *MtGras8* and miRNA5204* transcript levels could not be confirmed. Although the *MtPt4* transcript levels were not significantly altered in the miRNA5204* mis-expression lines, a lower arbuscule abundance and an increased proportion of deformed arbuscules were observed in MtPt4pro::*miRNA5204** roots. Hence the $MtPt4_{pro}$::*miRNA5204** roots mimic the phenotype of $MtPt4_{pro}$::*gras8-RNAi* roots, an affected MtGRAS8 function can be concluded. In MtPt4pro::*miRNA5204** as well as in $MtPt4_{pro}$::*gras8-RNAi* roots an increased abundance of round-shaped and less branched arbuscules were observed. Nevertheless, the RNAi-mediated gene silencing revealed a more stringent repression of fungal colonization and mycorrhizal marker gene expression.

Remarkably smaller arbuscules, as well as a significantly lower colonization intensity and arbuscule abundance were observed in MtPt4pro::*miRNA5204*** roots, as compared to UBQ_{pro}::*miRNA5204** roots. These facts indicate, that the expression of miRNA5204* under the mycorrhizal-specific *MtPt4* promoter affects the arbuscule development more than an ubiquitin promoter-driven expression of miRNA5204*. The *MtPt4* promoter enables a miRNA5204* expression in arbuscule-containing cells, where *MtGras8* was shown to be highly abundant. This might reveal a stronger effect on the fungal colonization. These findings indicate that the miRNA5204*-mediated regulation of *MtGras8* might control the fungal colonization in phosphate-dependent manner.

5.6 MtGRAS8 interacts with MtNSP2 and MtRAM1

It is well known that GRAS TFs form homo- and heterodimers. Protein-protein-interactions are facilitated by a LHRI domain, one of two highly conserved leucine-rich repeat domains present in GRAS proteins (Bolle, 2004; Cui et al., 2007; Hirsch et al., 2009). Previous studies confirmed the protein-protein-interaction of several GRAS TFs (Cui et al., 2007; Hirsch et al., 2009; Gobbato et al., 2012). As mentioned earlier, SCR and SHR control the root patterning upon heterodimer formation. This dimerization prevents the movement of SHR to the cortical cell layer. The complex leads to a self-activation upon binding to the SCR promoter and enables the differentiation of a single endodermis cell layer (Cui et al., 2007; Hirsch and Oldroyd, 2009). During root nodule and AM symbiosis the protein-protein-interaction of NSP2 with NSP1 or RAM1 was observed (Hirsch et al., 2009; Gobatto et al., 2012). These interactions seem to compete, because co-expression of either NSP1 or RAM1 negatively influences the interaction between NSP2 and RAM1 (Gobbato et al., 2012). Due to the fact that the DNA binding of NSP1 and RAM1 could be confirmed *in vivo*, NSP1 seems to rather activate the transcription of target genes during root nodule symbiosis and RAM1 activates the gene expression during AM symbiosis (Gobbato et al,. 2012). But recent studies showed that NSP1 plays also a role for the AMF colonization (Delaux et al., 2013). It is suggested, that NPS1 and NSP2 control the cortical colonization. RAM1 and NSP2 are rather involved in root penetration (Delaux et al., 2013). However, the strong and specific accumulation of *MtGras8* transcripts in arb cells points to a function of this proteins in arbuscule development or functioning. Recent experiment showed that the *Nsp2* promoter is active in arb cells (Devers et al., in preparation). This leads to the assumption that the here observed MtGRAS8::MtNSP2 heterodimer also occurs in arb cells. Additionally, the heterodimerization of MtGRAS8 and RAM1 was detected in this study. But so far, the cellular localization of RAM1 is unknown.

One might assume, that MtGRAS8 might be able to bind DNA and induces the expression of target genes. Accordingly, future electrophoretic mobility shift assays (EMSA) and Chromatin immunoprecipitation (ChIP) analysis are needed to confirm DNA-binding ability of MtGRAS8.

5.7 *MtGras8*, a link between phosphate homeostasis and arbuscule development?

The miRNA5204* mis-expression and *MtGras8* knock-down experiments suggested that MtGRAS8 might be related to arbuscule development and functioning. A time course experiment showed that miRNA5204* accumulates during the first two weeks of the AM symbiosis, where phosphate concentrations in the roots were higher as in later time points (Branscheid et al., 2012). Since Devers et al., (2011) identified miRNA5204* to be increased in roots grown at high phosphate concentrations, one might assume that the increased levels of miRNA5204* are related to the increased phosphate concentration in plants at the first two weeks of the time course experiment. However, no increased levels of miRNA5204* expression were found in non-mycorrhizal plants pointing to a link of miRNA5204* accumulation to AM symbiosis development. Further experiments like the localization of miRNA5204* accumulation in mycorrhizal roots at these early stages are needed to speculate about the role of the miRNA5204* at this time-point of symbiosis development.

The *MtGras8* silencing experiment strongly suggests a role of MtGRAS8 during arbuscule development and maintenance. Arbuscules have a limited life span of 8-10 days (Javot et al., 2007b). However, signals leading to arbuscule senescence or degeneration have not been identified. At early phases of arbuscule development, massively amounts of phospholipids are required for the arbuscule development and degradation processes (Gaude et al., 2012). This results in an increased phosphate consumption for the preparation of the PAM in the arbuscule-containing cells. The later transfer of phosphate across the PAM is likely to result in an increase in local phosphate concentrations. On the other hand, a high internal phosphate status of host plants is able to systemically suppress AM colonization particularly arbuscule abundance (Branscheid et al 2010). Therefore, putative signals leading to arbuscule degeneration might be related to the plant´s systemic phosphate status or to local phosphate concentration. It might be postulated that miRNA5204* with its phosphate-dependent expression is involved in a signaling mechanism linking phosphate signaling with arbuscule development and maintenance (figure 36).

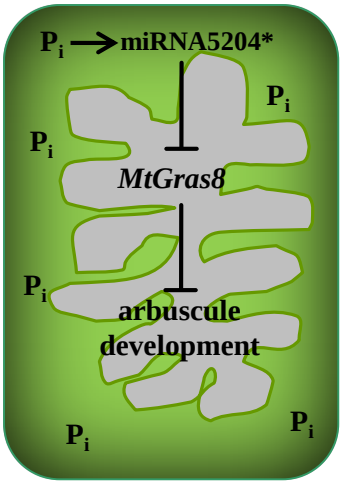

Figure 36: Model of a postulated phosphate-dependent control of mycorrhizal colonization. During AM symbiosis the phosphate (P_i) concentration rises in arbuscule containing cells of mycorrhizal roots, leading to an induction of miRNA5204*. The posttranscriptional regulation of *MtGras8* by miRNA5204* results in an increased number deformed arbuscules and reduced fungal colonization.

of

MiRNA5204* might be locally increased due to increasing phosphate concentrations. This miRNA5204* accumulation would result in lower *MtGras8* transcript accumulation due to transcript cleavage. As observed in the silencing experiment, lower *MtGras8* transcript abundances lead to an increase number of deformed arbuscules. Hence, miRNA5204* might be involved in the control of arbuscule degeneration in response to high phosphate signals. However, the reduction at earlier time points of AM symbiosis suggests additional functions for this miRNA, which need to be ruled out in future.

6 Summary

For the first time the transcriptional reprogramming of distinct root cortex cells during the arbuscular mycorrhizal (AM) symbiosis was investigated by combining Laser Capture Mirodissection of root cryosections and Affymetrix GeneChip® Medicago genome array hybridization. The establishment of cryosections facilitated the isolation of high quality RNA in sufficient amounts from three different cortical cell types. The transcript profiles of arbuscule-containing cells (arb cells), non-arbuscule-containing cells (nac cells) of *Rhizophagus irregularis* inoculated *Medicago truncatula* roots and cortex cells of non-inoculated roots (cor) were successfully explored. The data gave new insights in the symbiosis-related cellular reorganization processes and indicated that already nac cells seem to be prepared for the upcoming fungal colonization.

The mycorrhizal- and phosphate-dependent transcription of a GRAS TF family member (*MtGras8*) was detected in arb cells and mycorrhizal roots. MtGRAS8 shares a high sequence similarity to a GRAS TF suggested to be involved in the fungal colonization processes (MtRAM1). The function of *MtGras8* was unraveled upon RNA-interference- (RNAi-) mediated gene silencing. An AM symbiosis-dependent expression of a RNAi construct (*MtPt4*$_{pro}$::*gras8-RNAi*) revealed a successful gene silencing of *MtGras8* leading to a reduced arbuscule abundance and a higher proportion of deformed arbuscules in root with reduced transcript levels. Accordingly, *MtGras8* might control the arbuscule development and life-time. The targeting of *MtGras8* by the phosphate-dependent regulated miRNA5204* was discovered previously (Devers et al., 2011). Since miRNA5204* is known to be affected by phosphate, the posttranscriptional regulation might represent a link between phosphate signaling and arbuscule development. In this work, the posttranscriptional regulation was confirmed by mis-expression of miRNA5204* in *M. truncatula* roots. The miRNA-mediated gene silencing affects the *MtGras8* transcript abundance only in the first two weeks of the AM symbiosis and the mis-expression lines seem to mimic the phenotype of *MtGras8*-RNAi lines. Additionally, MtGRAS8 seems to form heterodimers with NSP2 and RAM1, which are known to be key regulators of the fungal colonization process (Hirsch et al., 2009; Gobbato et al., 2012). These data indicate that *MtGras8* and miRNA5204* are linked to the *sym* pathway and regulate the arbuscule development in phosphate-dependent manner.

7 Outlook

The transcription factors (TFs) gene expression analyses at cell type-specific level in mycorrhizal roots provides new insights in the transcriptional reprogramming of cortical cells during the arbuscular mycorrhizal symbiosis. Moreover, this work proposes that MtGRAS8 is a putative link between the *sym*-pathway and phosphate signaling. Further experiments are needed to unravel the role for this protein:

Mycorrhizal induced RNA-interference-mediated gene silencing resulted in an abberant arbuscule morphology. A high proportion of deformed arbuscules were detected. To distinguish the deformed arbuscules and degenerated arbuscules originated from the arbuscule turn-over, the arbuscules in roots expressing the $MtPt4_{pro}$::*gras8-RNAi* constructs have to be analyzed at an earlier time point, as described by Javot et al., 2007b. Further, time course experiments might answer the question, if the arbuscule life-time in affected due to the *MtGras8* knock-down.

The Bimolecular Fluorescence Complementation (BiFC) analysis revealed that MtGRAS8 interacts with two GRAS TFs, RAM1 and NSP2. Since DNA binding activity of RAM1 and NSP2, was not described so far, one might assume that MtGRAS8 is able to act as an TF and activate the transcription of target genes by binding to promoter *cis*-elements. The binding of promoter *cis*-elements by MtGRAS8 has to be investigated by electrophoretic mobility shift assays (EMSA).

A Chromatin immunoprecipitation (ChIP) analysis might give hints for putative downstream targets of MtGRAS8. Expression of the tagged MtGRAS8 proteins has to be controlled by an inducible promoter, such as the *MtPt4*- or alcR-promoter to obtain sufficient amounts DNA-protein-complexes. This will enable the identification of promoter *cis*-elements capable of binding MtGRAS8 proteins and unravel target genes directly regulated by MtGRAS8.

8 References

Akiyama K, Hayashi H (2006) Strigolactones: chemical signals for fungal symbionts and parasitic weeds in plant roots. Ann Bot **97:** 925-931

Alexander T, Meier R, Toth R, Weber HC (1988) Dynamics of Arbuscule Development and Degeneration in Mycorrhizas of Triticum-Aestivum L and Avena-Sativa L with Reference to Zea-Mays-L. New Phytologist **110:** 363-370

Alexander T, Toth R, Meier R, Weber HC (1989) Dynamics of Arbuscule Development and Degeneration in Onion, Bean, and Tomato with Reference to Vesicular-Arbuscular Mycorrhizae in Grasses. Canadian Journal of Botany-Revue Canadienne De Botanique **67:** 2505-2513

Allen JW, Shachar-Hill Y (2009) Sulfur Transfer through an Arbuscular Mycorrhiza. Plant Physiology **149:** 549-560

Andriankaja A, Boisson-Demier A, Frances L, Sauviac L, Jauneau A, Barker DG, de Carvalho-Niebel F (2007) AP2-ERF transcription factors mediate nod factor-dependent mt ENOD11 activation in root hairs via a novel cis-regulatory motif. Plant Cell **19:** 2866-2885

Ane JM, Kiss GB, Riely BK, Penmetsa RV, Oldroyd GE, Ayax C, Levy J, Debelle F, Baek JM, Kalo P, Rosenberg C, Roe BA, Long SR, Denarie JC, D.R. (2004) *Medicago truncatula* DMI1 required for bacterial and fungal symbioses in legumes. Science **303:** 1364-1367

Anisimova M, Gascuel O (2006) Approximate likelihood-ratio test for branches: A fast, accurate, and powerful alternative. Syst Biol **55:** 539-552

Arabidopsis Interactome Mapping C (2011) Evidence for network evolution in an Arabidopsis interactome map. Science **333:** 601-607

Ariel F, Diet A, Verdenaud M, Gruber V, Frugier F, Chan R, Crespi M (2010) Environmental Regulation of Lateral Root Emergence in Medicago truncatula Requires the HD-Zip I Transcription Factor HB1. Plant Cell **22:** 2171-2183

Asano T, Masumura T, Kusano H, Kikuchi S, Kurita A, Shimada H, Kadowaki K (2002) Construction of a specialized cDNA library from plant cells isolated by laser capture microdissection: toward comprehensive analysis of the genes expressed in the rice phloem. Plant J **32:** 401-408

Auge RM (2001) Water relations, drought and vesicular-arbuscular mycorrhizal symbiosis. Mycorrhiza **11:** 3-42

Auge RM, Kubikova E, Moore JL (2001) Foliar dehydration tolerance of mycorrhizal cowpea, soybean and bush bean. New Phytologist **151:** 535-541

Bago B, Pfeffer PE, Shachar-Hill Y (2000) Carbon metabolism and transport in arbuscular mycorrhizas. Plant Physiol **124:** 949-958

Balestrini R, Bonfante P (2005) The interface compartment in arbuscular mycorrhizae: A special type of plant cell wall? Plant Biosystems **139:** 8-15

Balestrini R, Cosgrove DJ, Bonfante P (2005) Differential location of alpha-expansin proteins during the accommodation of root cells to an arbuscular mycorrhizal fungus. Planta **220:** 889-899

Balestrini R, Gomez-Ariza J, Lanfranco L, Bonfante P (2007) Laser microdissection reveals that transcripts for five plant and one fungal phosphate transporter genes are contemporaneously present in arbusculated cells. Molecular Plant-Microbe Interactions **20:** 1055-1062

Baranowskij N, Frohberg C, Prat S, Willmitzer L (1994) A novel DNA binding protein with homology to Myb oncoproteins containing only one repeat can function as a transcriptional activator. Embo J **13:** 5383-5392

Bari R, Datt Pant B, Stitt M, Scheible WR (2006) PHO2, microRNA399, and PHR1 define a phosphate-signaling pathway in plants. Plant Physiol **141:** 988-999

Bariola PA, Retelska D, Stasiak A, Kammerer RA, Fleming A, Hijri M, Frank S, Farmer EE (2004) Remorins form a novel family of coiled coil-forming oligomeric and filamentous proteins associated with apical, vascular and embryonic tissues in plants. Plant Mol Biol **55:** 579-594

Barker SJ, Edmonds-Tibbett TL, Forsyth LM, Klingler JP, Toussaint JP, Smith FA, Smith SE (2005) Root infection of the reduced mycorrhizal colonization (rmc) mutant of tomato reveals

genetic interaction between symbiosis and parasitism. Physiological and Molecular Plant Pathology **67:** 277-283

Becard G, Fortin JA (1988) Early Events of Vesicular Arbuscular Mycorrhiza Formation on Ri T-DNA Transformed Roots. New Phytologist **108:** 211-218

Becard G, Piche Y (1989) Fungal Growth Stimulation by CO(2) and Root Exudates in Vesicular-Arbuscular Mycorrhizal Symbiosis. Appl Environ Microbiol **55:** 2320-2325

Benedito VA, Torres-Jerez I, Murray JD, Andriankaja A, Allen S, Kakar K, Wandrey M, Verdier J, Zuber H, Ott T, Moreau S, Niebel A, Frickey T, Weiller G, He J, Dai X, Zhao PX, Tang Y, Udvardi MK (2008) A gene expression atlas of the model legume Medicago truncatula. Plant J **55:** 504-513

Besserer A, Becard G, Jauneau A, Roux C, Sejalon-Delmas N (2008) GR24, a synthetic analog of strigolactones, stimulates the mitosis and growth of the arbuscular mycorrhizal fungus Gigaspora rosea by boosting its energy metabolism. Plant Physiology **148:** 402-413

Birnbaum K, Shasha DE, Wang JY, Jung JW, Lambert GM, Galbraith DW, Benfey PN (2003) A gene expression map of the Arabidopsis root. Science **302:** 1956-1960

Blancaflor EB, Zhao LM, Harrison MJ (2001) Microtubule organization in root cells of Medicago truncatula during development of an arbuscular mycorrhizal symbiosis with Glomus versiforme. Protoplasma **217:** 154-165

Boisson-Dernier A, Chabaud M, Garcia F, Becard G, Rosenberg C, Barker DG (2001) Agrobacterium rhizogenes-transformed roots of Medicago truncatula for the study of nitrogen-fixing and endomycorrhizal symbiotic associations. Molecular Plant-Microbe Interactions **14:** 695-700

Bolle C (2004) The role of GRAS proteins in plant signal transduction and development. Planta **218:** 683-692

Boualem A, Laporte P, Jovanovic M, Laffont C, Plet J, Combier JP, Niebel A, Crespi M, Frugier F (2008) MicroRNA166 controls root and nodule development in Medicago truncatula. Plant Journal **54:** 876-887

Brandt S, Kehr J, Walz C, Imlau A, Willmitzer L, Fisahn J (1999) A rapid method for detection of plant gene transcripts from single epidermal, mesophyll and companion cells of intact leaves. Plant Journal **20:** 245-250

Brandt S, Kloska S, Altmann T, Kehr J (2002) Using array hybridization to monitor gene expression at the single cell level. Journal of Experimental Botany **53:** 2315-2323

Branscheid A (2012) Phosphate homeostasis and posttranscriptional gene regulation during arbuscular mycorrhizal symbiosis in *Medicago truncatula*. Doctoral thesis **Uiversity of Potsdam, Germany**

Branscheid A, Devers EA, May P, Krajinski F (2011) Distribution pattern of small RNA and degradome reads provides information on miRNA gene structure and regulation. Plant Signal Behav **6:** 1609-1611

Branscheid A, Sieh D, Pant BD, May P, Devers EA, Elkrog A, Schauser L, Scheible WR, Krajinski F (2010) Expression Pattern Suggests a Role of MiR399 in the Regulation of the Cellular Response to Local Pi Increase During Arbuscular Mycorrhizal Symbiosis. Molecular Plant-Microbe Interactions **23:** 915-926

Brown RL, Kazan K, McGrath KC, Maclean DJ, Manners JM (2003) A role for the GCC-box in jasmonate-mediated activation of the PDF1.2 gene of Arabidopsis. Plant Physiol **132:** 1020-1032

Bustin SA (2000) Absolute quantification of mRNA using real-time reverse transcription polymerase chain reaction assays. J Mol Endocrinol **25:** 169-193

Büttner M, Singh KB (1997) Arabidopsis thaliana ethylene-responsive element binding protein (AtEBP), an ethylene-inducible, GCC box DNA-binding protein interacts with an ocs element binding protein. Proceedings of the National Academy of Sciences of the United States of America **94:** 5961-5966

Cai SQ, Lashbrook CC (2006) Laser capture microdissection of plant cells from tape-transferred paraffin sections promotes recovery of structurally intact RNA for global gene profiling. Plant Journal **48:** 628-637

Capoen W, Sun J, Wysham D, Otegui MS, Venkateshwaran M, Hirsch S, Miwa H, Downie JA, Morris RJ, Ane JM, Oldroyd GED (2011) Nuclear membranes control symbiotic calcium signaling of legumes. Proceedings of the National Academy of Sciences of the United States of America **108:** 14348-14353

Carthew RW, Sontheimer EJ (2009) Origins and Mechanisms of miRNAs and siRNAs. Cell **136:** 642-655

Casson S, Spencer M, Walker K, Lindsey K (2005) Laser capture microdissection for the analysis of gene expression during embryogenesis of Arabidopsis. Plant J **42:** 111-123

Castresana J (2000) Selection of conserved blocks from multiple alignments for their use in phylogenetic analysis. Mol Biol Evol **17:** 540-552

Catoira R, Galera C, de Billy F, Penmetsa RV, Journet EP, Maillet F, Rosenberg C, Cook D, Gough C, Denarie J (2000) Four genes of *Medicago truncatula* controlling components of a nod factor transduction pathway. Plant Cell **12:** 1647-1666

Cavagnaro TR, Smith FA, Ayling SM, Smith SE (2003) Growth and phosphorus nutrition of a Paris-type arbuscular mycorrhizal symbiosis. New Phytologist **157:** 127-134

Cerri MR, Frances L, Laloum T, Auriac MC, Niebel A, Oldroyd GED, Barker DG, Fournier J, de Carvalho-Niebel F (2012) Medicago truncatula ERN Transcription Factors: Regulatory Interplay with NSP1/NSP2 GRAS Factors and Expression Dynamics throughout Rhizobial Infection. Plant Physiology **160:** 2155-21**72**

Chandran D, Inada N, Hather G, Kleindt C, Wildemuth M C (2010) Laser microdissection of Arabidopsis cells at the powdery mildew infection site reveals site-specific processes and regulators. PNAS **107**: 460-465

Charpentier M, Bredemeier R, Wanner G, Takeda N, Schleiff E, Parniske M (2008) Lotus japonicus CASTOR and POLLUX Are Ion Channels Essential for Perinuclear Calcium Spiking in Legume Root Endosymbiosis. Plant Cell **20:** 3467-3479

Chen X, Liu J, Cheng Y, Jia D (2002) HEN1 functions pleiotropically in Arabidopsis development and acts in C function in the flower. Development **129:** 1085-1094

Chevenet F, Brun C, Banuls AL, Jacq B, Christen R (2006) TreeDyn: towards dynamic graphics and annotations for analyses of trees. Bmc Bioinformatics **7:** 439

Clark RB, Zeto SK, Ritchey KD, Baligar VC (2001) Mineral acquisition by maize grown in acidic soil amended with coal combustion products. Communications in Soil Science and Plant Analysis **32:** 1861-1884

Colebatch G, Desbrosses G, Ott T, Krusell L, Montanari O, Kloska S, Kopka J, Udvardi MK (2004) Global changes in transcription orchestrate metabolic differentiation during symbiotic nitrogen fixation in Lotus japonicus. Plant Journal **39:** 487-512

Combier JP, Frugier F, de Billy F, Boualem A, El-Yahyaoui F, Moreau S, Vernie T, Ott T, Gamas P, Crespi M, Niebel A (2006) MtHAP2-1 is a key transcriptional regulator of symbiotic nodule development regulated by microRNA169 in Medicago truncatula. Genes & Development **20:** 3084-3088

Courtial B, Feuerbach F, Eberhard S, Rohmer L, Chiapello H, Camilleri C, Lucas H (2001) Tnt1 transposition events are induced by in vitro transformation of Arabidopsis thaliana, and transposed copies integrate into genes. Mol Genet Genomics **265:** 32-42

Cox G, Tinker PB (1976) Translocation and Transfer of Nutrients in Vesicular-Arbuscular Mycorrhizas .1. Arbuscule and Phosphorus Transfer - Quantitative Ultrastructural-Study. New Phytologist **77:** 371-&

Cui HC, Levesque MP, Vernoux T, Jung JW, Paquette AJ, Gallagher KL, Wang JY, Blilou I, Scheres B, Benfey PN (2007) An evolutionarily conserved mechanism delimiting SHR movement defines a single layer of endodermis in plants. Science **316:** 421-425

d'Erfurth I, Cosson V, Eschstruth A, Lucas H, Kondorosi A, Ratet P (2003) Efficient transposition of the Tnt1 tobacco retrotransposon in the model legume Medicago truncatula. Plant J **34:** 95-106

Day RC, Grossniklaus U, Macknight RC (2005) Be more specific! Laser-assisted microdissection of plant cells. Trends Plant Sci **10:** 397-406

Delaux PM, Becard G, Combier JP (2013) NSP1 is a component of the Myc signaling pathway. New Phytol **199:** 59-65

Denarie J, Debelle F, Prome JC (1996) Rhizobium lipo-chitooligosaccharide nodulation factors: Signaling molecules mediating recognition and morphogenesis. Annual Review of Biochemistry **65:** 503-535

Dereeper A, Guignon V, Blanc G, Audic S, Buffet S, Chevenet F, Dufayard JF, Guindon S, Lefort V, Lescot M, Claverie JM, Gascuel O (2008) Phylogeny.fr: robust phylogenetic analysis for the non-specialist. Nucleic Acids Research **36:** W465-W469

Devers E (2011) Phosphate homeostasis and novel microRNAs are involved in the regulation of the arbuscular mycorrhizal symbiosis in *Medicago truncatula*. Doctoral thesis **University of Potsdam, Germany**

Devers EA, Branscheid A, May P, Krajinski F (2011) Stars and symbiosis: microRNA- and microRNA*-mediated transcript cleavage involved in arbuscular mycorrhizal symbiosis. Plant Physiol **156:** 1990-2010

Devers EA, Teply J, Reinert A, Gaude N, Krajinski F (2013) An endogenous artificial microRNA system for unraveling the function of root endosymbioses related genes in Medicago truncatula. BMC Plant Biol **13:** 82

Di Laurenzio L, Wysocka-Diller J, Malamy JE, Pysh L, Helariutta Y, Freshour G, Hahn MG, Feldmann KA, Benfey PN (1996) The SCARECROW gene regulates an asymmetric cell division that is essential for generating the radial organization of the Arabidopsis root. Cell **86:** 423-433

Eckardt NA (2002) Foolish seedlings and DELLA regulators: the functions of rice SLR1 and Arabidopsis RGL1 in GA signal transduction. Plant Cell **14:** 1-5

El Yahyaoui F, Küster H, Ben Amor B, Hohnjec N, Puhler A, Becker A, Gouzy J, Vernie T, Gough C, Niebel A, Godiard L, Gamas P (2004) Expression profiling in *Medicago truncatula* identifies more than 750 genes differentially expressed during nodulation, including many potential regulators of the symbiotic program. Plant Physiol **136:** 3159-3176

Emmert-Buck MR, Bonner RF, Smith PD, Chuaqui RF, Zhuang Z, Goldstein SR, Weiss RA, Liotta LA (1996) Laser capture microdissection. Science **274:** 998-1001

Endre G, Kereszt A, Kevei Z, Mihacea S, Kalo P, Kiss GB (2002) A receptor kinase gene regulating symbiotic nodule development. Nature **417:** 962-966

Endt DV, Kijne JW, Memelink J (2002) Transcription factors controlling plant secondary metabolism: what regulates the regulators? Phytochemistry **61:** 107-114

Fedorova M, van de Mortel J, Matsumoto PA, Cho J, Town CD, VandenBosch KA, Gantt JS, Vance CP (2002) Genome-wide identification of nodule-specific transcripts in the model legume *Medicago truncatula*. Plant Physiol **130:** 519-537

Ferrol N, Barea JM, Azcon-Aguilar C (2002) Mechanisms of nutrient transport across interfaces in arbuscular mycorrhizas. Plant and Soil **244:** 231-237

Fester T, Schmidt D, Lohse S, Walter MH, Giuliano G, Bramley PM, Fraser PD, Hause B, Strack D (2002) Stimulation of carotenoid metabolism in arbuscular mycorrhizal roots. Planta **216:** 148-154

Fester T, Strack D, Hause B (2001) Reorganization of tobacco root plastids during arbuscule development. Planta **213:** 864-868

Fiorilli V, Lanfranco L, Bonfante P (2013) The expression of *Gint PT*, the phosphate transporter of *Rhizophagus irregularis*, depents on the symbiotic status of phosphate availability. Planta **237**: 1267-1277

Frenzel A, Manthey K, Perlick AM, Meyer F, Puhler A, Küster H, Krajinski F (2005) Combined transcriptome profiling reveals a novel family of arbuscular mycorrhizal-specific *Medicago truncatula* lectin genes. Mol Plant Microbe Interact **18:** 771-782

Fujimoto SY, Ohta M, Usui A, Shinshi H, Ohme-Takagi M (2000) Arabidopsis ethylene-responsive element binding factors act as transcriptional activators or repressors of GCC box-mediated gene expression. Plant Cell **12:** 393-404

Gao Y, Yang SG, Yuan LY, Cui YH, Wu KQ (2012) Comparative Analysis of SWIRM Domain-Containing Proteins in Plants. Comparative and Functional Genomics

Gaude N, Bortfeld S, Duensing N, Lohse M, Krajinski F (2012) Arbuscule-containing and non-colonized cortical cells of mycorrhizal roots undergo extensive and specific reprogramming during arbuscular mycorrhizal development. Plant Journal **69:** 510-528

Genre A, Bonfante P (1997) A mycorrhizal fungus changes microtubule orientation in tobacco root cells. Protoplasma **199:** 30-38

Genre A, Bonfante P (1998) Actin versus tubulin configuration in arbuscule-containing cells from mycorrhizal tobacco roots. New Phytologist **140:** 745-752

Genre A, Bonfante P (2002) Epidermal cells of a symbiosis-defective mutant of Lotus japonicus show altered cytoskeleton organisation in the presence of a mycorrhizal fungus. Protoplasma **219:** 43-50

Genre A, Bonfante P (2005) Building a mycorrhizal cell: How to reach compatibility between plants and arbuscular mycorrhizal fungi. Journal of Plant Interactions **1:** 3-13

Genre A, Chabaud M, Faccio A, Barker DG, Bonfante P (2008) Pre-penetration apparatus assembly precedes and predicts the colonization patterns of arbuscular mycorrhizal fungi within the root cortex of both Medicago truncatula and Daucus carota. Plant Cell **20:** 1407-1420

Genre A, Chabaud M, Timmers T, Bonfante P, Barker DG (2005) Arbuscular mycorrhizal fungi elicit a novel intracellular apparatus in *Medicago truncatula* root epidermal cells before infection. Plant Cell **17:** 3489-3499

Genre A, Ivanov S, Fendrych M, Faccio A, Zarsky V, Bisseling T, Bonfante P (2012) Multiple Exocytotic Markers Accumulate at the Sites of Perifungal Membrane Biogenesis in Arbuscular Mycorrhizas. Plant and Cell Physiology **53:** 244-255

Gianinazzi-Pearson V, Brechenmacher L (2004) Functional genomics of arbuscular mycorrhiza: decoding the symbiotic cell programme. Canadian Journal of Botany-Revue Canadienne De Botanique **82:** 1228-1234

Gianinazzi-Pearson V, Gianinazzi S (1989) Cellular and Genetic-Aspects of Interactions between Hosts and Fungal Symbionts in Mycorrhizae. Genome **31:** 336-341

Gianinazzi-Pearson V, Gollotte A, Lherminier J, Tisserant B, Franken P, Dumasgaudot E, Lemoine MC, Vantuinen D, Gianinazzi S (1995) Cellular and Molecular Approaches in the Characterization of Symbiotic Events in Functional Arbuscular Mycorrhizal Associations. Canadian Journal of Botany-Revue Canadienne De Botanique **73:** S526-S532

Gillespie JW, Best CJM, Bichsel VE, Cole KA, Greenhut SF, Hewitt SM, Ahram M, Gathright YB, Merino MJ, Strausberg RL, Epstein JI, Hamilton SR, Gannot G, Baibakova GV, Calvert VS, Flaig MJ, Chuaqui RF, Herring JC, Pfeifer J, Petricoin EF, Linehan WM, Duray PH, Bova GS, Emmert-Buck MR (2002) Evaluation of non-formalin tissue fixation for molecular profiling studies. American Journal of Pathology **160:** 449-457

Gobbato E, Marsh JF, Vernie T, Wang E, Maillet F, Kim J, Miller JB, Sun J, Bano SA, Ratet P, Mysore KS, Denarie J, Schultze M, Oldroyd GED (2012) A GRAS-Type Transcription Factor with a Specific Function in Mycorrhizal Signaling. Current Biology **22:** 2236-2241

Goldsworthy SM, Stockton PS, Trempus CS, Foley JF, Maronpot RR (1999) Effects of fixation on RNA extraction and amplification from laser capture microdissected tissue. Mol Carcinog **25:** 86-91

Gomez-Ariza J, Balestrini R, Novero M, Bonfante P (2009) Cell-specific gene expression of phosphate transporters in mycorrhizal tomato roots. Biology and Fertility of Soils **45:** 845-853

Gomez-Roldan V, Fermas S, Brewer PB, Puech-Pages V, Dun EA, Pillot JP, Letisse F, Matusova R, Danoun S, Portais JC, Bouwmeester H, Becard G, Beveridge CA, Rameau C, Rochange SF (2008) Strigolactone inhibition of shoot branching. Nature **455:** 189-U122

Gomez SK, Javot H, Deewatthanawong P, Torres-Jerez I, Tang Y, Blancaflor EB, Udvardi MK, Harrison MJ (2009) *Medicago truncatula* and *Glomus intraradices* gene expression in cortical cells harboring arbuscules in the arbuscular mycorrhizal symbiosis. BMC Plant Biol **9:** 10

Gough C, Cullimore J (2011) Lipo-chitooligosaccharide Signaling in Endosymbiotic Plant-Microbe Interactions. Molecular Plant-Microbe Interactions **24:** 867-878

Gronlund M, Gustafsen C, Roussis A, Jensen D, Nielsen LP, Marcker KA, Jensen EO (2003) The Lotus japonicus ndx gene family is involved in nodule function and maintenance. Plant Mol Biol **52:** 303-316

Gu M, Xu K, Chen AQ, Zhu YY, Tang GL, Xu GH (2010) Expression analysis suggests potential roles of microRNAs for phosphate and arbuscular mycorrhizal signaling in Solanum lycopersicum. Physiologia Plantarum **138:** 226-237

Gu YQ, Yang C, Thara VK, Zhou J, Martin GB (2000) Pti4 is induced by ethylene and salicylic acid, and its product is phosphorylated by the Pto kinase. Plant Cell **12:** 771-785

Guether M, Balestrini R, Hannah M, He J, Udvardi MK, Bonfante P (2009) Genome-wide reprogramming of regulatory networks, transport, cell wall and membrane biogenesis during arbuscular mycorrhizal symbiosis in *Lotus japonicus*. New Phytol **182:** 200-212

Guindon S, Gascuel O (2003) A simple, fast, and accurate algorithm to estimate large phylogenies by maximum likelihood. Syst Biol **52:** 696-704

Gutterson N, Reuber TL (2004) Regulation of disease resistance pathways by AP2/ERF transcription factors. Current Opinion in Plant Biology **7:** 465-471

Hacquard S, Delaruelle C, Legué V, Tisserant E, Kohler A, Frey P, Martin F, Duplessis S (2010) Laser capture microdissection of uredinia formed by *Melampsora larici-populina* revealed a transcriptional switch between biotrphy and sporulation. MPMI **23**:175-1286

Hacquard S, Tisserant E, Brun A, Legué V, Martin F, Kohler A (2013) Laser microdissection and microarray analysis of *Tuber melanopsorum* ectomycorrhizas revealed functional heterogeneity between mantle and hartig net compartments. Envromental Microbiology **15**: 1853-1869

Harrison MJ (1999) Molecular and Cellular Aspects of the Arbuscular Mycorrhizal Symbiosis. Annu Rev Plant Physiol Plant Mol Biol **50:** 361-389

Harrison MJ (2005) Signaling in the arbuscular mycorrhizal symbiosis. Annu Rev Microbiol **59:** 19-42

Harrison MJ, Dewbre GR, Liu J (2002) A phosphate transporter from *Medicago truncatula* involved in the acquisition of phosphate released by arbuscular mycorrhizal fungi. Plant Cell **14:** 2413-2429

Harrison MJ, Dixon RA (1994) Spatial Patterns of Expression of Flavonoid/Isoflavonoid Pathway Genes during Interactions between Roots of Medicago-Truncatula and the Mycorrhizal Fungus Glomus Versiforme. Plant Journal **6:** 9-20

Heckmann AB, Lombardo F, Miwa H, Perry JA, Bunnewell S, Parniske M, Wang TL, Downie JA (2006) Lotus japonicus nodulation requires two GRAS domain regulators, one of which is functionally conserved in a non-legume. Plant Physiol **142:** 1739-1750

Hirochika H, Okamoto H, Kakutani T (2000) Silencing of retrotransposons in arabidopsis and reactivation by the ddm1 mutation. Plant Cell **12:** 357-368

Hirsch S, Kim J, Munoz A, Heckmann AB, Downie JA, Oldroyd GED (2009) GRAS Proteins Form a DNA Binding Complex to Induce Gene Expression during Nodulation Signaling in Medicago truncatula. Plant Cell **21:** 545-557

Hirsch S, Oldroyd GE (2009) GRAS-domain transcription factors that regulate plant development. Plant Signal Behav **4:** 698-700

Hogekamp C, Arndt D, Pereira PA, Becker JD, Hohnjec N, Küster H (2011) Laser Microdissection Unravels Cell-Type-Specific Transcription in Arbuscular Mycorrhizal Roots, Including CAAT-Box Transcription Factor Gene Expression Correlating with Fungal Contact and Spread. Plant Physiology **157:** 2023-2043

Hogekamp C and Küster H (2013) A roadmap of cell-type specific gene expression during sequential stages of the arbuscular mycorrhiza symbiosis. BMC Genomics **14**:306

Hohnjec N, Vieweg MF, Puhler A, Becker A, Küster H (2005) Overlaps in the transcriptional profiles of *Medicago truncatula* roots inoculated with two different Glomus fungi provide insights into the genetic program activated during arbuscular mycorrhiza. Plant Physiol **137:** 1283-1301

Horvath B, Yeun LH, Domonkos A, Halasz G, Gobbato E, Ayaydin F, Miro K, Hirsch S, Sun JH, Tadege M, Ratet P, Mysore KS, Ane JM, Oldroyd GED, Kalo P (2011) Medicago truncatula IPD3 Is a Member of the Common Symbiotic Signaling Pathway Required for Rhizobial and Mycorrhizal Symbioses. Molecular Plant-Microbe Interactions **24:** 1345-1358

Imaizumi-Anraku H, Takeda N, Kawaguchi M, Parniske M, Hayashi M, Kawasaki S (2005) Host genes involved in activation and perception of calcium spiking. Plant and Cell Physiology **46:** S5-S5

Irizarry RA, Bolstad BM, Collin F, Cope LM, Hobbs B, Speed TP (2003) Summaries of affymetrix GeneChip probe level data. Nucleic Acids Research **31**

Ivanov S, Fedorova E, Bisseling T (2010) Intracellular plant microbe associations: secretory pathways and the formation of perimicrobial compartments. Current Opinion in Plant Biology **13:** 372-377

Jarsch IK, Ott T (2011) Perspectives on Remorin Proteins, Membrane Rafts, and Their Role During Plant-Microbe Interactions. Molecular Plant-Microbe Interactions **24:** 7-12

Javot H, Penmetsa RV, Terzaghi N, Cook DR, Harrison MJ (2007b) A *Medicago truncatula* phosphate transporter indispensable for the arbuscular mycorrhizal symbiosis. Proc Natl Acad Sci U S A **104:** 1720-1725

Jiang CF, Gao XH, Liao L, Harberd NP, Fu XD (2007) Phosphate starvation root architecture and anthocyanin accumulation responses are modulated by the gibberellin-DELLA signaling pathway in Arabidopsis(1[OA]). Plant Physiology **145:** 1460-1470

Jin HL, Martin C (1999) Multifunctionality and diversity within the plant MYB-gene family. Plant Molecular Biology **41:** 577-585

Jones MA, Grierson CS (2003) A simple method for obtaining cell-specific cDNA from small numbers of growing root-hair cells in Arabidopsis thaliana. Journal of Experimental Botany **54:** 1373-1378

Journet EP, van Tuinen D, Gouzy J, Crespeau H, Carreau V, Farmer MJ, Niebel A, Schiex T, Jaillon O, Chatagnier O, Godiard L, Micheli F, Kahn D, Gianinazzi-Pearson V, Gamas P (2002) Exploring root symbiotic programs in the model legume *Medicago truncatula* using EST analysis. Nucleic Acids Res **30:** 5579-5592

Kakar K, Wandrey M, Czechowski T, Gaertner T, Scheible WR, Stitt M, Torres-Jerez I, Xiao Y, Redman JC, Wu HC, Cheung F, Town CD, Udvardi MK (2008) A community resource for high-throughput quantitative RT-PCR analysis of transcription factor gene expression in *Medicago truncatula*. Plant Methods **4:** 18

Kalo P, Gleason C, Edwards A, Marsh J, Mitra RM, Hirsch S, Jakab J, Sims S, Long SR, Rogers J, Kiss GB, Downie JA, Oldroyd GE (2005) Nodulation signaling in legumes requires NSP2, a member of the GRAS family of transcriptional regulators. Science **308:** 1786-1789

Karandashov V, Bucher M (2005) Symbiotic phosphate transport in arbuscular mycorrhizas. Trends in Plant Science **10:** 22-29

Kehr J (2001) High resolution spatial analysis of plant systems. Current Opinion in Plant Biology **4:** 197-201

Kerk NM, Ceserani T, Tausta SL, Sussex IM, Nelson TM (2003) Laser capture microdissection of cells from plant tissues. Plant Physiol **132:** 27-35

Kistner C, Parniske M (2002) Evolution of signal transduction in intracellular symbiosis. Trends in Plant Science **7:** 511-518

Kistner C, Winzer T, Pitzschke A, Mulder L, Sato S, Kaneko T, Tabata S, Sandal N, Stougaard J, Webb KJ, Szczyglowski K, Parniske M (2005) Seven *Lotus japonicus* genes required for transcriptional reprogramming of the root during fungal and bacterial symbiosis. Plant Cell **17:** 2217-2229

Kizis D, Pages M (2002) Maize DRE-binding proteins DBF1 and DBF2 are involved in rab17 regulation through the drought-responsive element in an ABA-dependent pathway. Plant Journal **30:** 679-689

Kosuta S, Chabaud M, Lougnon G, Gough C, Denarie J, Barker DG, Becard G (2003) A diffusible factor from arbuscular mycorrhizal fungi induces symbiosis-specific MtENOD11 expression in roots of Medicago truncatula. Plant Physiology **131:** 952-962

Kosuta S, Hazledine S, Sun J, Miwa H, Morris RJ, Downie JA, Oldroyd GE (2008) Differential and chaotic calcium signatures in the symbiosis signaling pathway of legumes. Proc Natl Acad Sci U S A **105:** 9823-9828

Krajinski F, Hause B, Gianinazzi-Pearson V, Franken P (2002) Mtha1, a plasma membrane H+-ATPase gene from *Medicago truncatula*, shows arbuscule-specific induced expression in mycorrhizal roots. Plant Biology **4:** 754-761

Kumagai H, Kouchi H (2003) Gene silencing by expression of hairpin RNA in Lotus japonicus roots and root nodules. Mol Plant Microbe Interact **16:** 663-668

Küster H, Hohnjec N, Krajinski F, El YF, Manthey K, Gouzy J, Dondrup M, Meyer F, Kalinowski J, Brechenmacher L, van Tuinen D, Gianinazzi-Pearson V, Puhler A, Gamas P, Becker A (2004) Construction and validation of cDNA-based Mt6k-RIT macro- and microarrays to explore root endosymbioses in the model legume *Medicago truncatula*. J Biotechnol **108:** 95-113

Lauressergues D, Delaux PM, Formey D, Lelandais-Briere C, Fort S, Cottaz S, Becard G, Niebel A, Roux C, Combier JP (2012) The microRNA miR171h modulates arbuscular mycorrhizal colonization of Medicago truncatula by targeting NSP2. Plant Journal **72:** 512-522

Lefebvre B, Timmers T, Mbengue M, Moreau S, Herve C, Toth K, Bittencourt-Silvestre J, Klaus D, Deslandes L, Godiard L, Murray JD, Udvardi MK, Raffaele S, Mongrand S, Cullimore J, Gamas P, Niebel A, Ott T (2010) A remorin protein interacts with symbiotic receptors and regulates bacterial infection. Proceedings of the National Academy of Sciences of the United States of America **107:** 2343-2348

Levy J, Bres C, Geurts R, Chalhoub B, Kulikova O, Duc G, Journet EP, Ane JM, Lauber E, Bisseling T, Denarie J, Rosenberg C, Debelle F (2004) A putative Ca2+ and calmodulin-dependent protein kinase required for bacterial and fungal symbioses. Science **303:** 1361-1364

Libault M, Joshi T, Benedito VA, Xu D, Udvardi MK, Stacey G (2009) Legume transcription factor genes: what makes legumes so special? Plant Physiol **151:** 991-1001

Limpens E, Franken C, Smit P, Willemse J, Bisseling T, Geurts R (2003) LysM domain receptor kinases regulating rhizobial Nod factor-induced infection. Science **302:** 630-633

Limpens E, Mirabella R, Fedorova E, Franken C, Franssen H, Bisseling T, Geurts R (2005) Formation of organelle-like N-2-fixing symbiosomes in legume root nodules is controlled by DMI2. Proceedings of the National Academy of Sciences of the United States of America **102:** 10375-10380

Lipsick JS, Manak J, Mitiku N, Chen CK, Fogarty P, Guthrie E (2001) Functional evolution of the Myb oncogene family. Blood Cells Mol Dis **27:** 456-458

Liu J, Blaylock LA, Endre G, Cho J, Town CD, VandenBosch KA, Harrison MJ (2003) Transcript profiling coupled with spatial expression analyses reveals genes involved in distinct developmental stages of an arbuscular mycorrhizal symbiosis. Plant Cell **15:** 2106-2123

Liu J, Maldonado-Mendoza I, Lopez-Meyer M, Cheung F, Town CD, Harrison MJ (2007) Arbuscular mycorrhizal symbiosis is accompanied by local and systemic alterations in gene expression and an increase in disease resistance in the shoots. Plant J **50:** 529-544

Liu W, Kohlen W, Lillo A, Op den Camp R, Ivanov S, Hartog M, Limpens E, Jamil M, Smaczniak C, Kaufmann K, Yang WC, Hooiveld GJEJ, Charnikhova T, Bouwmeester HJ, Bisseling T, Geurts R (2011) Strigolactone Biosynthesis in Medicago truncatula and Rice Requires the Symbiotic GRAS-Type Transcription Factors NSP1 and NSP2. Plant Cell **23:** 3853-3865

Liu Y, Jiang Y, Qiao DR, Cao Y (2002) [The mechanism and application of posttranscriptional gene silencing]. Sheng Wu Gong Cheng Xue Bao **18:** 140-143

Lohse M, Nunes-Nesi A, Kruger P, Nagel A, Hannemann J, Giorgi FM, Childs L, Osorio S, Walther D, Selbig J, Sreenivasulu N, Stitt M, Fernie AR, Usadel B (2010) Robin: An Intuitive Wizard Application for R-Based Expression Microarray Quality Assessment and Analysis. Plant Physiology **153:** 642-651

Lorenzo O, Piqueras R, Sanchez-Serrano JJ, Solano R (2003) ETHYLENE RESPONSE FACTOR1 integrates signals from ethylene and jasmonate pathways in plant defense. Plant Cell **15:** 165-178

Madsen EB, Madsen LH, Radutoiu S, Olbryt M, Rakwalska M, Szczyglowski K, Sato S, Kaneko T, Tabata S, Sandal N, Stougaard J (2003) A receptor kinase gene of the LysM type is involved in legume perception of rhizobial signals. Nature **425:** 637-640

Maillet F, Poinsot V, Andre O, Puech-Pages V, Haouy A, Gueunier M, Cromer L, Giraudet D, Formey D, Niebel A, Martinez EA, Driguez H, Becard G, Denarie J (2011) Fungal lipochitooligosaccharide symbiotic signals in arbuscular mycorrhiza. Nature **469:** 58-U1501

Manthey K, Krajinski F, Hohnjec N, Firnhaber C, Puhler A, Perlick AM, Küster H (2004) Transcriptome profiling in root nodules and arbuscular mycorrhiza identifies a collection of novel genes induced during *Medicago truncatula* root endosymbioses. Mol Plant Microbe Interact **17:** 1063-1077

Marin M, Ott T (2012) Phosphorylation of intrinsically disordered regions in remorin proteins. Front Plant Sci **3:** 86

Marin M, Thallmair V, Ott T (2012) The Intrinsically Disordered N-terminal Region of AtREM1.3 Remorin Protein Mediates Protein-Protein Interactions. Journal of Biological Chemistry **287**

Marschner H, Dell B (1994) Nutrient-Uptake in Mycorrhizal Symbiosis. Plant and Soil **159:** 89-102

Martin C, PazAres J (1997) MYB transcription factors in plants. Trends in Genetics **13:** 67-73

Matzke M, Matzke AJM, Kooter JM (2001) RNA: Guiding gene silencing. Science **293:** 1080-1083

McConnell JR, Emery J, Eshed Y, Bao N, Bowman J, Barton MK (2001) Role of PHABULOSA and PHAVOLUTA in determining radial patterning in shoots. Nature **411:** 709-713

Messinese E, Mun JH, Yeun LH, Jayaraman D, Rouge P, Barre A, Lougnon G, Schornack S, Bono JJ, Cook DR, Ane JM (2007) A novel nuclear protein interacts with the symbiotic DMI3 calcium- and calmodulin-dependent protein kinase of Medicago truncatula. Molecular Plant-Microbe Interactions **20:** 912-921

Middleton PH, Jakab J, Penmetsa RV, Starker CG, Doll J, Kalo P, Prabhu R, Marsh JF, Mitra RM, Kereszt A, Dudas B, VandenBosch K, Long SR, Cook DR, Kiss GB, Oldroyd GED (2007) An ERF transcription factor in Medicago truncatula that is essential for nod factor signal transduction. Plant Cell **19:** 1221-1234

Mitra RM, Gleason CA, Edwards A, Hadfield J, Downie JA, Oldroyd GE, Long SR (2004) A Ca2+/calmodulin-dependent protein kinase required for symbiotic nodule development: Gene identification by transcript-based cloning. Proc Natl Acad Sci U S A **101:** 4701-4705

Morandi D, Gollotte A, Camporota P (2002) Influence of an arbuscular mycorrhizal fungus on the interaction of a binucleate Rhizoctonia species with Myc+ and Myc- pea roots. Mycorrhiza **12:** 97-102

Nagy R, Drissner D, Amrhein N, Jakobsen I, Bucher M (2009) Mycorrhizal phosphate uptake pathway in tomato is phosphorus-repressible and transcriptionally regulated. New Phytologist **181:** 950-959

Nair MG, Safir GR, Siqueira JO (1991) Isolation and Identification of Vesicular-Arbuscular Mycorrhiza-Stimulatory Compounds from Clover (Trifolium repens) Roots. Appl Environ Microbiol **57:** 434-439

Nakagawa T, Kurose T, Hino T, Tanaka K, Kawamukai M, Niwa Y, Toyooka K, Matsuoka K, Jinbo T, Kimura T (2007) Development of series of gateway binary vectors, pGWBs, for realizing efficient construction of fusion genes for plant transformation. J Biosci Bioeng **104:** 34-41

Nakajima K, Sena G, Nawy T, Benfey PN (2001) Intercellular movement of the putative transcription factor SHR in root patterning. Nature **413:** 307-311

Nakano T, Suzuki K, Fujimura T, Shinshi H (2006) Genome-wide analysis of the ERF gene family in Arabidopsis and rice. Plant Physiology **140:** 411-432

Nakazono M, Qiu F, Borsuk LA, Schnable PS (2003) Laser-capture microdissection, a tool for the global analysis of gene expression in specific plant cell types: identification of genes expressed differentially in epidermal cells or vascular tissues of maize. Plant Cell **15:** 583-596

Nelson T, Tausta SL, Gandotra N, Liu T (2006) Laser microdissection of plant tissue: what you see is what you get. Annu Rev Plant Biol **57:** 181-201

Newman EI, Reddell P (1987) The Distribution of Mycorrhizas among Families of Vascular Plants. New Phytologist **106:** 745-751

Ohmetakagi M, Shinshi H (1995) Ethylene-Inducible DNA-Binding Proteins That Interact with an Ethylene-Responsive Element. Plant Cell **7:** 173-182

Okamuro JK, Caster B, Villarroel R, VanMontagu M, Jofuku KD (1997) The AP2 domain of APETALA2 defines a large new family of DNA binding proteins in Arabidopsis. Proceedings of the National Academy of Sciences of the United States of America **94:** 7076-7081

Olah B, Briere C, Becard G, Denarie J, Gough C (2005) Nod factors and a diffusible factor from arbuscular mycorrhizal fungi stimulate lateral root formation in *Medicago truncatula* via the DMI1/DMI2 signalling pathway. Plant J **44:** 195-207

Oldroyd GE (2013) Speak, friend, and enter: signalling systems that promote beneficial symbiotic associations in plants. Nat Rev Microbiol **11:** 252-263

Oldroyd GE, Downie JA (2006) Nuclear calcium changes at the core of symbiosis signalling. Curr Opin Plant Biol **9:** 351-357

Oldroyd GED, Downie JM (2008) Coordinating nodule morphogenesis with rhizobial infection in legumes. Annu Rev Plant Biol **59:** 519-546

Oldroyd GED, Long SR (2003) Identification and characterization of nodulation-signaling pathway 2, a gene of Medicago truncatula involved in Nod factor signaling. Plant Physiology **131:** 1027-1032

Olsson PA, Johansen A (2000) Lipid and fatty acid composition of hyphae and spores of arbuscular mycorrhizal fungi at different growth stages. Mycol Res **104:** 429-434

Onate-Sanchez L, Singh KB (2002) Identification of Arabidopsis ethylene-responsive element binding factors with distinct induction kinetics after pathogen infection. Plant Physiology **128:** 1313-1322

Op den Camp R, Streng A, De Mita S, Cao Q, Polone E, Liu W, Ammiraju SS, Kudrna D, Wing R, Untergassser A, Bisseling T, Geurts R (2011) LysM-Type Mycorrhizal Receptor Recruited for Rhizobium Symbiosis in Nonlegume Parasponia Science **331:** 909-912

Pant BD, Buhtz A, Kehr J, Scheible WR (2008) MicroRNA399 is a long-distance signal for the regulation of plant phosphate homeostasis. Plant Journal **53:** 731-738

Parniske M (2005) Plant-fungal associations: cue for the branching connection. Nature **435:** 750-751

Peel GJ, Pang YZ, Modolo LV, Dixon RA (2009) The LAP1 MYB transcription factor orchestrates anthocyanidin biosynthesis and glycosylation in Medicago. Plant Journal **59:** 136-149

Peiter E, Sun J, Heckmann AB, Venkateshwaran M, Riely BK, Otegui MS, Edwards A, Freshour G, Hahn MG, Cook DR, Sanders D, Oldroyd GED, Downie JA, Ane JM (2007) The Medicago truncatula DMI1 protein modulates cytosolic calcium signaling. Plant Physiology **145:** 192-203

Peng J, Carol P, Richards DE, King KE, Cowling RJ, Murphy GP, Harberd NP (1997) The Arabidopsis GAI gene defines a signaling pathway that negatively regulates gibberellin responses. Genes Dev **11:** 3194-3205

Peters W, Latka I (1986) Electron-Microscopic Localization of Chitin Using Colloidal Gold Labeled with Wheat-Germ-Agglutinin. Histochemistry **84:** 155-160

Pirozynski KA, Malloch DW (1975) The origin of land plants: a matter of mycotrophism. Biosystems **6:** 153-164

Popp C, Ott T (2011) Regulation of signal transduction and bacterial infection during root nodule symbiosis. Current Opinion in Plant Biology **14:** 458-467

Pumplin N, Harrison MJ (2009) Live-Cell Imaging Reveals Periarbuscular Membrane Domains and Organelle Location in Medicago truncatula Roots during Arbuscular Mycorrhizal Symbiosis. Plant Physiology **151:** 809-819

Pysh LD, Wysocka-Diller JW, Camilleri C, Bouchez D, Benfey PN (1999) The GRAS gene family in Arabidopsis: sequence characterization and basic expression analysis of the SCARECROW-LIKE genes. Plant Journal **18:** 111-119

Quandt HJ, Puhler A, Broer I (1993) Transgenic Root-Nodules of Vicia-Hirsuta - a Fast and Efficient System for the Study of Gene-Expression in Indeterminate-Type Nodules. Molecular Plant-Microbe Interactions **6:** 699-706

Radutoiu S, Madsen LH, Madsen EB, Felle HH, Umehara Y, Gronlund M, Sato S, Nakamura Y, Tabata S, Sandal N, Stougaard J (2003) Plant recognition of symbiotic bacteria requires two LysM receptor-like kinases. Nature **425:** 585-592

Raffaele S, Bayer E, Lafarge D, Cluzet S, Retana SG, Boubekeur T, Leborgne-Castel N, Carde JP, Lherminier J, Noirot E, Satiat-Jeunemaitre B, Laroche-Traineau J, Moreau P, Ott

T, Maule AJ, Reymond P, Simon-Plas F, Farmer EE, Bessoule JJ, Mongrand S (2009) Remorin, a Solanaceae Protein Resident in Membrane Rafts and Plasmodesmata, Impairs Potato virus X Movement. Plant Cell **21:** 1541-1555

Raffaele S, Mongrand S, Gamas P, Niebel A, Ott T (2007) Genome-wide annotation of remorins, a plant-specific protein family: Evolutionary and functional perspectives. Plant Physiology **145:** 593-600

Redecker D, Kodner R, Graham LE (2000) Glomalean fungi from the Ordovician. Science **289:** 1920-1921

Reinhart BJ, Weinstein EG, Rhoades MW, Bartel B, Bartel DP (2002) MicroRNAs in plants (vol 16, pg 1616, 2002). Genes & Development **16:** 2313-2313

Remy W, Taylor TN, Hass H, Kerp H (1994) Four hundred-million-year-old vesicular arbuscular mycorrhizae. Proc Natl Acad Sci U S A **91:** 11841-11843

Rhoades MW, Reinhart BJ, Lim LP, Burge CB, Bartel B, Bartel DP (2002) Prediction of plant microRNA targets. Cell **110:** 513-520

Riechmann JL, Heard J, Martin G, Reuber L, Jiang C, Keddie J, Adam L, Pineda O, Ratcliffe OJ, Samaha RR, Creelman R, Pilgrim M, Broun P, Zhang JZ, Ghandehari D, Sherman BK, Yu G (2000) Arabidopsis transcription factors: genome-wide comparative analysis among eukaryotes. Science **290:** 2105-2110

Riechmann JL, Meyerowitz EM (1998) The AP2/EREBP family of plant transcription factors. Biological Chemistry **379:** 633-646

Ruiz-Lozano JM (2003) Arbuscular mycorrhizal symbiosis and alleviation of osmotic stress. New perspectives for molecular studies. Mycorrhiza **13:** 309-317

Sabatini S, Heidstra R, Wildwater M, Scheres B (2003) SCARECROW is involved in positioning the stem cell niche in the Arabidopsis root meristem. Genes & Development **17:** 354-358

Sakuma Y, Liu Q, Dubouzet JG, Abe H, Shinozaki K, Yamaguchi-Shinozaki K (2002) DNA-binding specificity of the ERF/AP2 domain of Arabidopsis DREBs, transcription factors involved in dehydration- and cold-inducible gene expression. Biochem Biophys Res Commun **290:** 998-1009

Schad M, Mungur R, Fiehn O, Kehr J (2005) Metabolic profiling of laser microdissected vascular bundles of *Arabidopsis thaliana*. Plant Methods **1:** 2

Scheidl SJ, Nilsson S, Kalen M, Hellstrom M, Takemoto M, Hakansson J, Lindahl P (2002) mRNA expression profiling of laser microbeam microdissected cells from slender embryonic structures. American Journal of Pathology **160:** 801-813

Schoof H, Lenhard M, Haecker A, Mayer KFX, Jurgens G, Laux T (2000) The stem cell population of Arabidopsis shoot meristems is maintained by a regulatory loop between the CLAVATA and WUSCHEL genes. Cell **100:** 635-644

Schroeder A, Mueller O, Stocker S, Salowsky R, Leiber M, Gassmann M, Lightfoot S, Menzel W, Granzow M, Ragg T (2006) The RIN: an RNA integrity number for assigning integrity values to RNA measurements. BMC Mol Biol **7:** 3

Schüssler A, Schwarzott D, Walker C (2001) A new fungal phylum, the Glomeromycota: phylogeny and evolution. Mycol Res **105:** 1413-1421

Schwab R, Ossowski S, Riester M, Warthmann N, Weigel D (2006) Highly specific gene silencing by artificial microRNAs in Arabidopsis. Plant Cell **18:** 1121-1133

Schweizer P, Pokorny J, Schulze-Lefert P, Dudler R (2000) Double-stranded RNA interferes with gene function at the single-cell level in cereals. Plant Journal **24:** 895-903

Shinshi H, Usami S, Ohmetakagi M (1995) Identification of an Ethylene-Responsive Region in the Promoter of a Tobacco Class-I Chitinase Gene. Plant Molecular Biology **27:** 923-932

Siciliano V, Genre A, Balestrini R, Cappellazzo G, deWit PJ, Bonfante P (2007) Transcriptome analysis of arbuscular mycorrhizal roots during development of the pre-penetration apparatus. Plant Physiol **144:** 1455-1466

Sieberer BJ, Chabaud M, Fournier J, Timmers AC, Barker DG (2012) A switch in Ca2+ spiking signature is concomitant with endosymbiotic microbe entry into cortical root cells of Medicago truncatula. Plant Journal **69:** 822-830

Silverstone AL, Ciampaglio CN, Sun T (1998) The Arabidopsis RGA gene encodes a transcriptional regulator repressing the gibberellin signal transduction pathway. Plant Cell **10:** 155-169

Simon L, Bousquet J, Levesque RC, Lalonde M (1993) Origin and Diversification of Endomycorrhizal Fungi and Coincidence with Vascular Land Plants. Nature **363:** 67-69

Smit P, Raedts J, Portyanko V, Debelle F, Gough C, Bisseling T, Geurts R (2005) NSP1 of the GRAS protein family is essential for rhizobial Nod factor-induced transcription. Science **308:** 1789-1791

Smith SE, Read DJ (1997) Mycorrhizal Symbiosis. CA:Academic

Smith SE, Smith FA, Jakobsen I (2003) Mycorrhizal fungi can dominate phosphate supply to plants irrespective of growth responses. Plant Physiol **133:** 16-20

Smyth GK (2004) Linear models and empirical bayes methods for assessing differential expression in microarray experiments. Stat Appl Genet Mol Biol **3:** Article3

Soltis DE, Smith SA, Cellinese N, Wurdack KJ, Tank DC, Brockington SF, Refulio-Rodriguez NF, Walker JB, Moore MJ, Carlsward BS, Bell CD, Latvis M, Crawley S, Black C, Diouf D, Xi Z, Rushworth CA, Gitzendanner MA, Sytsma KJ, Qiu YL, Hilu KW, Davis CC, Sanderson MJ, Beaman RS, Olmstead RG, Judd WS, Donoghue MJ, Soltis PS (2011) Angiosperm phylogeny: 17 genes, 640 taxa. American Journal of Botany **98:** 704-730

Sprent JI, James EK (2007) Legume evolution: Where do nodules and mycorrhizas fit in? Plant Physiology **144:** 575-581

Strack D, Fester T, Hause B, Schliemann W, Walter MH (2003) Arbuscular mycorrhiza: Biological, chemical, and molecular aspects. Journal of Chemical Ecology **29:** 1955-1979

Stracke S, Kistner C, Yoshida S, Mulder L, Sato S, Kaneko T, Tabata S, Sandal N, Stougaard J, Szczyglowski K, Parniske M (2002) A plant receptor-like kinase required for both bacterial and fungal symbiosis. Nature **417:** 959-962

Sunkar R, Girke T, Jain PK, Zhu JK (2005) Cloning and characterization of MicroRNAs from rice. Plant Cell **17:** 1397-1411

Sunkar R, Zhu JK (2004) Novel and stress-regulated microRNAs and other small RNAs from Arabidopsis. Plant Cell **16:** 2001-2019

Takeda N, Maekawa T, Hayashi M (2012) Nuclear-Localized and Deregulated Calcium- and Calmodulin-Dependent Protein Kinase Activates Rhizobial and Mycorrhizal Responses in Lotus japonicus. Plant Cell **24:** 810-822

Talbert PB, Adler HT, Parks DW, Comai L (1995) The Revoluta Gene Is Necessary for Apical Meristem Development and for Limiting Cell Divisions in the Leaves and Stems of Arabidopsis-Thaliana. Development **121:** 2723-2735

Tellström V, Usadel B, Thimm O, Stitt M, Küster H, Niehaus K (2007) The lipopolysaccharide of *Sinorhizobium meliloti* suppresses defense-associated gene expression in cell cultures of the host plant *Medicago truncatula*. Plant Physiol **143:** 825-837

Thimm O, Blasing O, Gibon Y, Nagel A, Meyer S, Kruger P, Selbig J, Muller LA, Rhee SY, Stitt M (2004) MAPMAN: a user-driven tool to display genomics data sets onto diagrams of metabolic pathways and other biological processes. Plant J **37:** 914-939

Thompson JD, Higgins DG, Gibson TJ (1994) Clustal-W - Improving the Sensitivity of Progressive Multiple Sequence Alignment through Sequence Weighting, Position-Specific Gap Penalties and Weight Matrix Choice. Nucleic Acids Research **22:** 4673-4680

Tian C, Kasiborski B, Koul R, Lammers PJ, Bucking H, Shachar-Hill Y (2010) Regulation of the nitrogen transfer pathway in the arbuscular mycorrhizal symbiosis: gene characterization and the coordination of expression with nitrogen flux. Plant Physiol **153:** 1175-1187

Tian C, Wan P, Sun S, Li J, Chen M (2004) Genome-wide analysis of the GRAS gene family in rice and Arabidopsis. Plant Mol Biol **54:** 519-532

Tisserant E, Kohler A, Dozolme-Seddas P,. Balestrini R, Benabdellah K, Colard A. Croll D, Da Silva C. Gomez S K, Koul R, Ferrol N, Fiorilli V, Formey D, Franken Ph, Helber N, Hijri M, Lanfranco L, Lindquist E, Liu Y, Malbreil M, Morin E, Poulain J, Shapiro H, van Tuinen D, Waschke A, Azco´n-Aguilar C, Be´card G, Bonfante P, Harrison M J, Küster H, Lammers P, Paszkowski U, Requena N, Rensing S A, Roux C, Sanders I R, Shachar-Hill Y, Tuskan G,Young J P W, Gianinazzi-PearsonV and Martin F (2012) The transcriptome of the arbuscular mycorrhizal fungus *Glomus intraradices* (DAOM 197198) reveals functional tradeoffs in an obligate symbiont. New Phytologist **193**: 755–769

Toth K, Stratil TF, Madsen EB, Ye JY, Popp C, Antolin-Llovera M, Grossmann C, Jensen ON, Schussler A, Parniske M, Ott T (2012) Functional Domain Analysis of the Remorin Protein LjSYMREM1 in Lotus japonicus. PLoS One **7**

Toth R, Miller RM (1984) Dynamics of Arbuscule Development and Degeneration in a Zea-Mays Mycorrhiza. American Journal of Botany **71:** 449-460

Trouvelot A, Fardeau JC, Plenchette C, Gianinazzi S, Gianinazzapearson V (1986) Nutritional Balance and Symbiotic Expression in Mycorrhizal Wheat. Physiologie Vegetale **24:** 300-300

Udvardi MK, Kakar K, Wandrey M, Montanari O, Murray J, Andriankaja A, Zhang JY, Benedito V, Hofer JM, Chueng F, Town CD (2007) Legume transcription factors: global regulators of plant development and response to the environment. Plant Physiol **144:** 538-549

Usadel B, Nagel A, Thimm O, Redestig H, Blaesing OE, Palacios-Rojas N, Selbig J, Hannemann J, Piques MC, Steinhauser D, Scheible WR, Gibon Y, Morcuende R, Weicht D, Meyer S, Stitt M (2005) Extension of the visualization tool MapMan to allow statistical analysis of arrays, display of coresponding genes, and comparison with known responses. Plant Physiology **138:** 1195-1204

Usadel B, Poree F, Nagel A, Lohse M, Czedik-Eysenberg A, Stitt M (2009) A guide to using MapMan to visualize and compare Omics data in plants: a case study in the crop species, Maize. Plant Cell and Environment **32:** 1211-1229

Valdes-Lopez O, Arenas-Huertero C, Ramirez M, Girard L, Sanchez F, Vance CP, Luis Reyes J, Hernandez G (2008) Essential role of MYB transcription factor: PvPHR1 and microRNA: PvmiR399 in phosphorus-deficiency signalling in common bean roots. Plant Cell Environ **31:** 1834-1843

Voets L, de la Providencia IE, Declerck S (2006) Glomeraceae and Gigasporaceae differ in their ability to form hyphal networks. New Phytologist **172:** 185-188

Volpe V, Dell'Aglio E, Giovannetti M, Ruberti C, Costa A, Genre A, Guether M, Bonfante P (2013) An AM-induced, MYB-family gene of Lotus japonicus (LjMAMI) affects root growth in an AM-independent manner. Plant J **73:** 442-455

Wais RJ, Galera C, Oldroyd G, Catoira R, Penmetsa RV, Cook D, Gough C, Denarie J, Long SR (2000) Genetic analysis of calcium spiking responses in nodulation mutants of Medicago truncatula. Proceedings of the National Academy of Sciences of the United States of America **97:** 13407-13412

Walter M, Chaban C, Schutze K, Batistic O, Weckermann K, Nake C, Blazevic D, Grefen C, Schumacher K, Oecking C, Harter K, Kudla J (2004) Visualization of protein interactions in living plant cells using bimolecular fluorescence complementation. Plant Journal **40:** 428-438

Wang ET, Schornack S, Marsh JF, Gobbato E, Schwessinger B, Eastmond P, Schultze M, Kamoun S, Oldroyd GED (2012) A Common Signaling Process that Promotes Mycorrhizal and Oomycete Colonization of Plants. Current Biology **22:** 2242-2246

Wesley SV, Liu Q, Wielopolska A, Ellacott G, Smith N, Singh S, Helliwell C (2003) Custom knock-outs with hairpin RNA-mediated gene silencing. Methods Mol Biol **236:** 273-286

Wienkoop S, Saalbach G (2003) Proteome analysis. Novel proteins identified at the peribacteroid membrane from Lotus japonicus root nodules. Plant Physiology **131:** 1080-1090

Wulf A, Manthey K, Doll J, Perlick AM, Linke B, Bekel T, Meyer F, Franken P, Küster H, Krajinski F (2003) Transcriptional changes in response to arbuscular mycorrhiza development in the model plant *Medicago truncatula*. Mol Plant Microbe Interact **16:** 306-314

Yang KY, Liu YD, Zhang SQ (2001) Activation of a mitogen-activated protein kinase pathway is involved in disease resistance in tobacco. Proceedings of the National Academy of Sciences of the United States of America **98:** 741-746

Zhu YG, Smith FA, Smith SE (2003) Phosphorus efficiencies and responses of barley (Hordeum vulgare L.) to arbuscular mycorrhizal fungi grown in highly calcareous soil. Mycorrhiza **13:** 93-100

9 Appendix

9.1 List of chemicals

Table 10: Chemicals

Reagent	Manufacturer
2-(*N*-morpholino)ethanesulfonic acid (MES) ($C_6H_{13}NO_4S$)	*Sigma-Aldrich*, Seelze, Germany
3-(N-Morpholino)-propanesulfonate (MOPS)	*Carl Roth*, Karlsruhe, Germany
5-Brom-4-chlor-3-indolyl-β-D-glucuronsäure (X-Gluc)	*Carl Roth*, Karlsruhe, Germany
5-bromo-4-chloro-indolyl-β-D-galactopyranoside (X-Gal	*Carl Roth*, Karlsruhe, Germany
6 x DNA loading dye	*Thermo Fisher Scientific*, Henningsdorf, Germany
Acetic acid (CH_3CO_2H)	*Riedel de Häen*, Seelze, Germany
Acetosyringone	*Sigma-Aldrich*, Seelze, Germany
Ammonium nitrate (NH_4NO_3)	*Carl Roth*, Karlsruhe, Germany
ß-mercaptoethanol	*Sigma-Aldrich*, Seelze, Germany
Bacto™ Agar	*Becton Dickinson*, Heidelberg, Germany
Bacto™ Trypton	*Becton Dickinson*, Heidelberg, Germany
Beef extract	*Duchefa Biochemie B.V.*, Haarlem, Netherlands
Biozym LE agarose	*Biozym Scientific*, Hess. Oldendorf, Germany
Boric acid (H_3BO_3)	*Carl Roth*, Karlsruhe, Germany
Bromphenol blue 6x	*Sigma-Aldrich*, Seelze, Germany
Calcium chloride ($CaCl_2$)	*Duchefa Biochemie B.V., Haarlem*, Netherlands
Calcium nitrate ($Ca(NO_3)_2$)	*Carl Roth*, Karlsruhe, Germany
Citric acid anhydrous ($C_6H_8O_7$)	*Carl Roth*, Karlsruhe, Germany
CTAB (N-Cetyl- N,N,N- Trimethyl - ammoniumbromid)	*Sigma-Aldrich*, Seelze, Germany
Cobald chloride ($CoCl_2$ x $6H_2O$)	*Carl Roth*, Karlsruhe, Germany
Copper sulfate ($CuSO_4$ x $5H_2O$)	*Carl Roth*, Karlsruhe, Germany
Diethylpyrocarbonate (DEPC)	*Sigma-Aldrich*, Seelze, Germany

Table 10: Chemicals

Reagent	Manufacturer
Dithiothreitol; Threo-1,4-dimercapto-2,3-butandiol (DTT)	*Thermo Fisher Scientific*, Henningsdorf, Germany
Dimethyl sulfoxide (DMSO)	*Carl Roth*, Karlsruhe, Germany
EDTA ($C_{10}H_{16}N_2O_8$)	*Carl Roth*, Karlsruhe, Germany
Ethanol absolute (C_2H_6O)	*VWR international*, Darmstadt, Germany
Ethidium bromide (EhtBr)	*Sigma-Aldrich*, Seelze, Germany
Formaldehyde (CH_2O)	*Carl Roth*, Karlsruhe, Germany
Formamide (CH_3NO)	*Carl Roth*, Karlsruhe, Germany
Gene Ruler™ 100bp Plus DNA Ladder	*Thermo Fisher Scientific*, Henningsdorf, Germany
GeneRuler™ 1kbPlus DNA Ladder	*Thermo Fisher Scientific*, Henningsdorf, Germany
Glucose ($C_6H_{12}O_6$)	*Carl Roth*, Karlsruhe, Germany
Glycin ($C_2H_5NO_2$)	*Carl Roth*, Karlsruhe, Germany
Glycerol 87 %	*Merck*, Darmstadt, Germany
Guanidinium chloride (GdmCl) (CH_5N_3HCl)	*Carl Roth*, Karlsruhe, Germany
Hydrochloric acid (HCl)	*Fluka Riedel de Haën*, Seelze, Germany
IPTG	*Carl Roth*, Karlsruhe, Germany
Isopropyl ethanol (C_3H_8O)	*Fluka Riedel de Häen*, Seelze, Germany
Manganese chloride ($MnCl_2$ x $4H_2O$)	*Carl Roth*, Karlsruhe, Germany
Manganese sulfate ($MnSO_4$ x H_2O)	*Sigma-Aldrich*, Seelze, Germany
Magnesium chloride ($MgCl_2$)	*Carl Roth*, Karlsruhe, Germany
Magnesium sulfate ($MgSO_4$ x $7H_2O$)	*Duchefa Biochemie B.V., Haarlem*, Netherlands
Myo-inositol ($C_6H_{12}O_6$)	*Merck*, Darmstadt, Germany
Nickel sulfate ($NiSO_4$ x $6H_2O$)	*Carl Roth*, Karlsruhe, Germany
Nicotinic acid ($C_6H_5NO_2$)	*Duchefa Biochemie B.V., Haarlem*, Netherlands
NN-dimethyl formamide (DMF)	*Sigma-Aldrich*, Seelze, Germany
Peptone	*Becton Dickinson*, Heidelberg, Germany

Table 10: Chemicals

Reagent	Manufacturer
Phytagel™	*Sigma-Aldrich*, Seelze, Germany
Potassium acetate (CH_3O_2K)	*Carl Roth*, Karlsruhe, Germany
Potassium chloride (KCl)	*Carl Roth*, Karlsruhe, Germany
Potassium ferricyanide ($K_3[Fe(CN)_6]$)	*Sigma-Aldrich*, Seelze, Germany
Potassium ferrocyanide ($K_4[Fe(CN)_6] \times 3H_2O$)	*Sigma-Aldrich*, Seelze, Germany
Potassium hydroxide (KOH)	*Fluka Riedel de Häen*, Seelze, Germany
Potassium phosphate (KH_2PO_4)	*Carl Roth*, Karlsruhe, Germany
PVP (Polyvinylpolypyrrolidone)	*Duchefa Biochemie B.V., Haarlem*, Netherlands
Pyridoxin	*Sigma-Aldrich*, Seelze, Germany
RNaseZAP®	*Sigma-Aldrich*, Seelze, Germany
Fe-EDTA	*Duchefa Biochemie B.V., Haarlem*, Netherlands
Roti® -Phenol/Chloroform/Isoamyl alcohol	*Carl Roth*, Karlsruhe, Germany
Select Agar®	*Thermo Fisher Scientific*, Henningsdorf, Germany
Sodium acetate (NaOAc) ($C_2H_3NaO_2$)	*Merck*, Darmstadt, Germany
Sodium chloride (NaCl)	*Carl Roth*, Karlsruhe, Germany
Sodium dodecyl sulfate (SDS) ($C_{12}H_{25}NaO_4S$)	*Bio-Rad laboratories*, Munich, Germany
Sodium hydroxide (NaOH)	*Fluka Riedel de Häen*, Seelze, Germany
Sodium hypochloride (NaOCl)	*Carl Roth*, Karlsruhe, Germany
Sodium molybdate ($Na_2MoO_4 \times 2H_2O$)	*Sigma-Aldrich*, Seelze, Germany
Sodium phosphate dibasic ($Na_2HPO_4 \times H_2O$)	*Carl Roth*, Karlsruhe, Germany
Sulforic acid (H_2SO_4)	*Sigma-Aldrich*, Seelze, Germany
Sucrose ($C_{12}H_{22}O_{11}$)	*AppliChem, Berlin,Germany*
Thiamin HCl	*Sigma-Aldrich*, Seelze, Germany
Tris-acetate ($(HOCH_2)_3CNH_2$))	*Carl Roth*, Karlsruhe, Germany
Trisodium citrate ($Na_3C_6H_5O_7$)	*Fluka Riedel de Haën*, Seelze, Germany

Table 10: Chemicals

Reagent	Manufacturer
Trypan blue	*Fluka Riedel de Häen*, Seelze, Germany
Yeast Extract	*Duchefa Biochemie B.V.*, Haarlem, Netherlands
Zinc sulfate ($ZnSO_4$ x $7H_2O$)	*Sigma-Aldrich*, Seelze, Germany

9.2 List of consumables

Table 11: Consumables

Equipment	Type	Manufacturer
1 kb DNA ladder	Gene Ruler 1 kb Ladder 250 – 10000 bp	*Thermo Fisher Scientific*, Henningsdorf, Germany
1 kb plus DNA ladder	Gene Ruler 1 kb Plus Ladder 75 – 20000 bp	*Thermo Fisher Scientific*, Henningsdorf, Germany
100 bp DNA ladder	Gene Ruler 100 bp Plus Ladder 100 – 3000 bp	*Thermo Fisher Scientific*, Henningsdorf, Germany
1,5 ml and 2 ml reaction tubes		*Eppendorf*, Hamburg, Germany
384 well micortiter plates	MicroAmp® Optical 384 well reaction plate	*Life Technologies*, Darmstadt, Germany
50 ml reaction tubes		*BD Biosciences Clontech*, Heidelberg, Germany
Adhesive caps	Adhesive caps 500 clear	*Carl Zeiss Micro imaging*, Berlin, Germany
Affymetrix Microarray	Affymetrix GeneChip® Medicago Genome Array	Affymetrix, Wooburn Green, UK
Cover glasses	24x50 mm Deckgläser	*Carl Roth*, Karlsruhe, Germany
Electroporation cuvettes	Electroporade cuvettes 2mm electrode gap	*PeqLab*, Erlangen, Germany
Microfluid chip for Bionalyzer Measurements	RNA 600 Picolab Chip	*Agilent*™, Berlin, Germany
Microscope slides		*Paul-Marienfeld GmbH &CoKG*, Lauda-Königshofen, Germany
Nail polish		*Science Service*, Munich, Germany
Oligo(dT) primer	Oligo(dT)$_{12-18}$ Primer	*Thermo Fisher Scientific*, Henningsdorf, Germany
Parafilm®		*American National Can*, Menasha, USA
PCR foil	G060/UC-RT	*G. Kisker GbR*, Steinfurt, Germany
Petri dishes, circulare 92/16 mm		*Grainer Bio-one*, Kremsmünster, Germany
Petri dishes, square 120/717 mm		*Sarsted AG & Co.*, Nürnbrecht, Germany
Pipettes	Reference, Research Pro	*Eppendorf*, Hamburg, Germany
Poly-L-lysine coated slides	Poly-Prep Slides	*SIGMA-Aldrich*, Seelze, Germany
RNA ladder for Bioanalyzer measurements	RNA 6000 ladder	*Agilent*™, Berlin, Germany
scalpel blade		*C. Bruno Bayha*, Tuttlingen, Germany

Table 11: Consumables

Equipment	Type	Manufacturer
Shredder columns	QIAShredder™ (50)	*Qiagen*™, Hilden, Germany
Slide boxes		*Carl Zeiss Micro imaging*, Berlin, Germany
Syringe (1ml)	1 ml NORM-JECT®	*Henke-Sass, Wolf GmbH*, Tuttlingen, Germany
Tips 10µl, 100µl, 1000µl		*Eppendorf*, Hamburg, Germany
Tissue freezing medium	TMF™ tissue freezing medium	*Science Service*, Munich, Germany

9.3 List of technical devices

Table 12: Technical devices

Technical device	Type	Manufacturer
Bioanalyzer	Agilent™ 2100 Bioanalyzer	*Agilent™*, Berlin, Germany
Thermomixer	Thermomixer comfort	*Eppendorf*, Hamburg, Germany
Centrifuge	MiniSpin plus incl. stadardrotor	*Eppendorf*, Hamburg, Germany
Centrifuge	NeoLab	*NeoLab*, Heidelberg, Germany
Clean bench	Hera safe	*Thermo Scientific*, Langenselbold, Germany
Confocal microscope	TCP SP5 confocal	*Leica*, Wetzlar, Germany
Cryostat	Leica CM 1950 Cryostat	*Leica Mikrosystemes*, Wetzlar, Germany
Electroporator	Electroporator2150	*Eppendorf*, Hamburg, Germany
Epifluorescence microscope	Olymus BX-51TF-5	*Olympus Deutschland GmbH*, Hamburg, Germany
Gel documentation incl. PC system and CCD camera	ChemiDoc	*Bio-Rad Laboratories*, Munich, Germany
Glass container	Färbekasten nach Schiefferdecker	*CARL ROTH*, Karlsruhe, Germany
Heating plate	Präzitherm	*Störk-Tronic*, Stuttgart, Germany
Laser Assisted Microdissection system	P.A.L.M.® LCM Microbeam 02027	*P.A.L.M. Microlaser technologies*, Bernried, Germany
Nanodrop ND-1000	ND1000	*NanoDrop*®, Willington, Delaware, USA
PCR-mashine /thermocycler	MJ research PTC-200 Peltier	*Biozym*, Hess. Oldendorf, Germany
Photometer		*Eppendorf*, Hamburg, Germany
Real-Time PCR-mashine	ABI PRISM 7900HT fast Real-Time PCR system	*Life Technologies*, Darmstadt, Germany,
Retsch mill	Retsch® MM200	*Retsch*®, Haan, Germany
Slide boxes		*Carl Zeiss Micro Imaging*, Bernried, Germany
Spectral photometer	NanoDrop® ND-1000	*NanoDrop® products*, Willington, Delaware, USA
Spring steel forceps	forceps 100mm, pointed	*VWR*, Darmstadt, Germany
Stereo microscope	M37	*Leica*, Wetzlar, Germany

Table 12: Technical devices

Technical device	Type	Manufacturer
Thermomixer	Eppendorf Thermomixer comfort 5355	*Eppendorf*, Hamburg, Germany
Vacuum centrifuge	Concentrator 5301 Gesamtsystem	*Eppendorf*, Hamburg, Germany
Vibrating blade microtome	Leica VT 1000S	*Leica*, Wetzlar, Germany
Vortexer	Vortex Genie 2	*Bender Hobein AG*, Zürich, Swiss
Water bath	C 10	*Thermo Haake*, Karlsruhe, Germany

9.4 Primer list

Table 13: Oligonucleotides. All primers were ordered by *MWG Operon* (Ebersberg, Germany) as desalted oligonucleotides. Appropriate restriction enzyme sites are labeled in green. Sequences of the miRNA5204* and appropriate complementary strand are highlighted in red. for: forward primer, rev: reverse primer, GW: primer for Gateway® Cloning.

Name	Sequence (5´ 3´)	Reference
qRT-PCR		
Housekeeping genes		
MtPfd2 for	GTGTTTTGCTTCCGCCGTT	Kakar et al.,
*MtPfd2*rev	CCAAATCTTGCTCCCTCATCTG	2008
MtEf1-α for	GACAAGCGTGTGATCGAGAGATT	Kakar et al.,
MtEf1-α rev	TTTCACGCTCAGCCTTAAGCT	2008
MtGapdh for	TGCCTACCGTCGATGTTTCAGT	Kakar et al.,
MtGapdh rev	TTGCCCTCTGATTCCTCCTTG	2008
MtUbiquitin exon for	GCAGATAGACACGCTGGGA	Kakar et al.,
MtUbiquitin exon rev	AACTCTTGGGCAGGCAATAA	2008
*MtUbiquitin*intron for	GTCCTCTAAGGTTTAATGAACCGG	Kakar et al.,
*MtUbiquitin*intron rev	GAAAGACACAGCCAAGTTGCAC	2008
Transcription factors		
MtCbf1 for	CCGCAGCATTGTTAATAGCCA	This work
MtCbf1 rev	AAACAATTGGAGCTACCCCTGA	This work
MtCbf2 for	TGGTTTCTAATTCTGATTCCACTGAT	This work
MtCbf2 rev	TTTCCATTTGCATGACAGTGGTAT	This work
MtErf2 for	5CATAACACCTATTGCTGCTGCA	This work
MtErf2 rev	TCAGCCGACATATTCCCATG	This work
MtGras8 for	CATTGAGGATGGAGAGGCATG	This work
MtGras8 rev	TGATTCTCCTCCTCCATCGATCA	This work
MtHomeobox1 for	CCGGATTCCATTGGAATCG	This work
MtHomeobox1 rev	GGATTTCAGCAACCCTTGCA	This work
MtHomeobox40 for	CCAGCTTGTGAATACACCCAA	This work
MtHomeobox40 rev	GCACTGTTTTCTCCACCTTTGT	This work
*MtMyb1*for	GCCCTCTCTTTCCGAGGAAT	This work
*MtMyb1*rev	TCGCTGTTCGATGTTCTTCGT	This work
MtSYMREM for	CCCTGTTGTGGAAAAGGATTCA	This work
MtSYMREM rev	TGCTGATTAGGCTCCTGACTGA	This work
MtSWIRM1 for	TTGTTGGTAGGACCGACAAGGA	This work
MtSWIRM1 rev	TCAATGCAAGGAGCAGACTCG	This work
MtZinc1 for	ATGGCGAAGCAGCTACCTTGT	This work
MtZinc1 rev	TGGAGTTGCACATGTTCGACA	This work

Continuation table 13: Oligonuleotides

Name	Sequence (5´ 3´)	Reference
Mycorrizhal marker genes		
Copper transporter for	CTCGAAAGACACACATGACAGCA	Gaude et al.,
Copper transporter rev	GAGAGAGTGGAGGTGCAATGAAC	2012
Expansin for	GCTGTTGAGATGTGGCAGAA	Gaude et al.,
Expansin rev	AAGACCGACGCATGTACTCC	2012
MtAmt for	ACAGATGGTGATCCAAATTGAG	Gaude et al.,
MtAmt rev	CTGATTGCGCTTAATGTTCAC	2012
MtHa1 for	CTTTGTGCTTTTCGCACATAACAT	Krajinski et
MtHa1 rev	AGACAAAAAAATATAAAACAATAGCCAATG	al., 2002
MtPt4 for	CAAGAAAGATTAGACGCGCAA	Harrison et al.,
MtPt4 rev	GTTTCCGTCACCAAGAACGTG	2002
Protease inhibitor for	GTGCCCTACAGAGGCTTGTC	Gaude et al.,
Protease inhibitor rev	AACACAACTGGAAGGGCATC	2012
Phosphate stress marker genes		
Mt4 for	AATGATTGCTGGGAATGAACCTT	Branscheid.,
Mt4 rev	TTCCAAAGAGAAAATCCCATCAA	et al 2010
Phospholipase D for	TTGATGAATGGAAAGCCGTGG	Branscheid., et al 2010
Phospholipase D rev	GCGGAGGCTATGGGAAAATTT	Branscheid., et al 2010
Rhizophagus irregularis transcripts		
R. irregularis translation elongation factor for	TGTTGCTTTCGTCCCAAT	Helber et al., 2011
R. irregularis translation elongation factor rev	GGTTTATCGGTAGGTCGA	Helber et al., 2011
Stem-loop cDNA synthesis		
Stem-loop miRNA5204*	GTCGTATCCAGTGCAGGGTCCGAGGTATTCGCAC TGGATACGACATACTG	accoding to Devers et al., 2013
Stem-loop miRNA5204	GTCGTATCCAGTGCAGGGTCCGAGGTATTCGCAC TGGATACGACGTTCCTA	accoding to Devers et al., 2013
Stem-loop qRT-PCR		
MiRNA5204* for	CAGTCCCTCAAAGGCTTC	This work
Stem-loop rev primer	CCAGTGCAGGGTCCGAGGT	Devers et al., 2013

Continuation table 13: Oligonuleotides

Name	Sequence (5´ 3´)	Reference
***Erf2-1/Tnt1*mutant screening**		
Confirmation read through		
Erf2-1infront Tnt1-for	CTCTTATTGTTCCATCCGGT	This work
Erf2-1infront Tnt1-rev	TTACCCCACTTTCTCATCCT	This work
Confirmation of Tnt1 insertion		
Erf2-1/Tnt1 for	GAGGAATAAGGATGAGAAAGTG	This work
Erf2-1/Tnt1 rev	ACACAGCAGTATCATAAGCA	This work
Gateway® Cloning		
Promoter::uidA fusions		
GW-*MtAba1*pro for	CACCTCCAAGCATACATGAAAGAC	This work
GW-*MtAba1*pro rev	ACAACGTTAGTTCTTGTCC	This work
GW-*MtCbf1*pro for	CACCGGCAAAGCCATTATT AACTCAC	This work
GW-*MtCbf1*pro rev	AAGAAGATGTTGCTTCTGCTG	This work
GW-*MtCbf2*pro for	CACCACTATGCCAGAAAGCTA TTACG	This work
GW-*MtCbf2*pro rev	AATATGCACCTGCTTGTCTC	This work
GW-*MtErf2*pro for	CACCTTACGAGAACAAACCAATCC	This work
GW-*MtErf2*pro rev	CTTCCATACCCTACCTACCT	This work
GW-*MtGras8*pro rev	CGTTCTTTCAGAGCTTTCTTCA	This work
GW-*MtGras8*pro rev	CGTTCTTTCAGAGCTTTGTTGA	This work
GW-*MtHomeobox1* pro for	ATCATCCTAATTAAGCTACC	This work
GW*MtHomeobox1* pro rev	ATCATCCTAATTAAGCTACC	This work
GW-*MtMyb1*pro for	CACCCGATTTCTTCATGTGTTTCC	This work
GW-*MtMyb1* pro rev	CCTATGTTATTCAGTTGCTGG	This work
GW-*MtSWIRM1*pro for	CACCAATCGTCCATGTAATTTGGGTC	This work
GW-*MtSWIRM1*pro rev	CATTCGTTTACCACTTGTCC	This work
BiFC constructs		This work
GW-MtGRAS8 for	CACCGAGAAATTAATATGTC ACCTGC	This work
GW-MtGRAS8 rev stop	TCAGCATTTCCAGCAAGAA	This work
GW-MtNSP1for	CACCACAATGACTATGGAAC	This work
GW-MtNSP1 rev stop	CTACTCTGGTTGTTTATCCAG	This work
GW-MtNSP2for	CACCATGGGATTTGATGGACATG	This work
GW-MtNSP2 rev stop	CTATAAATCAGAATCTGAAG AAGAACAAGTC	This work

Continuation table 13: Oligonuleotides

Name	Sequence (5´ 3´)	Reference
GW-MtPHO2 for	CACCATGACTGATTCAGACTGGGAGTC	This work
GW-MtPHO2 rev stop	CTTCGTCGAGTTTTCATTTTTGG	This work
GW-MtRAM1for	CACCATGATCAATTCACTTTGTGG	This work
GW-MtRAM1rev stop	TCAGCATCGCCATGCAGAA	This work
***MtGras8* RNAi constructs Medtr4g104020.1**		
GW-*MtGras8* 3´UTR for	CACCTTAGGATCACAGCGATTGGT	This work
GW-*MtGras8* 3´UTR rev	GTCATCACTTTATTTCTGCTCC	This work
BamHI-MtGras8 3´UTR sense for	5´ATGGACGGATCCTTAGGATCACAGCGATTGGT	This work
Acc65I-MtGras8 3´UTR sense rev	5´ATGCTGGGTACCGTCATCACTTTATTTCTGCTCC	This work
MluI-MtGras8 3´UTR antisense for	5´TCAGGAACGCGTTTAGGATCACAGCGATTGGT	This work
BspEI-MtGras83´UTR antisense rev	5´TGACTGTCCGGAGTCATCACTTTATTTCTGCTCC	This work
3´UTR *MtGras8* for	CTTAGGATCACAGCGATTGGT	This work
3´UTR *MtGras8* rev	GTCATCACTTTATTTCTGCTCC	This work
Amplification miRNA5204*		
Primer A	CTGCAAGGCGATTAAGTTGGGTAAC	Devers et al., 2013
Primer B	GCGGATAACAATTTCACACAGGAAACAG	Devers et al., 2013
Primer I:	5´GTTCCCTCAAAGGCTTCCAGTATAAATTGGACAC GCGTCT	This work
Primer II:	5´TTATACTGGAAGCCTTTGAGGGAACAAAAAGAT CAAGGC	This work
Primer III:	5´TTATACTGGAAGAATTTGAGGGCTCTAAAAGGA GGTGATAG	This work
Primer IV:	5´TAGCCCTCAAATTCTTCCAGTATAATTAGGTTAC TAGT	This work
Colony PCR miR5204* for	ATACTGGAAGAATTTGAGGGC	This work
Colony PCR miR5204* rev	ATACTGGAAGCCTTTGAGGGA	This work

Continuation table 13: Oligonuleotides

Name	Sequence (5´ 3´)	Reference
Sequencing primer		
Sequencing pENTR®/D-TOPO®		
M13 for	GTAAAACAGCGGCCAG	*LGC genomics*
SeqL-E rev	GTTGAATATGGCTCATAACAC	*LGC genomics*
Sequencing RNAi vectors		
MtPt4pro for	TCTCCTAAGCTAACTTAGGAC TAAACGTCACATTG	This work
NOS terminator rev	ATAGGCGTCTCGCATATCTCATTAAAGCAGGG	This work
pKDsRed *FAD* intron for	GCAATCCTTTCACAAC	This work
pKDsRed *FAD* intron rev	CAAACATCAGATTCTCGAC	This work
Sequencing expression vectors for mis-expression miRNA5204*		
AtUbiquitin3pro for	GGTATATGTTCGCTGATTGG	This work
OSC terminator rev	AATATCATGCGATCATAGGC	This work
Sequencing expression vectors (pE-SPYNE-GW and pE-SPYCE-GW) for BiFC		
C-terminal YFP for	ACAAGCAGAAGAACGGCATC	This work
N-terminal YFP for	GTAAACGGCCACAAGTTCAG	This work
MtNsp2 rev	CCAGGTGCAACCATAATCCTC	This work
*MtNsp1*rev	GATGGAAAGAAAGAGACAGAACCT	This work
MtGras8 rev	TCCATGTTGAAGTAGCACTG	This work
MtRam1 rev	CACATTGAACTATCTGGTGATTGG	This work
MtPho2 rev	TGAGCTTGGCCACCATAGAG	This work

Eidesstattliche Erklärung

Hiermit erkläre ich, dass ich die Arbeit ohne fremde Hilfe verfasst und keine als die angegebenen Hilfsmittel benutzt habe. Außerdem versichere ich, dass die Arbeit nicht veröffentlicht oder in einem anderen Prüfungsverfahren vorgelegt worden ist.

Potsdam, den 26. Juni 2013

Unterschrift

Danksagung

Ich bedanke mich ganz besonders bei Prof. Dr. Franziska Krajinski für die ausführliche Betreuung während meiner Promotion und Bereitstellung dieses spannenden Themas. Vielen Dank für die langjährige Zusammenarbeit und das Vertrauen und die Unterstützung, die mir in den letzten sechs Jahren entgegen gebracht wurden.

Besonders danke ich Dr. Nicole Gaude für die jahrelange moralische Unterstützung, die Beantwortung unzähliger Fragen und ihre unendliche Geduld.

Dr. Emanuel Devers danke ich für hilfreiche Diskussionen und Anregungen.

Dr. Daniela Sieh möchte ich für manche ausgesprochene Wahrheit und den Stupps in die richtige Richtung danken!

Bei der gesamten AG Krajinski möchte ich mich für die sehr harmonische und entspannte Arbeitsatmosphäre und die Unterstützung bedanken. Ich werde die gemeinsamen Mittagspausen und Brunch-Büffets vermissen (nicht nur wegen des Essens ☺).

Bei meinem Evaluierungskommitee, bestehend aus Dr. Staffan Persson, Dr. Dirk Hincha und Dr. Alisdair Fernie möchte ich mich für viele hilfreiche Anregungen und Diskussionen bedanken.

Weiterhin möchte ich meinem Partner Christian Kautz und meiner Familie meinen herzlichsten Dank aussprechen, da sie mich während des Studiums und der Promotion unterstützt und immer hinter mir gestanden haben.

Danke, dass ihr alle an mich geglaubt habt, obwohl es mir manchmal schwer fiel!